

STRUCTURAL AND PETROFABRIC ANALYSIS OF AN "ALPINE-TYPE" PERIDOTITE:
THE LHERZOLITE OF THE FRENCH PYRENEES

BY

H. G. AVÉ LALLEMANT

ABSTRACT

A narrow E-W-striking "graben" containing Mesozoic sediments is separated from the Hercynian mountain chain of the Pyrenees in the south by the North-Pyrenean fault and in the north by a detachment plane. In the region around Vicdessos and the Etang de Lers (Ariège, France), three Alpine phases of deformation are recognized: the first and strongest has an E-W-trending fold axis and a subvertical axial-plane cleavage, the second and weakest also has an E-W-trending axis but a northward dipping axial-plane cleavage, and the third a subvertical axis and subvertical N-S-striking axial-plane cleavage. The northernmost zone has ultramafic bodies consisting principally of lherzolite. This zone is also characterized by the occurrence of metamorphism and brecciation. The metamorphism is of a dynamo-thermal type, resembling the Abukuma-type of metamorphism, with a climax during the first Alpine deformational phase. Petrofabric analyses of some metamorphic minerals (calcite, dolomite, phlogopite, scapolite, and tremolite) indicate that this was a flattening phase. Although the lherzolites did not suffer from the Alpine metamorphism, they show fracture cleavages of the first and the third Alpine phases. However, the lherzolites contain many more older structures, such as a layering of spinel pyroxenites, an isoclinal folding with an axial-plane cleavage, and a weak, more open folding of these structures. Petrofabric analyses of olivine, enstatite, and diopside indicate that the fabric of the lherzolites is determined by the axial-plane cleavage of the isoclinal folds (α -olivine, α -enstatite, and α -diopside lying perpendicular to the axial-plane cleavage, and γ -olivine, γ -enstatite, and γ -diopside lying parallel to the fold axis) which arose from a pre-Alpine syntectonic recrystallization. In general, the olivine grains show a fabric habit, i.e. they are referable to a triaxial ellipsoid, the short axis perpendicular to the axial-plane cleavage, the long axis parallel to the fold axis, but these axes do not always coincide with the optic elasticity axes. All these phenomena form indications that the lherzolites intruded as solid blocks. There is no indication of a tectonic intrusion; faults in the country rock and shear zones and slickenside structures in the lherzolites are absent. The brecciation of the lherzolites, which occurred principally along their margins, and of the country rock just in the zone containing lherzolites, is definitely linked to the emplacement of the lherzolites. Indications that the breccias originated by explosions are provided by such features as the funnel-shaped breccia bodies and the discordant nature of the breccias, which cut across the bedding planes. This situation suggests that the solid intrusion of the lherzolites could have been caused by degassing of the upper mantle followed by gaseous explosions, just before the Alpine orogeny. It seems highly probable that the lherzolites originated in the upper mantle, where their pre-Alpine structures and fabric would also have been formed. The gabbroic intrusions (ophites) are truly magmatic, and are probably genetically related to the lherzolites, but this relationship would also date back to the upper mantle.

RÉSUMÉ

Un fossé, de direction E-O, contenant des sédiments Mésozoïques, est séparé de la zone axiale des Pyrénées, au sud par la faille Nord-Pyrénéenne, et au nord par une surface de décollement. Dans la région autour de Vicdessos et de l'Etang de Lers (Ariège, France) trois phases de déformation Alpines sont reconnues: la première est la plus forte avec des plis de direction E-O, et un clivage axial subvertical, la deuxième plus faible, aussi avec des axes E-O, mais ayant un clivage axial, plongeant faiblement au nord, et la troisième avec un axe subvertical et un clivage axial N-S. Dans la zone septentrionale, des massifs ultramafiques sont fréquents, composés principalement de la lherzolite. Cette zone est aussi caractérisée par la présence d'un métamorphisme et d'une bréchification. Le métamorphisme est d'une type dynamo-thermique, ressemblant au type d'Abukuma, avec un maximum pendant la première phase de plissement. "Petrofabric analysis" de quelques minéraux métamorphiques (calcite, dolomite, phlogopite, scapolite, et trémolite) indique que cette phase est une phase d'aplatissement. Bien que les lherzolites n'aient pas été éprouvées par le métamorphisme Alpin, elles montrent des clivages (type "fracture cleavage") de la première phase Alpine et de la troisième. Les lherzolites contiennent de nombreuses structures plus anciennes, comme la stratification de pyroxénolites à spinelle, de plis isoclinaux de cette stratification avec un clivage axial, et un plissement faible de toutes ces structures. "Petrofabric analysis" d'olivine, d'enstatite, et de diopside indique que la texture des lherzolites dépend du clivage axial des plis isoclinaux (α -olivine, α -enstatite, et α -diopside étant perpendiculaires au clivage axial, et γ -olivine, γ -enstatite, et γ -diopside étant parallèles à l'axe du pli), et est produit par une récrystallisation syntectonique pré-Alpine. Généralement les grains d'olivine montrent un "fabric habit", c.-à-d. ils sont comparables à une ellipsoïde triaxiale avec l'axe court perpendiculaire au clivage axial, et l'axe long parallèle à l'axe du pli; cependant, les axes de l'ellipsoïde ne correspondent pas toujours aux axes de l'indicatrice. Tous ces faits indiquent que les lherzolites sont introduites en blocs solides. Il n'y a pas d'indications d'une intrusion tectonique; des failles dans la roche environnante et des zones de faille et des miroirs de glissement dans les lherzolites sont absents. La bréchification des lherzolites, qui avait pris lieu principalement dans la bordure des massifs lherzolitiques, et de la roche environnante, exactement dans la zone contenant les lherzolites, est liée clairement à l'intrusion des lherzolites. Il y a des indications que les brèches sont de nature explosive: des massifs de brèche en forme de cheminée, et la nature discordante de la brèche recoupant la stratification sédimentaire. Ces faits indiquent que l'intrusion solide des lherzolites pouvait être causée par des explosions de gaz, libéré dans le manteau supérieur, juste avant l'orogénèse Alpine. Le manteau supérieur est probablement à l'origine des lherzolites, d'où les structures et la texture pré-Alpines pourraient prendre naissance. Des intrusions gabbroïdes (les ophites) sont vraiment magmatiques. Elles sont probablement reliées aux lherzolites, bien que la relation n'ait existé que dans le manteau supérieur.

CONTENTS

I. Introduction	2	Structural analysis of the lherzolites	18
II. Mesozoic country rocks of the lherzolites	3	General remarks	18
Stratigraphy	3	Lherzolite of the Etang de Lers	18
Structural geology	4	Lherzolite of the Forêt de Freychinède	24
Phases of deformation	4	V. Fabric analysis of the ultramafic rocks	25
Explosion breccias	6	Introduction	25
Faults	6	Fabrics	26
III. Fabrics of the Mesozoic country rocks	7	Conclusions based on the fabrics	41
Alpine metamorphism	7	Grain shape	44
Calcareous and dolomitic rocks	7	Granulation and mylonitization	45
Liassic marls and limy arkoses	7	Geological evidence derived from the fabric analyses	45
Albian marls	8	Comparison with other fabrics from the literature	46
Fabric analysis	8	Mechanism causing the observed fabrics	48
Conclusions	12	Ophites	49
IV. Lherzolites and related ultramafic rock types	13	VI. Origin and emplacement of the lherzolites	50
Petrography	13	Emplacement of the lherzolites	50
General character	13	Other "Alpine-type" peridotites	51
Lherzolite	14	Origin of the lherzolites	52
Harzburgitic lherzolite	15	Nature of the upper mantle	52
Spinel pyroxenites	16	Orogenic interpretation of the lherzolites	52
Garnet pyroxenites	16	References	54
Garnet-plagioclase pyroxenite	16	6 Plates	
Hornblendites	17	3 Appendices (in back flap)	
Breccias	17		

CHAPTER I

INTRODUCTION

The origin and emplacement of peridotites in orogenic terrains is a fundamental problem in geology. These peridotites, generally referred to as "Alpine-type" peridotites, have some varieties whose composition is almost uniform throughout the world. One of these varieties is lherzolite. When, in 1797, de la Métherie (*vide* Lacroix, 1894) proposed this name for the rock he had found at the Etang de Lers¹⁾ in Ariège, French Pyrenees, he did not know either the mineralogical or the precise chemical composition of the rock. At present, it still seems warranted to give this rock type a special name, but the name spinel peridotite would be more self-explanatory than lherzolite. According to Zirkel (1866), lherzolite contains principally olivine, with orthopyroxene and clinopyroxene, spinel always being an accessory.

One of the most useful approaches for determining the origin and emplacement of any geological body whose occurrence among the country rocks is strange, is the comparative microstructural investigation. Petrofabric analyses of individual mineral grains with a universal-stage microscope are also useful in this respect, and have been performed in the present study for some lherzolites. The Northern Pyrenees, containing the type locality of lherzolite, form an excellent terrain for this type of investigation.

The Pyrenees are principally a Hercynian orogene which was only uplifted to its present level in Alpine times (de Sitter and Zwart, 1962). Mesozoic sediments

were folded only slightly and underwent no metamorphism during the Alpine orogeny, with the exception of a very narrow but extensive E-W-striking belt, bordered in the south by the great North-Pyrenean fault and in the north by some of the external Hercynian massifs. The Mesozoic rocks in this zone were tightly folded and relatively strongly metamorphosed during several phases of the Alpine orogeny. All lherzolite bodies occur within this narrow Mesozoic belt and never outside it. Ophites, which are believed to be genetically related to the lherzolites, occur throughout the Pyrenees, both inside or outside this belt.

Within the Mesozoic belt, the lherzolite bodies are not evenly distributed. They are generally concentrated in groups, of which four can be distinguished: 1. near Prades (Ariège), 2. near Vicdessos and the Etang de Lers (Ariège), 3. near Couledoux (Haute-Garonne), 4. near Moncaup and Arguénos (Haute-Garonne). Some isolated small bodies occur in the Departments of Hautes-Pyrénées and Basses-Pyrénées (Fig. 1).

The present author visited most of the occurrences in 1964 while searching for the most suitable terrain for a petrostructural investigation. The group near Vicdessos and the Etang de Lers was found to offer the most interesting phenomena and the best exposure. The field work was carried out in this region during the summers of 1965 and 1966, and was supported by substantial grants from the *Van Oosterom Onderwijsfonds*.

There are many theories about these lherzolites, one

¹⁾ modern spelling; formerly Etang de Lherz.

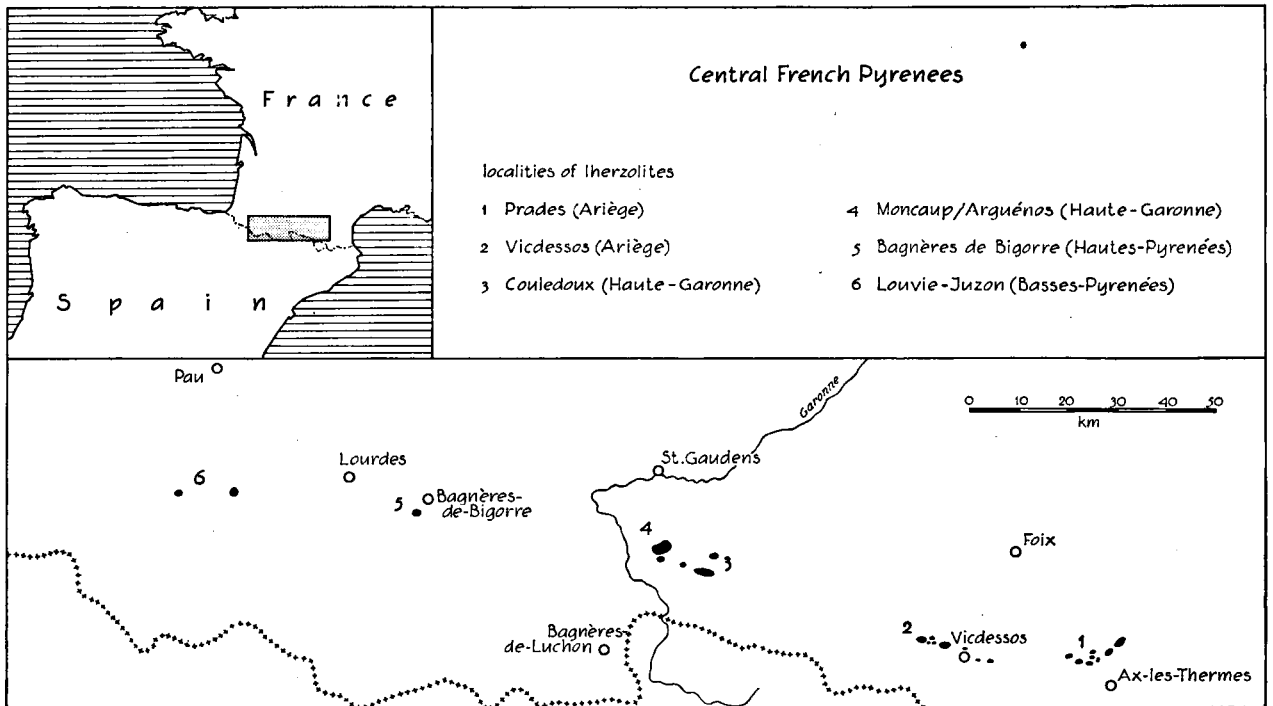


Fig. 1. Map showing the occurrence of lherzolite in the Pyrenees.

of the oldest being that they are of sedimentary origin. Some geologists have considered that they were unchanged sediments, others thought them to be metasediments (Longchambon, 1912). This controversy about metamorphism persisted, although the idea of a sedimentary origin was abandoned. Lacroix (1894, 1894/95, 1901) believed that the lherzolites were igneous and had been intruded into the Mesozoic sediments, causing contact metamorphism. Ravier (1959) and Monchoux (1965) showed that the metamorphism of the Mesozoic rocks was not caused by the lherzolites. The fabric of the lherzolites could have been caused by the Alpine orogeny after their emplacement (Collée, 1962), or the fabric could be older, thus precluding a magmatic intrusion into the present level.

To unravel the structural history of the Pyrenean lherzolites, the Mesozoic rocks were investigated first; the stratigraphy and structures are reported in Chapter II, metamorphism and petrofabrics in

Chapter III. In Chapter IV the composition and structures of the lherzolites and their associated rock types are described, in Chapter V the fabrics. After subtraction of the overprinted Alpine structures, older structures could be recognized. Chapter VI gives the conclusions drawn from the preceding chapters and a comparison of the present data with the findings from other regions.

The region studied was mapped on a scale of 1 : 10,000, based on enlarged copies of the 1 : 20,000 topographical maps of the Institut Géographique National: sheets XXI-48-1/2 (Vicdessos) and XX-48-4 (Aulus-Bains). The final geological map (Appendix I) was again reduced to a scale of 1 : 20,000. The various structures are shown on a separate map in Appendix II, cross-sections in Appendix III. All maps and also the text figures were drawn by Mr. J. Bult.

Samples with numbers preceded by V are taken from the area covered by the Vicdessos sheet, those with an L derive from the Aulus-les-Bains sheet.

CHAPTER II

MESOZOIC COUNTRY ROCKS OF THE LHERZOLITES

STRATIGRAPHY

Since the scope of this study did not include an extensive stratigraphic examination of the region, the stratigraphic sequences of Casteras (1933) have been followed. Briefly summarized, the first post-Hercynian sedimentation in the Pyrenees took place during the

Stephanian, but in the region studied the oldest post-Hercynian sediments are of Jurassic age, which Casteras ascribed to removal by erosion of the Stephanian, Permian, and Triassic.

Although a detailed subdivision of the Mesozoic sediments can be made for other regions of the French

Pyrenees, this is rather difficult to do here because of the strong Alpine metamorphism. Few fossils have been found in this region. French geologists have demonstrated the stratigraphy elsewhere, and since the lithology of the units is very similar throughout the Pyrenees a stratigraphic sequence could be arrived at.

The first unit of sediments consists of Lower Liassic dolomites, which are greyish, fine-grained, and sometimes banded, passing into dolomitic limestones and even into pure, compact limestones. This unit is not always present. Often it wedges out, as in the western part of the region, the thickness varying from zero to at least 400 m.

The next unit consists of thin alternating bands of light-coloured marly arkoses and darkish marls of Middle and Upper Liassic age. This unit is sometimes 10 or 20 m thick, but in places measures as much as 100 m and even more in the fold hinges. This group is very easily distinguished, forming a good marker horizon.

Upon the Liassic lies a series of dolomites of Middle Jurassic age. They are generally black and sometimes white or pink. There are limestone intercalations, which led Cayeux (1931) to suppose an epigenetic origin of the dolomites. Because they are difficult to distinguish, these Middle Jurassic rocks were not separately mapped (see map, Appendix I) with respect to the Cretaceous marbles, although there is a large hiatus between the two units. The distinction is also complicated by later brecciation due to gaseous explosions. Because of strong Alpine metamorphism in this region, these rocks are very coarsely recrystallized, as a result of which they have lost their black colour. At present, they are mostly greyish to white, or sometimes pink, dolomitic marbles.

The white or occasionally greyish limestones of Cretaceous (Aptian) age, which often contain bands of dolomites and are also coarsely metamorphosed and brecciated, are shown on the map together with the Middle Jurassic as a single unit. The thickness of this comprehensive unit is 200 to 1000 m (see cross-sections in Appendix III). The upper part of these Aptian limestones shows a constantly increasing quantity of marly intercalations. Thus, the Aptian limestones pass gradually into another lithofacies, finally making place for the Albian marls.

In the region under discussion the Albian comprises the last Mesozoic sediments. It generally consists of marls with many intercalations of black limestone and sedimentary breccia. This unit is still at least about 300 m thick. In other parts of the Pyrenees, Cenomanian sedimentation took place on an already folded, metamorphosed, and eroded pre-Cenomanian mountain chain. The Alpine orogeny must therefore have taken place between the Albian and the Cenomanian. During this interval the Iherzolites and ophites, which will be described in Chapters IV and V, were emplaced among the sediments. In other regions, new work on microfossils in marls until recently considered to be Albian, has shown that the upper part of these

sediments is of Senonian age (Mattauer *et al.*, 1964). A measure of sericitization in these Senonian rocks is indicative of a somewhat longer duration of the Alpine metamorphism.

The latest sediments are glacial deposits like those near Lercoul, Sem, Olbier, Saleix, Port de Saleix, and Sentenac, and some are fluvial deposits, located mainly in the valley of the Ruisseau de Vicdessos.

In the field, use was made of the geological map (1 : 80,000) of Casteras (1933). On the present map (see Appendix I) the boundaries indicated by dashed lines appear on Casteras' map but were not found by the present author, e.g. near Sem and Lercoul, where no Liassic marls were found even in the scree, although they may have been present before 1933. Some modifications were necessary; for instance, an anticline with a Liassic core was found south of the Etang de Lers, which changed the cross-section in this locality considerably.

STRUCTURAL GEOLOGY

Before studying the structures of the Iherzolites, the structures of their Mesozoic country rocks must be examined. Subtraction of these unequivocally Alpine structures from the total structural picture of the Iherzolites reveals their pre-Alpine history, if any. A rapid structural survey of the region was therefore made. The following rather brief account of the Alpine structural history in this region should suffice for the present purpose. As already mentioned, the Mesozoic rocks are preserved by an E-W-striking "graben" structure or a step fault.

Phases of deformation

First phase of deformation (F_1). — The structural map (Appendix II) gives the measurements of the various structural phenomena. Nine cross-sections, taken roughly N-S, are given in Appendix III. The geological map (Appendix I) clearly shows that the most important Alpine structures are the E-W-trending folds.

In the east, between Siguer and Vicdessos, there is only one syncline. North of Vicdessos, two small anticlines are developed in the northern flank. Farther to the west, the large southernmost syncline dies out against the North-Pyrenean fault, as does the next anticline near the Port de Saleix. West of the Etang de Lers a new small anticline developed, forming beyond it a total of two anticlines and three synclines. The syncline in the south is taken from the French geological map (1 : 80,000), and was not mapped in this study. These E-W-striking folds belong to the first phase of deformation (F_1) of the Alpine orogeny. The Albian marls and the Liassic marly limestones seem to have been very incompetent during the folding. The Albian marls near Vicdessos were folded isoclinally, whereas the limestones form open concentric folds. Where Liassic cores in anticlines are exposed, it can

be observed that these beds are also folded isoclinally, but the limestones are always concentrically folded. Almost without exception throughout this region, the axial plane of the folds strikes between NW-SE and WSW-ENE and dips steeply to the north or is vertical. The fold axes seem themselves to be folded, plunging and rising with great regularity.

In addition to the large S_1 -folds, there are also folds of medium size (e.g. north of Vicdessos) with a wavelength of about 100 m. Minor folds and microfolds of the first phase are very scarce.

An axial-plane cleavage (S_1) has been developed almost everywhere. This cleavage is well developed in the Albian part of the syncline near Vicdessos. The S_1 -cleavage and the bedding often enclose a small angle, which is well illustrated in a quarry between Auzat and Vicdessos (Fig. 3 and Plate I, a). In the limestones both the cleavage and the bedding are very difficult to recognize because of recrystallization during the Alpine metamorphism. Fanning of the axial-plane cleavage occurs everywhere.

The cleavage-bedding intersection, or l_1 -lineation, often pitches far more steeply than the fold axes in the isoclinally folded Albian marls. A slight rotation of the stress field or a small tilting of the rocks before F_1 , may have caused this discrepancy.

Second phase of deformation (F_2). — The second phase has a very local nature. However, F_2 acted rather strongly on the Albian marls and the interlayered

limestone beds. Asymmetrical folds with axial planes striking E-W and generally dipping 30° to 40° to the north, have E-W-trending fold axes (B_2) which plunge only slightly. All sizes of folds are present: microfolds (Fig. 3), folds with a 20 cm wavelength (Plate I, c), and major folds such as those visible on the slope of the limestone hill near the village of Olbier, 0.5 km south of Vicdessos (Fig. 2).

In the Albian marls, but also in some instances in the Liassic, a second axial-plane cleavage (S_2) developed (Fig. 3 and Plate I, a), on which some calcite veins are present.

In an outcrop near the eastern bridge of Vicdessos some shaly layers are slightly boudinaged (Plate I, d). Fissures in the shale layers running perpendicular to the fold axis (B_2) are filled with calcite. During the crystallization of the calcite a small continuous



Fig. 2. View from the road between Auzat and Saleix, toward the east: S_2 -folds in the Aptian limestones near the village of Olbier.

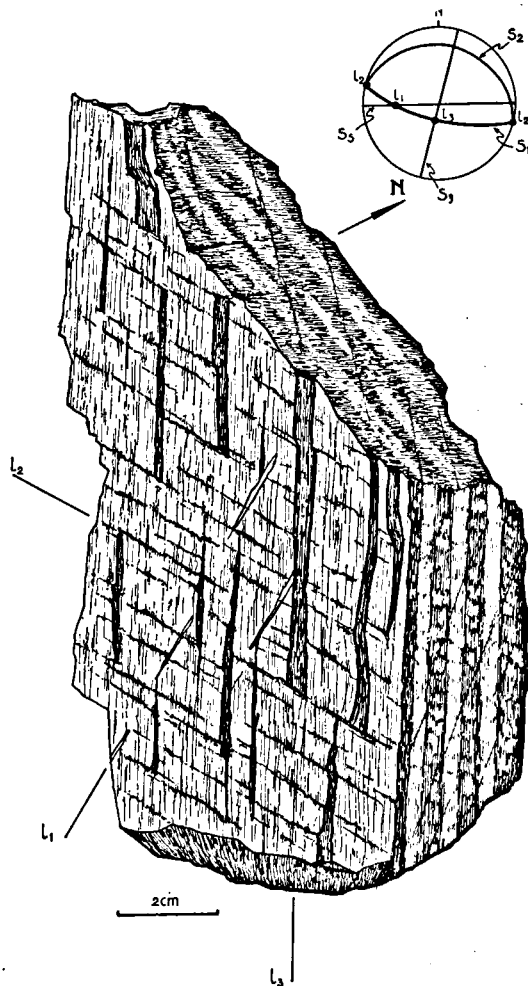


Fig. 3. Hand specimen from a quarry between Vicdessos and Auzat. Thin layers of darkish marl interbedded with lighter-coloured marly limestones. The bedding S_8 , the cleavage S_1 , S_2 , and S_3 , and the intersections of S_1 with S_8 , S_2 , and S_3 (lineations l_1 , l_2 , and l_3) are clearly visible. The stereographic projection shows all these structures.

rotation of each shaly block gave the calcite crystals a sigmoidal shape showing no undulatory extinction in thin sections. In some instances quartz crystallized after the calcite in the same way, giving rise to a zoned vein.

Third phase of deformation (F_3). — The third phase acted very strongly throughout the region, much more so than the second phase. The bending of Mesozoic beds, which is visible near Vicdessos, was due to a large-scale folding by F_3 . Smaller folds are scarce. Only a few small-scale folds, with a wavelength of several centimetres, were found. The fold axis (B_3) seems to be almost vertical, depending on the position of the strata before F_3 . Their axial planes strike roughly NNE-SSW and are subvertical.

Roughly parallel to the axial plane, the development of a strong cleavage (S_3) is very clearly visible in the Albian marls and less so in the limestones. Fig. 3 clearly demonstrates the three cleavages in a marl with some thin marly limestone intercalations. On the top face of the hand specimen it is evident that the lighter-coloured marly limestone laminae were broken up into boudins parallel to the first fold axis or the l_1 -lineation. In Plate I, b, taken in the plane parallel to the S_1 -cleavage, the clearest lineation is the intersection of the S_1 - and S_3 -cleavages (l_3) plunging 68° to the east. The almost horizontal lineation is the fold axis of S_2 -microfolds (l_2), the very vague lineation parallel to the pencil being the bedding- S_1 intersection, the l_1 -lineation.

There appears to be a consistent pattern governing the direction of dip of the S_3 -cleavages. The structural map (Appendix II) shows that the S_3 -cleavage may dip to the west in one N-S-striking zone, and in the following zone to the east. This could be explained by fanning of the cleavage in S_3 -folds, the intermediate strain or deformation axis of which (B_3) does not coincide with the vertical S_3 -fold axis but makes an angle with it. If the E-W-striking and vertical S_1 -cleavages, which are in general more easily recognized than the bedding planes, were folded during F_3 by a not too steeply northward-plunging deformation axis (B_3), vertical fold axes would have originated (Ramsay, 1960); the axial-plane cleavage S_3 , however, would show fanning around the northward-plunging B_3 -axis, with the above-mentioned result.

An alternative explanation is that a fourth phase of only slight folding, with a N-S-striking axis, was responsible for this picture, which would also explain the slight bending or undulation of the S_1 -fold hinges in the E-W direction.

Explosion breccias

The northern zone of the Mesozoic belt contains calcareous breccias whose origin is not sedimentary. These breccias cut across the bedding. The anticlinal hinges of the limestone folds are often far more brecciated than their flanks. However, these are not

fault breccias, as may be concluded from several facts: the fragments in the breccia are angular; they are not tabular, elongate, or disposed in a parallel manner; and irregular funnel-shaped patches of breccia occur within well-bedded limestones in some places.

It is rather difficult to see much of the bedding here, but because of the local nature of the breccia a general idea of the position of the bedding plane can be formed. The local nature of the breccia is shown by Plate II, a, in which the fragments are not far removed from their original position in the bedding. In Plate II, b this is less distinct, and in Plate II, c an Alpine cleavage obscures any indication of bedding. The limestone breccias generally occur in the same zone as the lherzolites. The present author believes that the emplacement of the lherzolites and the brecciation were both caused by the same process. In the neighbourhood of the lherzolites the limestone breccia often contains lherzolite fragments. Two such fragments can be seen in Plate II, d; some flow lines around the fragments are also visible.

These observations suggest that the breccias were caused by gaseous explosions. Because S_1 -cleavages occur in the breccia, the intrusion of the lherzolites and the brecciation must have taken place before or during the first deformation phase (F_1) of the Alpine orogeny, although also some brecciation took place after F_1 .

Faults

The Mesozoic rocks are separated from the Paleozoic rocks in the south by a large fault: the great North-Pyrenean fault (de Sitter, 1953; de Sitter and Zwart, 1959; 1962), whose plane is subvertical, striking ENE-WSW to ESE-WNW. West of Auzat there is a very wide (200 m) zone of fault breccia: granitic blocks in the limestone and brecciated limestone veins in the granite.

Some of the fragments of shaly marl are elongate, lying parallel to a subvertical striation. The latest large-scale movement along this fault was therefore a vertical one that lifted the axial zone of the Pyrenees, the Mesozoic rocks subsiding. This fault movement must have been active after Albian times but before the Cenomanian, which elsewhere covers the fault discordantly (de Sitter, 1953).

North of the Mesozoic zone lies the external Paleozoic Trois Seigneur Massif. The Mesozoic strata are disposed parallel to the contact, which led Casteras (1933) to think that this contact had not been disturbed. But some movements must have occurred along this plane. The intensive folding of the Mesozoics, for example north of Vicdessos (cross-section 6, Appendix III), must have involved gliding on this plane during the first Alpine folding phase.

Some anticlinal hinges with cores of Liassic marls were probably broken through; this is certainly the case in the northernmost anticline, north of Vicdessos. This fault also originated during the first folding phase.

FABRICS OF THE MESOZOIC COUNTRY ROCKS

ALPINE METAMORPHISM

The Mesozoic rocks in this region are randomly metamorphosed. In some places they show no visible change, in others they have undergone high-grade metamorphism. In some localities the metamorphic minerals have a distinct preferred orientation, in others they are totally unoriented. Ravier (1959) tried to explain this by assuming the occurrence of two metamorphic phases: one dynamic, the other thermal. Lacroix (1894, 1894/95) thought that the latter phase was caused by the intrusion of the lherzolites. The Mesozoic rocks have indeed undergone a high-grade metamorphism near their contacts with the lherzolites, but there are also instances where no such metamorphism near a lherzolite body is evident (Monchoux, 1965), and there are also high-grade rocks with no lherzolites in their vicinity.

The northern zone of this narrow Mesozoic strip can be distinguished from its southern border by three important phenomena. Firstly, the rocks in the north are better recrystallized; secondly, they have undergone strong brecciation, probably due to gaseous explosions; and in the third place, they contain all the lherzolite bodies (Fig. 4). The genetic relationship of these three phenomena will be discussed below.

Calcareous and dolomitic rocks

The Lower Liassic, Upper Jurassic, and Lower Cretaceous limestones and dolomites have been metamorphosed into marbles showing no great mutual differences. The calcite grains seem to have grown larger with increasing grade of metamorphism. This is also, albeit less evidently, the case for the dolomite grains. In some places a limestone bed changes laterally into dolomite. It is not known whether this change is of metamorphic or an older diagenetic origin. In most cases thin sections show that elongate calcite and dolomite grains lie parallel to the S_1 -cleavage.

The same metamorphic minerals are almost always present:

Scapolite. — A sodium-rich scapolite occurs very frequently, showing a black to grey colour caused by

many very small organic inclusions; when weathered it is white. Often the scapolites are concentrated in certain stratigraphic horizons found throughout the Mesozoic sequence. They are developed as short prisms measuring up to 3 cm in length. When there is a definite S_1 -cleavage in the marble they lie with their long axis [001] in this plane, often even parallel to the tectonic B_1 -axis.

Phlogopite. — A colourless uniaxial mica occurs in all the marbles. In some places the mica flakes have a preferred orientation parallel to the S_1 -cleavage, but only in areas where the S_1 -cleavage is strongly developed.

Biotite. — Besides phlogopite, a light-brown biotite is encountered in some grey to black marbles.

Chlorite. — A colourless chlorite occurs mostly in small blebs. It is probably an alteration product of higher-grade Fe/Mg-minerals.

Tremolite. — In some samples tremolite occurs in large quantities as a colourless variety with $2V\alpha$ between 82° and 85° and $\gamma \wedge [001]: 15^\circ-17^\circ$, usually developed as long thin needles, up to 3 cm long, lying in the S_1 -cleavage plane.

Tourmaline. — A dark blue-green tourmaline often occurs, predominantly in zones parallel to the S_1 -cleavage or the bedding plane.

Apatite. — In these rocks apatite with a perfectly idiomorphic shape is a very rare mineral.

Accessories. — Other newly-formed minerals are quartz (rounded grains), titanite, hematite, chalcopyrite, and magnetite. The rounded grains of zircon and rutile are probably of detrital origin.

Liassic marls and limy arkoses

The marls and arkoses of the Middle and Upper Liassic form a very heterogeneous group, constituting an alternating sequence of beds, generally 0.5 to 4 cm

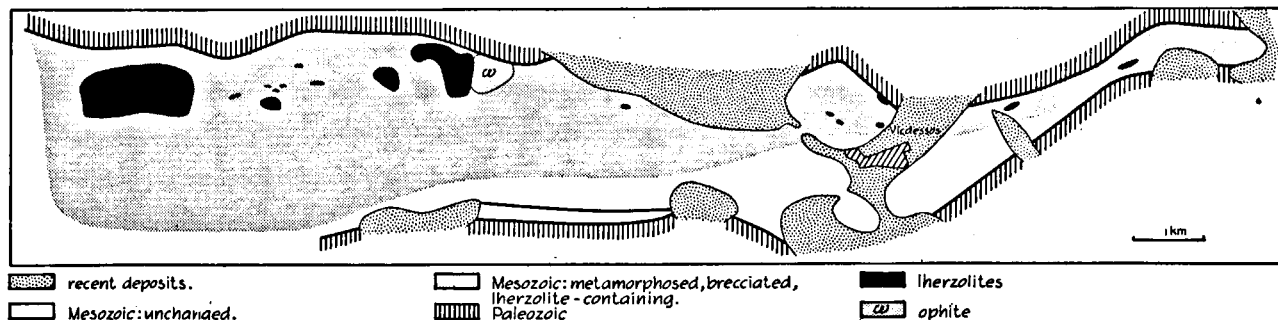


Fig. 4. Simultaneous occurrence of lherzolites, explosion breccias, and metamorphism.

thick, of greyish arkoses and blackish marls. West of Auzat, they show no effects of the Alpine metamorphism. In the northern zone of the region, to the contrary, they contain many neo-mineralizations. In general, they are very fine-grained rocks, the average grain size being 0.1 mm. The metamorphic minerals also have very fine grains; some porphyroblasts are larger, measuring up to 3 mm. Near the contact with the larger Iherzolite body, southwest of Port de Lers, the Liassic rocks show a higher grade of metamorphism, resulting in coarser grains, principally of clinopyroxene. In some places there seems to be a preferred orientation of the minerals parallel to the Alpine S_1 -cleavage, in others they are randomly disposed.

Calcite. — In the limy arkoses, little calcite remained after crystallization of the lime-silicate material. In the limy marls there is far more calcite, but here there are fewer lime-silicates.

Quartz. — Almost all the samples contain quartz, not, as in the limestones, in the form of rounded grains, but as irregular or somewhat hexagonal grains giving rise to mosaic textures.

Plagioclase. — A very calcic plagioclase occurs here: labradorite, bytownite, and sometimes even almost pure anorthite. Twinning occurs by the pericline- and albite-laws. The plagioclase has often developed as porphyroblasts containing many inclusions of the other minerals.

Microcline. — A sometimes cross-hatched alkali-feldspar is often present as very small allotriomorphic grains between the other minerals. These grains are usually concentrated with quartz and plagioclase in thin light-coloured laminae.

Scapolite. — A peculiar observation is that the scapolites occurring in the marls have a much higher birefringence (up to 0.020) than those found in the limestones, indicating a higher calcium content. They are generally concentrated in layers parallel to the bedding, and are allotriomorphic and equidimensional, forming a kind of mosaic texture, an additional divergence from the idiomorphic nature of the scapolites in the limestones.

Phlogopite. — A colourless uniaxial mica occurs frequently.

Biotite. — A light-brown biotite is far more frequent than the phlogopite. In some places it is oriented with the basal cleavage plane parallel to the S_1 -cleavage, in others it has grown perpendicular to this cleavage. In one sample some of these "cross"-biotites show evidence of having been folded and broken along the S_2 -cleavage. Chloritization of biotite took place on a small scale.

β -zoisite. — Colourless β -zoisite grains are in general irregularly shaped, but sometimes they are elongate parallel to their [010]-axis. $2V\gamma$ is about 30° with $r \gg v$. In some places they are found concentrated in zones lying parallel to the bedding.

Clinopyroxene. — In most samples a very light-green clinopyroxene is developed as irregular, equidimensional, very small grains (0.1 mm). In a locality southwest of Port de Lers they show larger sizes, measuring up to 1.5 mm. $2V\gamma$ is about 58° , $[001] \wedge \gamma$ about 40° .

Tremolite. — Colourless tremolite crystals with $2V\alpha = 80^\circ$ and $[001] \wedge \gamma = 12^\circ$ have ragged shapes. Sometimes they are porphyroblastic with many inclusions.

Amphibole. — A light-green to blue-green amphibole is sometimes developed around the pyroxene crystals.

Titanite. — The marls are relatively rich in titanite, which is sometimes irregularly shaped, sometimes idiomorphic.

Tourmaline. — Small dark bluish-green to brown crystals of tourmaline, elongate along their [001]-axis, occur preferentially in zones parallel to the bedding.

Accessories. — Zircon, hematite, and opaque ore minerals occur as accessories.

Albian marls

It is unfortunate that the only outcrops of Albian marls in this region are situated in the southern zone where the Alpine metamorphism was very slight. The alternating sequence of calcareous and shaly beds was very strongly affected by the Alpine deformation, but the only sign that syntectonic metamorphism took place consists of the growth of very fine sericite flakes along the cleavage planes.

FABRIC ANALYSIS

Samples of metamorphic Mesozoic rocks from five localities were subjected to petrofabric analysis. The localities are shown on the map (Appendix I).

Fabric analysis was done in thin sections taken parallel to the horizontal plane or perpendicular to the obvious fold axis. For the latter case, the measured optic or crystallographic directions were rotated into the horizontal plane. Measurements were made in runs perpendicular to the mineral foliation. The orientation data were projected on the lower hemisphere of an equal-area projection, using the Schmidt net. The letter N on the diagrams indicates the geographic north; the horizontal is parallel to the plane of the drawing. The points in the diagrams were counted with the hexagonal counting net of Kalsbeek (1963) instead of the time-consuming free-counter method (Turner and Weiss, 1963). In cases where 200 measurements were made, the 1% contour is represented by a bold line, and the area below the 1% contour is shaded. Where

only 100 measurements were made, the bold line is the 2% contour, the broken line being the 1% contour; the area below the 2% contour is shaded. In some cases more than 200 or fewer than 100 grains were measured. An explanation of the contours is always given in the legend to the diagram.

In most samples the average grain size was measured. To get a three-dimensional picture of the average grain shape, many length-width measurements were made in three thin sections perpendicular to the fabric *a*-, *b*-, and *c*-axes (the *c*-axis was chosen perpendicular to the Alpine *S*₁-plane; the *b*-axis parallel to the fold axis *B*₁, and the *a*-axis perpendicular to *c* and *b*).

Sample L-95-A: Scapolite-tremolite-phlogopite marble (Fig. 5)

This marble contains calcite, scapolite, tremolite, phlogopite, and some chalcopyrite.

Calcite. — The fabric is rather homogeneous: the first 200 grains of calcite measured were compared to a second set of 200 measurements. The differences were

small. Therefore, all 400 measurements of [0001] were used for the diagram. There is an incomplete but rather conspicuous cleft-girdle with an angular radius of 75°, whose axis coincides with fabric *b* and with the regional fold axis *B*₁. No definite maximum is found in the girdle, but rather a minimum near fabric *a*. The *S*₃-cleavage, which is very obvious in the hand specimen, does not seem to have affected the microfabric.

The calcite grains generally have a tabular form parallel to the *S*₁-cleavage, but in this plane there is also a weak elongation parallel to the fabric *a*-axis. The average grain sizes, in the directions of *a*, *b*, and *c*, are 0.7, 0.6, and 0.4 mm, respectively. The stout scapolite prisms and the tall needles of tremolite, which are diamond-shaped in cross-section, seem to have an orientation parallel to the same cleavage plane.

Phlogopite. — In one sample, 193 measurements of {001}-cleavages and 7 of α (= [001]) of phlogopite were made. A 13% maximum was found near the

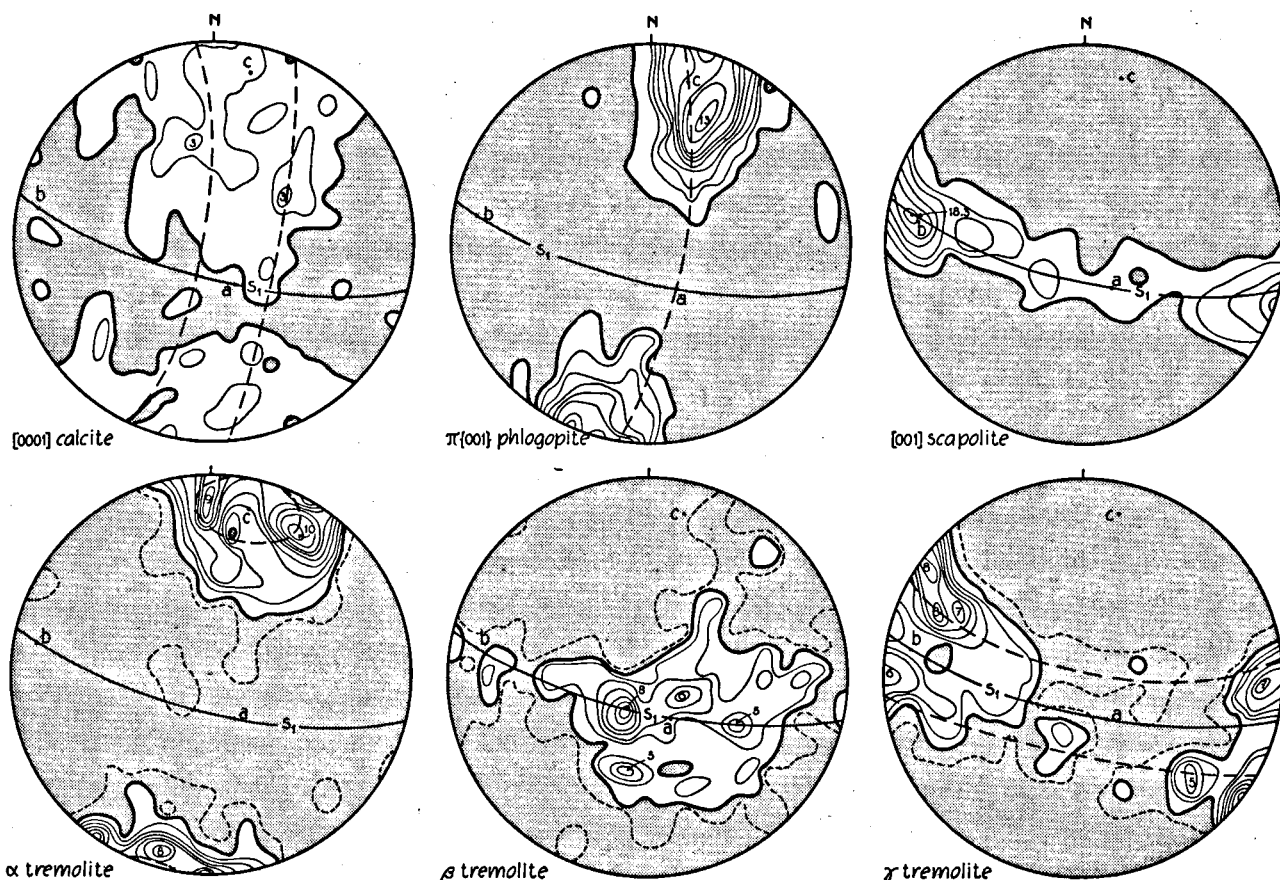


Fig. 5. Scapolite-tremolite-phlogopite marble (Sample L-95-A). 400 [0001]-calcite; contours at 1%, 2%, and 3% per 1% area; dashed lines: cleft-girdle around *b* with angular radius of 75°. 200 poles to {001}-phlogopite; contours at 1%, 2%, 3%, 4%, 5%, 6%, 7%, 8%, 9%, and 10% per 1% area (point-maximum of 13%). 60 [001]-scapolite; contours at 1.6%, 5.0%, 8.3%, 11.6%, 15.0%, and 18.3% per 1% area. 100 α -, β -, and γ -tremolite; contours at 1% (dashed lines), 2%, 3%, 4%, 5%, 6%, 7%, 8%, 9%, and 10% per 1% area. In the α -tremolite diagram a cleft-girdle has been drawn around *c* with angular radius of 17°, in the γ -diagram a cleft-girdle around *c* with an angular radius of 73°.

fabric c -axis. This maximum is somewhat elongated and forms a very incomplete girdle around the tectonic B_1 -axis.

Scapolite. — Only 60 scapolites could be measured in this thin section, but this number seemed sufficient to reveal a pronounced preferred orientation. The [001] of scapolite lies in a girdle in the S_1 -cleavage plane. An 18.3% point-maximum (11 points) in this girdle runs parallel to the tectonic B_1 -axis.

Tremolite. — The optic elasticity axes of 100 grains of tremolite were measured. Many of the grains were too small to permit measurement of {110}-cleavages. The α -tremolite (= X) shows a cleft-girdle pattern with an angular radius of 17° around the fabric c -axis, suggesting that {100} has a preferred orientation in the cleavage plane. The fact that two point-maxima (9% and 10%) in the cleft-girdle lie opposite each other in the fabric bc -plane, suggests that the [001] of tremolite also has a preferred orientation. This is supported by the diagram of γ -tremolite (= Z). γ lies in an incomplete cleft-girdle with an angular radius of 73° around the fabric c -axis. A 7% and an 8% point-maximum lie symmetrically with respect to the fabric b -axis (= B_1) in the bc -plane. β -tremolite (= [010]) has orientation maxima near fabric a , as could be expected from its α and γ orientations. Tendencies toward girdle formation are visible in both the ab and ac fabric planes.

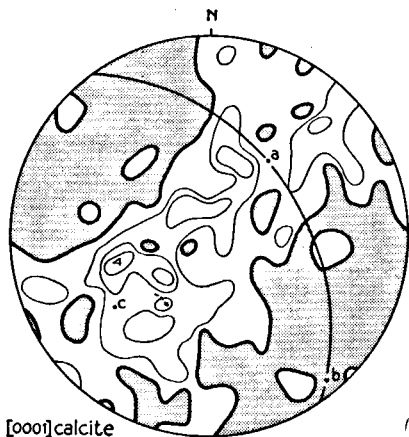


Fig. 6. Scapolite-phlogopite marble (Sample L-38). 200 [0001]-calcite. Contours at 1%, 2%, 3%, and 4% per 1% area.

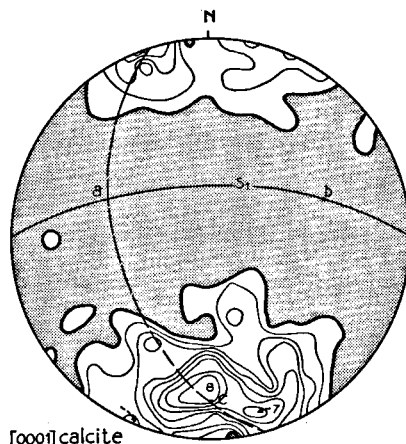
Sample L-38: Scapolite-phlogopite marble (Fig. 6)

This sample shows no clear cleavage plane, but in a thin section there is a pronounced orientation according to the shape of the calcite grains from which a S_1 -plane can be derived. The marble has recrystallized so thoroughly that no vestige of sedimentary banding can be seen.

Calcite. — [0001] of calcite, of which 200 were measured, have a preferred orientation without obvious point-maxima. With some imagination, the girdle

pattern could be considered a cleft-girdle pattern with an angular radius of 75° . The axis of the girdle coincides roughly with the regional B_1 -axis.

The average grain size is about 2.0, 3.3, and 1.0 mm for a , b , and c , respectively, demonstrating a clear elongation parallel to the B_1 -axis. It is evident that the shape of the calcite grains is independent of the crystallographic axes; calcite therefore has a fabric habit.



[0001] calcite

Fig. 7. Phlogopite marble (Sample L-101). 200 [0001]-calcite. Contours at 1%, 2%, 3%, 4%, 5%, 6%, 7%, and 8% per 1% area. S_1 = axial-plane cleavage.

Sample L-101: Phlogopite marble (Fig. 7)

This marble, which also contains some dolomite, phlogopite, rounded quartz, and hematite, has a distinct orientation of platy calcite grains parallel to the S_1 -cleavage.

Calcite. — 200 [0001] of calcite were measured. A preferred orientation is rather clearly visible in the diagram. There is only one point-maximum, of 8%. This maximum is somewhat elongate in the fabric ac -plane.

In the S_1 -plane there is a weak elongation parallel to b . The average grain size is 3.5, 4.0, and 2.5 mm for a , b , and c , respectively.

Sample L-92: Scapolite-phlogopite dolomite (Fig. 8)

This sample of a medium-grained rock consists principally of dolomite, with some calcite, scapolite, phlogopite, an opaque ore mineral, hematite, and some rounded quartz grains. There is a notable orientation of platy dolomite crystals parallel to S_1 .

Dolomite. — A definite cleft-girdle pattern of dolomite [0001] is present. The tectonic B_1 -axis is the axis of this girdle. The S_2 -cleavage is macroscopically visible in this sample, but seems to have no relation to the fabric. This girdle does not contain a definite point-maximum, but there seems to be a relative minimum near fabric c , thus differing from the fabric pattern of calcite [0001] observed in the marbles, whose girdle

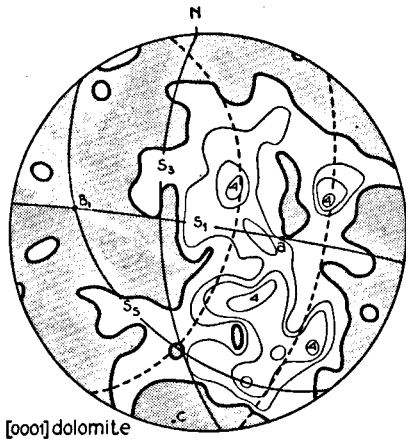


Fig. 8. Scapolite-phlogopite dolomite (Sample L-92). 200 [0001]-dolomite. Contours at 1%, 2%, 3%, and 4% per 1% area. Cleft-girdle around $b = B_1$ with angular radius of 70° .

contains maxima near fabric c and minima near fabric a . This tendency of dolomite is also found in sample V-99-B.

The average size of the dolomite grains is 1.1, 1.1, and 0.5 mm in the directions of a , b , and c , respectively. Therefore, dolomite also displays a fabric habit.

Sample V-99-A and C: Phlogopite marble and Sample V-99-B: Phlogopite dolomite (Fig. 9)

These three samples are from an isoclinal S_1 -fold occurring just east of the village of Sentenac. Sample A is from the northern flank, B from the fold hinge, and C from the southern flank. Sample B comes from the same bed as samples A and C but contains principally dolomite instead of calcite. All three also contain phlogopite, an opaque ore mineral, hematite, and some quartz.

Calcite. — In sample A, 200 calcite grains were measured. Maximum concentration of [0001] occurs perpendicular to the bedding and the S_1 -cleavage, which are parallel here. Two point-maxima are seen, both near fabric c . In the diagram two coaxial small-circles with an angular radius of 75° have been drawn, their axes parallel to the fold axis B_1 . The cleft-girdle pattern observed in the other marbles is not very clear here, perhaps due to the F_3 -phase which could have caused a new preferred orientation: a cleft-girdle with an angular radius of 75° around the vertical B_3 -axis. In sample C, in which 200 calcites were measured, the cleft-girdle pattern with an angular radius of 75° around the fold axis B_1 is far more definite. Two point-maxima (4% and 5%) lie in the cleft-girdles roughly perpendicular to the bedding and cleavage. The B_3 cleft-girdle is less clear.

The calcite grains having average grain sizes of 1.1, 0.9, and 0.7 mm in the directions of a , b , and c , respectively, are much coarser than the equidimensional dolomite, which has an average grain size of 0.2 mm.

Dolomite. — In each of two mutually perpendicular thin sections of sample V-99-B, 200 dolomite [0001] were measured. Both yielded the same pattern. Upon rotation, all 400 were counted and contoured in a diagram. Fig. 8 shows that dolomite [0001] tends to be concentrated in the fabric a direction, whereas the [0001]-axes of calcite are concentrated in the fabric c direction. Here, the same relation is established. There is a very broad maximum near the fabric a -axis. A cleft-girdle pattern around the fold axis B_1 is hardly visible. The other cleft-girdle pattern around the vertical B_3 -axis may be present. It therefore seems possible that here the recrystallization took place not only during the first Alpine phase F_1 but also during the third, F_3 ; this latter fabric, however, is probably developed only very locally.

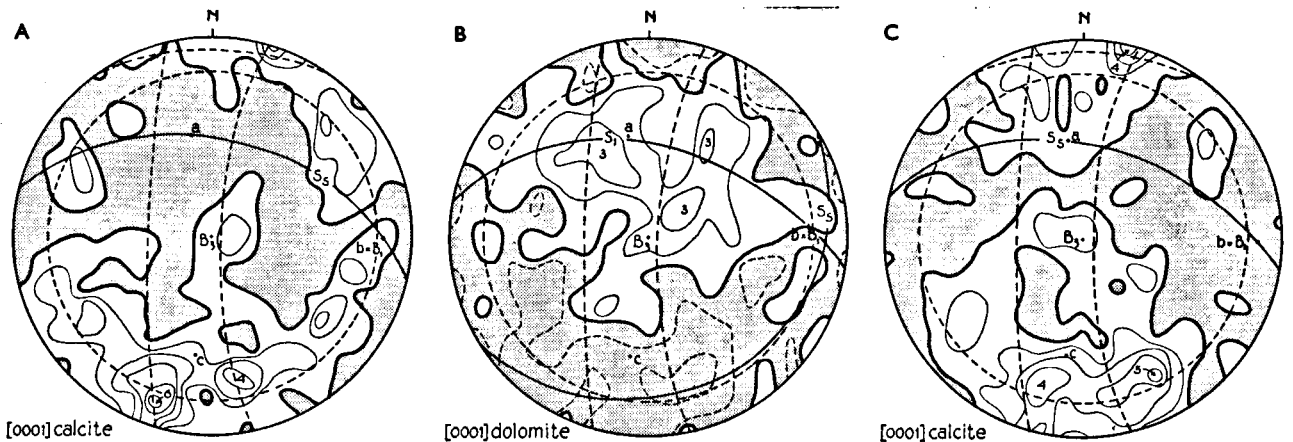


Fig. 9. Sample V-99. A. Phlogopite marble; 200 [0001]-calcite; contours at 1%, 2%, 3%, 4%, 5%, and 6% per 1% area. B. Phlogopite dolomite; 400 [0001]-dolomite; contours at 0.5% (dashed lines), 1%, 2%, and 3% per 1% area. C. Phlogopite marble; 200 [0001]-calcite; contours at 1%, 2%, 3%, 4%, and 5% per 1% area. For all diagrams: two cleft-girdles with angular radii of 75° around $b = B_1$ and B_3 . S_3 = bedding; S_1 = axial-plane cleavage.

CONCLUSIONS

According to many authors (e.g. Lacroix, 1894; 1894/95), the metamorphism in this region is a contact metamorphism caused by the intrusion of the lherzolites and the ophites. In the following chapters it will be shown that the lherzolites were emplaced among the Mesozoic rocks as relatively cold and rigid bodies. Monchoux (1965) has demonstrated that the lherzolite body of Moncaup (Haute-Garonne) has no contact metamorphism at all. The Mesozoic country rock of some lherzolite bodies in the Dépt. des Basses-Pyrénées are not at all or only very slightly metamorphosed (Rio, 1966). It therefore seems impossible to find an immediate link with respect to cause and effect between the extensive Alpine metamorphism and the lherzolites. The ophites are too scarcely represented here to explain all the metamorphism.

Ravier (1959) examined the metamorphism of the Mesozoic rocks of the Northern Pyrenees in an extensive study. He suggested that the crystallization of sericite in the Albian marls was the only result of dynamic metamorphism during the Alpine orogeny. The higher-grade metamorphic rocks often greatly resemble hornfels. He explained their formation as the result of heat flow from fractures in the basement. In the same paper Ravier also suggested that this metamorphism took place before the Alpine deformations, but de Sitter and Zwart (1959), and later Collée (1962) considered it more likely that the metamorphism outlasted the Alpine deformation.

On the basis of the petrofabric data, it is concluded here that most of the Mesozoic rocks underwent a more or less regional metamorphism during the first and strongest phase of deformation (F_1). The calcite and dolomite fabrics are all consistent with the S_1 -cleavage. The most frequent fabric pattern of calcite [0001] has a broad girdle around $b = B_1$ in which minima occur near the ac -plane. It is therefore very likely that this fabric represents a cleft-girdle pattern. In general, the angular radius of this cleft-girdle is 75° . These findings are in agreement with those of Sander (1930), who observed cleft-girdles of calcite [0001] with angular radii between 60° and 80° . Most cases show a point-maximum in the girdle near the fabric c -axis, perpendicular to the S_1 -cleavage, but in some this maximum is split up into two submaxima lying symmetrically with respect to the ac -plane. The dolomite [0001] fabric also seems to have a cleft-girdle pattern around $b = B_1$, but point-maxima lie near fabric a rather than fabric c , as for calcites.

Thus, with the exception of samples V-99-A, B, and C, the fabrics have an orthorhombic symmetry caused by flattening between relatively fixed jaws ("*Einen-gung*" in the sense of Sander, 1948).

The measured grain shape of the calcites and dolomites is also consistent with the F_1 deformation. In all cases a flattening parallel to S_1 occurred. The extension in the S_1 -plane in the direction of the fold axis B_1 ($= b$) does not always exceed that in the a -direction: sometimes the longest diameter of the calcite grains lies

parallel to a , sometimes to b . Calcites and dolomites consistently display a fabric habit.

The crystallization of phlogopite, scapolite, and tremolite (Fig. 5) could have taken place during or right after the S_1 -folding. It must be assumed, however, that in the southern zone the temperature was so low that sericite was the only product of neo-mineralization. The randomly-oriented fabric of some rocks in the northern area suggests that in some localities metamorphism continued after the first and perhaps even after the third phase of deformation, or that the stresses were locally relaxed, perhaps by a gas-release mechanism. The second folding phase is so restricted that it is impossible to relate it to metamorphism. The calcite fabrics in Fig. 9 suggest some recrystallization during the third phase, but at that time the temperature must have been rather low. In the Liassic marls some biotites that grew after S_1 were cleaved and kinked by the S_3 -cleavage. Here, therefore, it seems that the climax of metamorphism was already over during the S_3 -folding, and that the S_2 - and S_3 -cleavages are of the fracture-cleavage type.

The grade of metamorphism in most of the marbles is rather low. Scapolite is not a critical mineral in any metamorphic facies (Shaw, 1960). The scapolitization of plagioclases in some ophites was ascribed by Lacroix (1891) to hydrothermal, and, in a later paper (1916), to ground-water action. The latter hypothesis does not seem very likely, however. The scapolites derived from ophites have optical properties identical to those from the Liassic marls in which scapolites and plagioclases seem to be in equilibrium. This fact and the occurrence in the marbles of Ca-poor scapolites always showing preferred orientations, suggest a syn- or late-tectonic origin attributable to hydrothermal or pneumatolytic action. The latter assumption seems more likely if the associated phenomena were caused by gaseous activity.

Phlogopite seems to be stable over a large temperature range, and thus cannot be a critical mineral (Yoder and Eugster, 1954).

Paired tremolite-calcite is critical for the albite-epidote hornfels and the greenschist facies (Winkler, 1965). It is interesting to note that the northern Liassic marls and limy arkoses generally show a higher grade of metamorphism. These rocks are mostly exposed in anticlinal hinges of isoclinal folds that are often accompanied by faults. It is therefore rather probable that the rate of heat flow was higher here, resulting in higher-grade metamorphic assemblages.

On the other hand, lower-grade assemblages are also found, indicating that equilibrium was not reached. Furthermore, retrograde alterations are present, obscuring the highest stages of metamorphism. Therefore, calcite, tremolite, and diopside sometimes occur together in the same rock. The association of diopside and biotite appears to be critical for the hornblende hornfels facies (Turner and Verhoogen, 1960). The presence of highly calcic plagioclases — up to almost pure anorthite — also suggests a grade higher than albite-epidote hornfels. Scapolite and titanite are not

critical. Zoisite seems to occur not only in the greenschist facies and the albite-epidote hornfels facies, but also in the hornblende hornfels facies (Deer *et al.*, 1962; Winkler, 1965). However, rocks with much diopside developed as large grains show no zoisite, whereas in fine-grained rocks with only a few small diopside grains, the zoisite content is higher.

The occurrence of blue-green hornblende around some diopside grains suggests a retrograde period after the climax of the metamorphism. Part of the zoisite could also be of retrograde origin.

From an outcrop that the present author was unable to relocate, Lacroix (1894/95) described andalusite, suggesting that the metamorphism of this region was of a very low-pressure type. He also found some sillimanite, which indicates either the higher temperature conditions of the pyroxene hornfels facies or the higher partial water pressures of the cordierite amphibolite facies (Winkler, 1965). Sillimanite was also found by Ravier (1959) in other regions. The absence of wollastonite may be explained by high partial pressures of CO₂.

Because of the absence of large igneous masses and because of the tectonite fabrics of the Mesozoic rocks, it may be concluded that the Alpine metamorphism was a very locally-developed "regional" metamorphism. The nature of the metamorphic mineral assemblages implies a very high geothermal gradient. They resemble the metamorphic assemblages of the truly regional dynamo-thermal metamorphism of the Abukuma-type (Winkler, 1965).

In agreement with Ravier (1959), the Alpine metamorphism is best explained by the assumption of an increased heat flow through large fractures in the basement, principally during and after the first phase

of strong orogenic movements. Indeed, the zone of metamorphic rocks is a very narrow but long belt parallel to the great North-Pyrenean fault. It is believed that this fault is a fault zone rather than a single fault. One or another of these faults, which must have extended very far into the basement, served as a conduit not only for the extreme heat flow but also for the lherzolites. This would explain the concentration in this region of all the lherzolite bodies in the zone of the highest grade of metamorphism. Another corroborating fact is the exclusive occurrence in the same northernmost zone of extensive brecciation of the Mesozoic rocks, generally in elongated areas parallel to the E-W-striking structures of the first folding phase (F₁). However, this brecciation outlasted the F₁-phase: some marble fragments in the breccia have a pronounced mineral foliation (S₁), whereas the matrix shows no sign of it.

A general explanation consistent with all these facts is that degassing occurred at deep levels, after which the gas rose along the fractures and caused metamorphism, its sudden release being responsible for the brecciation of the Mesozoic rocks and the emplacement of the lherzolites.

The ophites, which occur as small bodies in the same belt as the lherzolites, are of igneous origin and have typically igneous textures. Monchoux (1965) recorded contact metamorphism around some ophites near Arguénos (Haute-Garonne) in limestones showing no signs of thermal metamorphism at all at the contact with the lherzolites. As can be seen on the map (Appendix I), there are only a very few small bodies of ophite in this region; they could not have been responsible for the Alpine metamorphism in the whole region.

CHAPTER IV

LHERZOLITES AND RELATED ULTRAMAFIC ROCK TYPES

PETROGRAPHY

General character

On most of the geological maps made by previous workers, the intrusive rocks in this region are divided into two types: lherzolites and ophites. While ophites are wide-spread throughout the Pyrenees, occurring in Mesozoic as well as in Paleozoic rocks, lherzolite bodies are encountered only in a very narrow belt of folded and sometimes metamorphosed Mesozoic rocks north of the great North-Pyrenean fault. No lherzolites occur outside this belt. Most writers saw a close relationship between these two types of rock. Structurally, however, the differences between them are greater than the resemblances, which led the present author to separate them. A brief description of the ophites is given at the end of Chapter V.

The area described here contains numerous small and a few larger lherzolite bodies. From east to west,

the small bodies are found as follows: one west of Lercoul, one north of Sem, four north of Vicdessos, one in the Bois de Soubrouque, and many southwest of Port de Lers, having diameters ranging from a few centimetres — these are in fact inclusions in the limestone breccia — up to some fifty metres. Of the larger bodies, one is found in the Forêt de Freychinède, one southeast of Port de Lers, and, of course, the one that is the type locality of the lherzolites, around the Etang de Lers.

One of the most striking features of the lherzolites is that they are all concentrated in the northernmost zone of the Mesozoic belt, narrow as this belt is, and that it is just in this zone that the rocks have undergone a strong brecciation and a relatively high-grade metamorphism. In the present writer's opinion, these three phenomena are genetically interrelated, although the emplacement of the lherzolites itself did not cause the other two.

Another common feature is the external form of the lherzolite bodies. They are always lenticular, oval, or rectangular, with their longitudinal axis parallel to the Alpine S_1 -structures of the country rock. An apparent exception on the map (Appendix I) is the lherzolite of the Forêt de Freychinède, but this body is possibly composed of various separate entities. The degree of exposure is so poor that this point cannot be demonstrated.

The lherzolite bodies also contain other ultramafic rocks, but lherzolite is by far the most important rock type. The most striking structural feature is the parallel banding occurring in almost all of the bodies (Plate V, c). This banding or layering generally consists of alternating layers of lherzolite and spinel pyroxenite. Whereas the lherzolite layers vary in thickness, the spinel pyroxenite layers are mostly only a few centimetres thick, rarely measuring as much as 30 or 40 cm. In some places this layering consists only of concentrations of spinel or clinopyroxene grains, or both, in very thin layers. These laminae are always parallel and seem to be very continuous.

The ultramafic bodies also have in common the presence of lherzolic breccia, mostly concentrated at the contact with the limestones. Some of the small bodies consist exclusively of this breccia.

The larger bodies, e.g. from the Forêt de Freychinède and the Etang de Lers, contain other types of ultramafic rocks besides lherzolite, spinel pyroxenite, and lherzolic breccia. Parallel to the described layering are some thick bands whose clinopyroxene and spinel content is very low. This type may be called a harzburgitic lherzolite, and is in fact only a variety of lherzolite.

The lherzolites furthermore contain numerous dykes, sometimes concordant but often discordant to the layering. These dykes are made up of many different types of rock: garnet pyroxenite in many variations, garnet-plagioclase pyroxenite, pyroxene hornblendite, and biotite hornblendite.

Serpentinization is generally very weak and is concentrated along fracture zones or cleavages. The lherzolite body of Lercoul, however, is strongly serpentinized.

Lherzolite

The most important member of the ultramafic rocks in the Northern Pyrenees is of course lherzolite. Lherzolite bodies are easy to distinguish in the field because they carry a very scanty vegetation (there are exceptions to this, however; the lherzolite bodies of Prades are heavily timbered, while the surrounding Mesozoic marbles are not). If they are only slightly or not at all serpentinized, these bodies are recognizable from great distances because of their orange to wine-red colour against the white or grey of the marbles. The serpentinized lherzolite bodies are green to black and are therefore less easily recognizable from a distance.

Furthermore, erosion led to totally different aspects, so that the lherzolite bodies can be mapped with field-glasses. An excellent example is the Etang de Lers body (Plate III). Whereas the calcareous rocks have a typical karst topography, the lherzolites weather to rounded boulders. Strongly serpentinized lherzolites decompose into very small fragments rather than boulders.

In a fresh hand specimen, no distinct minerals are recognizable; the rock seems to have a homogeneous blackish-green colour. On weathered surfaces, however, most of the constituent minerals are easy to distinguish: the emerald-green clinopyroxenes, the bronze-brown orthopyroxenes, and the black spinels. None of these minerals shows much weathering. Only the olivines are weathered and changed into a powdery yellow to orange material easily removed by erosive action, so that the other minerals generally protrude above a yellow background. The soil locally covering the lherzolite has the same orange colour.

In general, the lherzolite is medium-grained, but in places it contains much coarser grains of all four minerals. The elongation of all grains, mostly parallel to the layering, can be distinguished with the naked eye. Serpentinized surfaces cut across the rock in several directions, but the zones of serpentinization are rather narrow. Whereas olivine, clinopyroxene, orthopyroxene, and spinel are recognizable with the naked eye, hornblende and the opaque ore minerals are only distinguishable in thin sections. The lherzolites contain 45% to 85% by volume of olivine, 10% to 35% orthopyroxene, 5% to 20% diopside, and 1% to 6% spinel, with hornblende and opaque ore minerals as minor accessories. These great differences in mineralogical composition are caused by the layered structure of the lherzolite. Macroscopically, in some the pyroxene content increases in distinguishable bands and the olivine content decreases. In others, to the contrary, olivine predominates and the pyroxene content decreases. Spinel enrichment generally occurs in pyroxene-rich layers. The content of serpentine was not measured. In most cases only the olivines are serpentinized along cracks, the pyroxenes being fresh. Sometimes, when the serpentinization is strong, the orthopyroxenes are also serpentinized, however slightly. A brief description of the mineral components of lherzolite is given below. Lacroix described them in detail in 1894. French geologists are presently working on their mineralogy and chemistry.

Olivine. — The olivines have a very light olive-green colour, but in thin sections they are colourless. They are totally xenomorphic; yet in thin sections they show mostly the same elongate cross-section, generally parallel to the layering. The boundaries of an olivine crystal are very irregular, however. In almost all of the samples strong tectonic influence on the texture is apparent. There are many kink bands parallel to {100}, which themselves have an undulatory extinction. Differences in extinction between two adjacent kink bands can be as high as 60°. The {010}-

cleavage is rather well developed. In many samples a large number of measurements of the optic angle were performed. The same value was consistently found: $2V\gamma = 87^\circ$. The olivines are therefore very homogeneous, not only in the Etang de Lers occurrence but also in the other bodies. According to Kennedy's graph (1947), the olivines have a composition of $Fe_{96}Fa_4$. A chemical analysis quoted by Collée (1962) gave $Fe_{92.3}Fa_{7.7}$.

The olivine grains are frequently fractured by constantly recurring cleavage systems. Along these planes only fracturing took place, usually without mylonitization or granulation. When the olivine grains are serpentinized, it is just along these planes. There are also shear zones with very fine-grained, granulated, and mylonitized olivines; these granulated zones are never serpentinized.

Orthopyroxene. — Many measurements of the optic angle gave a constant value of $2V\gamma = 81^\circ$, which points to an enstatite of the composition $En_{91}Fs_9$. Collée (1962) obtained almost the same value: $En_{91.2}Fs_{8.1}$, from a chemical analysis. The enstatite grains are a light bronze-brown in hand specimens, and in thin section colourless or very pale pink. Almost all the grains contain exsolution lamellae of clinopyroxene parallel to $\{100\}$, the lamellae having $[010]$ and $[001]$ in common with the host. Kink bands lying roughly parallel to $\{001\}$ are very common. Often the grains are also contorted.

In general, the enstatite grains are coarser than those of diopside and olivine. They are xenomorphic with very irregular boundaries. Enstatite is often concentrated together with spinel in zones lying parallel to the layering.

Clinopyroxene. — The emerald-green clinopyroxene grains are best recognized on a weathered surface. In thin sections they are a very pale green. No pleochroism is visible. The optic angle $2V\gamma = 61^\circ$ is rather constant. The extinction angle $\gamma \wedge [001] = 39^\circ-42^\circ$ seems to be slightly variable. A chemical analysis quoted by Collée (1962) shows that the clinopyroxene is a Cr-diopside containing some sodium. Some dispersion on optic axes occurs with $r > v$. $\{100\}$ twins occur. Exsolution lamellae parallel to $\{100\}$ are made up of enstatite having $[010]$ and $[001]$ in common with diopside. The cleavages parallel to $\{100\}$, $\{010\}$, and $\{110\}$ are all well developed.

The grain form of diopside is also very irregular. Almost all the grains are contorted or broken up, but less so than the olivine grains.

Diopside grains are less elongate or tabular than olivine. Often the diopside content increases in zones where orthopyroxene and spinel are concentrated.

Spinel. — Very irregular, xenomorphic spinel grains are in general evenly distributed in the lherzolite. In some places neat octahedra were found (Sandberger, 1866, *vide* Lacroix, 1894). Sometimes the spinel is concentrated with enstatite in very fine laminae or

thicker bands parallel to the layering. In hand specimen they are black, in thin sections brown, olive-brown, or olive-green. This is a Cr-spinel or picotite, according to the chemical analysis given by Lacroix (1894).

According to Lacroix (1894), the four foregoing minerals all have liquid or two-phases inclusions.

Hornblende. — All of the samples contained hornblende, but in very small quantities, as small xenomorphic grains with a pleochroism of light-brown (γ) to colourless (β , α). The optic angle is $2V\alpha = 89^\circ$. The extinction angle is $\gamma \wedge [001] = 7^\circ-10^\circ$. The hornblende sometimes occurs as a rim around diopside, suggesting a secondary origin; in other cases a primary origin is conceivable.

Serpentine. — The only lherzolite body showing very strong serpentinization is that of Lercoul. The other occurrences are only slightly serpentinized. Serpentinization took place along planes of mostly Alpine cleavage systems. In general, only the olivines are serpentinized. The thin veinlets of serpentine are often zoned parallel to the boundary containing some varieties of serpentine.

Ore minerals. — In places where serpentinization was stronger, small opaque ore minerals were developed. Babkine *et al.* (1966) have described the opaque minerals from the lherzolites and pyroxenites. Pentlandite, pyrrhotite, and chalcopyrite are the most frequent sulphide ore minerals. Ilmenite occurs in fresh samples; magnetite and chromite occur in serpentinized samples. The pyroxenites contain more and coarser ore minerals than the lherzolites.

The optic properties of the minerals of the lherzolites seem to be very constant in all bodies in the Pyrenees. This means that the chemical composition of the minerals will show little variation. The composition of the lherzolites is more variable, because of differences in the quantities of olivine and pyroxenes. All the grains are xenomorphic and have very irregular boundaries. In general, the grains are tabular or elongate in directions parallel to the layering. The strong deformation of the grains (undulatory extinction, kink bands, granulation zones, cleavages) precludes the establishment of a crystallization sequence.

Harzburgitic lherzolite

Parallel to the spinel pyroxenite layering are some continuous bands with a composition differing slightly from the normal lherzolite. These bands attain thicknesses of some twenty metres. In the field they are easily recognizable by their weathering; they are orange-yellow instead of dark-red. Clinopyroxene and spinel grains are far less conspicuous; the enstatite content is the same or even greater than that of the normal lherzolites. Thus, this lherzolite tends to be a harzburgitic variety. The minerals have the same optic properties as those found in the normal type.

The harzburgitic lherzolite is far more deformed than the normal type. Layers of spinel pyroxenite are present, but they are very strongly deformed. In general, pencil-shaped spinel pyroxenite bodies lying parallel to the layering occur more often than continuous layers such as are predominant in the normal lherzolite (Fig. 26). Serpentinization had a much stronger effect in these rocks.

Spinel pyroxenites

Thin layers ranging in thickness from several millimetres up to 40 cm or more but usually 2 to 4 cm thick occur in all lherzolite bodies. Running roughly parallel, they are very continuous, often throughout the whole body. These layers are composed of a green spinel pyroxenite, which Lacroix first called "pyroxénolites" (1894) and later (1901) "ariégites pyroxéniques normales".

The spinel pyroxenites are much coarser than the lherzolites and show much less deformation. They are also more resistant, so that on weathered surfaces they seem to protrude. The thickness of these layers is often constant, but may vary to form lenticular bodies. In fold hinges they may attain great thickness, and they become very thin in fold flanks.

These spinel pyroxenites contain principally diopside, with less enstatite and accessory spinel; some secondary hornblende is also present. As in the lherzolites, all grains have irregular boundaries and are xenomorphic. In thin sections a slight elongation in the shape of the grains is recognizable, the longitudinal axis being parallel to the layering. However, they are not as elongated or tabular as in the lherzolites. These layers are much less deformed internally than the lherzolites. Kink bands are still present in the pyroxenes, but granulation is absent.

Clinopyroxene. — The clinopyroxenes at the boundary with the lherzolite have the same emerald-green colour as in the lherzolites, but in the centre they are greyish-green and in thin sections colourless. Nevertheless, they seem to have the same optical properties: $2V\gamma = 61^\circ$ and $\gamma \wedge [001] = 39^\circ - 43^\circ$. Lacroix (1901) thought that the clinopyroxenes in the central part of a layer contain less Cr. The clinopyroxenes often contain exsolution lamellae of enstatite.

Orthopyroxene. — This is an enstatite with the same composition as in the lherzolites.

Spinel. — All varieties are present. In general, the spinels are olive-green, but sometimes they are brown or blue-green. In the last case the spinels are Fe-rich, a pleonast according to Lacroix (1901).

Garnet pyroxenites

The lherzolite bodies of the Etang de Lers and the Forêt de Freychinède contain several sills of garnet pyroxenite (see map, Fig. 12). These sills lie almost

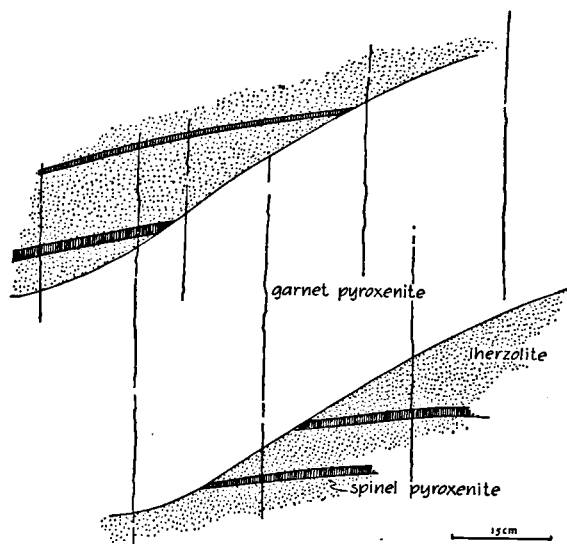


Fig. 10. Dyke of garnet pyroxenite, cutting across the spinel pyroxenite-lherzolite layering. Location: on the border between subareas II and III of Fig. 12.

parallel to the layering, but in one instance a cross-cutting dyke-like relationship has been established (Fig. 10). These dykes are in fact composite sills, because a distinct zoning parallel to the boundary is present. These sills are generally 30 to 40 cm thick, but in some places they bulge into lenses.

Thin sections through one of these sills near the Etang de Lers (hand specimen L-34; see map, Fig. 12) show symmetrical zoning. The 1.5 cm thick external zone against the lherzolite is a spinel orthopyroxenite (the "bronzitite" of Lacroix, 1894), containing enstatite and, as accessories, Cr-diopside and brown spinel. The next zone is a 5 cm wide spinel diopsidite, containing the same emerald-green Cr-diopside with a little enstatite and a grass-green spinel. Within a space of 0.5 cm the spinel changes colour from brown to grass-green. The central and thickest zone consists of garnet (spinel) diopsidite (the "ariégite pyroxénique à grenat" of Lacroix, 1901; or internal eclogite of Eskola, *in* Barth, Correns, and Eskola, 1939). This rock type is composed mainly of the same diopside and a pink pyrope-rich ($n = 1.74$; $a_0 = 11.54$) garnet. The garnet occurs as a rim around the green spinel. The centre of the sheet lacks any trace of spinel. In some instances a small amount of enstatite may also be present in this inner zone. The mineralogical composition of the pyroxenes is always the same as described above.

Along some cleavage planes, retrograde metamorphism has taken place. Keliphitic rims have developed around the garnet. These contain small vermicules of clinopyroxene, green spinel, a very calcic plagioclase, and rarely some chestnut-brown hornblende.

Garnet-plagioclase pyroxenite

In the first small saddle west of the highest peak of the lherzolite crest of the Etang de Lers, occurs a 30 cm thick dyke cutting discordantly across the spinel

pyroxenite layers. This dyke strikes E-W and dips 25° to the north. It is composed of a dark-brown rock with some white patches in which pink-coloured garnets are immediately recognizable. This rock shows some resemblances to the garnet pyroxenite. It contains principally garnet and clinopyroxene. The clinopyroxene, however, is a light-brown variety which is almost colourless in thin sections. A calcic plagioclase occurs frequently, not only as vermicules around garnets but also in coarse grains between them. Hornblende and biotite occur, both being strongly pleochroic from chestnut-brown to almost colourless. Accessory minerals are a grass-green spinel and opaque ore minerals; in cracks some serpentinous matter occurs. Deformation affected the rock strongly: the cleavages of the clinopyroxene and the plagioclase twins are exceptionally contorted, and all the crystals show strong undulatory extinction.

Hornblendites

Hornblendite dykes, veins, and veinlets cut across all the previously described rocks. In general, their thickness varies from several millimetres to several centimetres, but in some places they are much thicker, reaching several decimetres. The dykes have no preferred direction of strike or dip; sometimes they run parallel to the spinel pyroxenite layers, suddenly cutting across them over short distances and then becoming parallel again. In general, however, they cut across the layering at a wide angle. These dykes may split up in two or more branches or disappear suddenly; they are never continuous over long distances.

This rock is black and very coarse-grained. Hornblendes measuring some cm in length are easily recognizable. Thin sections reveal that there are two varieties of hornblendites, one with hornblende and light-brown clinopyroxene (the "ariégite pyroxénique et amphibolique" of Lacroix, 1901), and a second type with hornblende and chestnut to reddish-brown biotite (the "hornblendite" of Lacroix, 1901). All transitions between these two types are present. Both types contain some opaque ore minerals as accessories. All grains show signs of strong deformation.

The hornblendites are the youngest dykes belonging to the probably igneous suite that is genetically related to the lherzolites. Lacroix described another variety, containing garnet, which the present author has not encountered.

Breccias

There are two types of lherzolite breccia, with some transitional forms. One of these types will be called normal breccia, because it occurs far more frequently than the second type, which is a tectonic breccia.

Normal breccia. — An important phenomenon shared by almost all lherzolite bodies is an outer rim of normal breccia. In some places this breccia also occurs in zones lying parallel to the E-W- and N-S-striking

Alpine structures in the centre of a lherzolite body, as is clearly shown on the map of the Etang de Lers (Fig. 12).

The normal breccia consists of angular or somewhat rounded fragments of lherzolite and all the associated rock types (even of the youngest hornblendites), sometimes even of limestone (Plate IV). The inclusions are found in all sizes, from several millimetres to several decimetres, generally averaging 10 cm. The lherzolite fragments often show layers of spinel pyroxenite and mineral foliation with a random orientation (Fig. 23, a). The matrix is very fine-grained; microscopic examination reveals broken and splintered grains of diopside, enstatite, spinel, and calcite, and many serpentine blebs with mesh texture and sometimes a core of olivine. Thus, the matrix is a strongly serpentinized lherzolic microbreccia with some contamination from the calcareous country rock.

Lacroix (1894/95) thought that this breccia was of sedimentary origin. In a later paper (1901) reporting definite evidence to the contrary, he suggested that it was a tectonic breccia. There are no indications to support this assumption, however: the matrix is rather homogeneous without mineral foliation; the fragments are not elongate; there are no slickenside structures. Furthermore, it is not a magmatic intrusion breccia, since magmatic traces are totally lacking. Ravier (1959) concluded that it was an explosion breccia. The present author also thinks that this is the best explanation. The lherzolite bodies occur as elongate plugs parallel to the Alpine structures in the Mesozoic rocks. The fact that the outer zone is almost always brecciated suggests that this brecciation took place during the emplacement of the solid lherzolite bodies.

It is interesting to compare these breccias with those of southwestern Greenland described in detail by Bondesen (1964). Dykes and zones of breccia are disposed parallel to the regional structural trend. The breccia contains many fragments of the country rock and of ultramafic rocks. The matrix is a microbreccia, containing the same minerals — in crushed and broken fragments — as the country rock. There is no evidence of magmatic action. Bondesen therefore concluded that the breccia was emplaced by some kind of gaseous action, perhaps as a fluidized intrusion breccia, in the sense described by Reynolds (1954).

Green (1961) described peridotite breccias from the Papuan Ultramafic Belt. These breccias greatly resemble the Greenland type, and Green also suggests that their origin may be ascribed to fluidization by volcanic gasses. However, he thought the brecciation had occurred after the emplacement of the peridotites, whereas in Greenland the ultramafic inclusions are assumed to have been brought up by the fluidization.

In an extensive paper Reynolds (1954) gave many examples of breccias that she thought to have originated by fluidization. Fluidization, as she described it, is analogous to an industrial process in which gasses are passed through a bed of fine-grained solid particles to facilitate chemical reactions. At a certain velocity

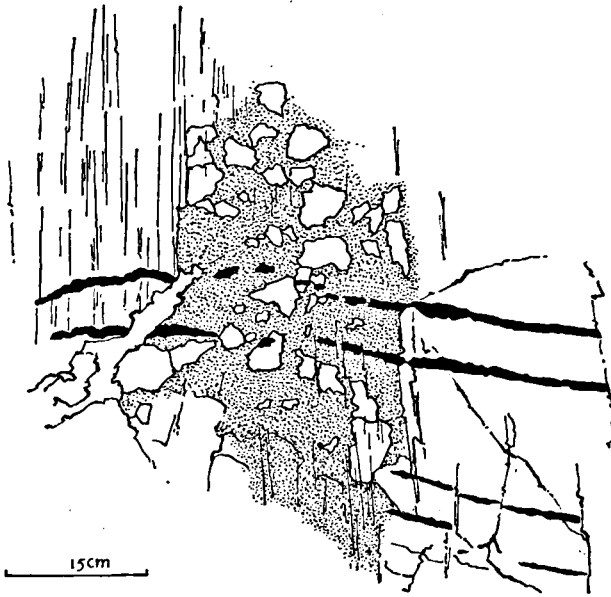


Fig. 11. An E-W-striking zone of a tectonic breccia along the Alpine S_1 -cleavage. The lherzolite of the Etang de Lers, near L-53. (White = lherzolite; black = spinel pyroxenite; stippled = microbreccia.)

of the gas flow, the bed expands and the particles begin to move. At higher velocities, gas bubbles form and travel upward, at which the bed becomes fluidized. At still higher velocities, the particles are transported by the gas ("boiling bed"). In these fluidized systems, conditions are ideal for chemical reactions between gas and solid.

The breccia rim of the lherzolite bodies does not always have the same thickness. The map of the occurrence at the Etang de Lers shows that it may measure as much as 150 metres, but sometimes the rim is lacking altogether. It is important that the boundary of the body as a whole is a very sharp and straight or somewhat arcuate line. Near the outer border the lherzolite breccia contains more limestone inclusions, whereas the limestone breccia surrounding it is richer in lherzolite fragments near its inner border. Nevertheless, the border is marked very sharply. It is believed here that this picture is best explained not by fluidization but by an explosive emplacement. Some serpentine-limestone breccias in Italy, which greatly resemble the present breccias, have been described by Bailey and McCallien (1960), who concluded that they were explosion breccias. Additional brecciation may have been caused by fluidization immediately following this emplacement. The origin of the E-W- and N-S-striking zones of the breccia lying parallel to the Alpine S_1 - and S_3 -cleavages could be interpreted in this manner.

The limestone breccia contains limestone and some lherzolite fragments (even when the main lherzolite bodies are far away) embedded in a fine-grained, pink calcareous matrix. The over-all structures of the limestones are preserved, even when the rock is totally brecciated. The shattering effect of the explosion

brecciated the whole rock without transporting material any great distance, except for the lherzolite fragments which could, however, have been blasted away from the main bodies. The material seems to have been sufficiently plastic to permit flow: some concentric lines around lherzolite fragments (Plate II, d) in the limestone breccia resemble flow structures.

In the lherzolite bodies, but also outside them in the limestone, there are dykes of lherzolititic microbreccia. These dykes show an irregular, meandering form. They have the same mineralogy as the other microbreccias. In some places they are homogeneous, but elsewhere they are layered parallel to the wall rock, showing some sort of graded bedding. These dykes could be explained by fluidization.

Tectonic breccia. — The second type of breccia is tectonic, and has nothing to do with the solid intrusion of the lherzolites because it originated after their emplacement during the first or third Alpine phases (F_1 or F_3). The tectonic breccia is developed in narrow vertical E-W- and N-S-striking zones at places where the cleavage is locally intensified (Fig. 11). Plate V, b shows that two vertical sets of cleavages, which make a small angle with S_3 , sometimes also played a role in the formation of the tectonic breccia. It is conceivable that later fluidization occurred preferentially in these brecciated zones, giving rise to transitional types.

STRUCTURAL ANALYSIS OF THE LHERZOLITES

General remarks

As has already been mentioned, all lherzolite bodies have an elongated form, either oval or rectangular. The longitudinal diameter is always parallel to the Alpine structures of the first folding phase (F_1). All lherzolite bodies show a banding caused by parallel layers of spinel pyroxenite. This layering is never parallel to either the contact or the Alpine structures. Comparison of the layering in the several bodies shows no consistent pattern: the attitudes of the layering planes are totally random in the different bodies. Lacroix (1894) and Longchambon (1912) thought that all lherzolite bodies were connected to each other at deeper levels, but structurally this seems impossible.

Lherzolite of the Etang de Lers

The lherzolite body of the Etang de Lers (Fig. 12) has a somewhat rectangular outcrop whose longitudinal axis measures about 1600 m and strikes ESE-WNW, parallel to the Alpine F_1 -structures. The width is about 700 m.

The contact with the surrounding Mesozoic rocks often resembles a fault contact. It is always a sharp line, straight or arcuate. The country rock, however, shows no indications of a true fault. The synclinal form of the Cretaceous rocks is hardly faulted.

A remarkable fact is that almost the whole body has an outer zone of lherzolititic breccia of variable thickness (Fig. 12). The surrounding marble is also

brecciated. This breccia has been described in the preceding section. The most important structure of the lherzolite is the parallel banding or interlayering of lherzolite and spinel pyroxenite. In the body of the Etang de Lers the strike of this layering is not uniform. In the west it strikes N-S, and in the east almost E-W. It is in any case evident that this layering is always discordant with respect to the contact of the lherzolites and also to the Alpine structures of the country rock.

For this study, the Etang de Lers body was divided into nine structurally almost homogeneous subareas (Fig. 12). As many measurements of the layering as possible were made in each subarea. Fold axes and fold mullions were also measured. Because of the scarcity of fold hinges, only a few fold axes could be measured. Therefore, β -diagrams of the layering planes were made. Many sets of cleavages are present. In most cases they are of the fracture-cleavage type. Cleavages and joints differ in that cleavages are rather regular, very closely spaced (some mm) fractures, whereas joints are always very widely spaced. The strike and dip of cleavages change during the transition between lherzolite and spinel pyroxenite. In each subarea, 100 cleavages were measured.

Cleavages. — The poles to the 100 cleavage planes measured in each subarea were plotted on the lower hemisphere of an equal-area net. The resulting nine diagrams are shown in Fig. 13. It is evident that there is a preferred orientation in each diagram. Most obvious are two sets of cleavages that do not rotate clock-wise from west to east, as does the layering, but constantly have the same strike and dip. The weaker of the two is the E-W- or ESE-WNW-striking subvertical set of cleavages. The stronger one is the N-S- or NNW-SSE-striking subvertical set. Both these sets are visible almost everywhere at Lers. In general, they have fractured the rock along very narrowly-spaced planes.

Often, a maximum in the π -diagrams is split up into two peaks. Sometimes the maxima are very wide, giving rise to partial girdles. This is not caused by regional rotation. In an outcrop the strike of a cleavage can often be seen to change considerably over a short distance. The deviations therefore appear to be of no importance. These cleavages are sometimes also found in the lherzolithic breccia and microbreccia. If the breccia resulted from the emplacement of the lherzolites and this occurred during or just before the first Alpine deformational phase (pages 6 and 17-18), it follows that these two sets of cleavages must be of Alpine age. The weaker (E-W) set corresponds to the F_1 deformation, the stronger (N-S) to F_3 .

These cleavages are often planes on which serpentinization occurred preferentially. Thin sections show clearly that these cleavages cut across all grains, almost without contorting or crushing them. Only in olivines did the serpentinization take place along the cleavages. Sometimes, however, movement took place along the cleavages. In those cases, brecciation and granulation are evident. This type of breccia has been

referred to above as tectonic breccia. In the north-western sector of each diagram there is another maximum, corresponding to a set of cleavages dipping 20° to 50° to the southeast. This maximum rotates clockwise from west to east (diagrams I to IX). In general, this cleavage (to be referred to henceforth as S_0) runs almost parallel to the layering. The rotation of the average pole to the S_0 -cleavage from west to east is identical to the rotation of the layering.

The S_0 -cleavage and the layering therefore seem to be older structures having nothing to do with the Alpine orogeny. In thin sections it is evident that the S_0 -cleavage is older than the two other sets (S_1 and S_3).

Pre-Alpine folding. — In previous chapters it has been argued that the emplacement of the lherzolites took place in the beginning of the Alpine orogeny. To determine the pre-Alpine structural history of the ultramafic rocks, the Alpine structures in the Mesozoic country rock were examined. The Alpine S_1 - and S_3 -cleavages are also present in the ultramafic rocks, but the other structures — the S_0 -cleavage and the layering (S_L), both of which are always discordant with respect to the contact and to the Alpine structures — are absent in the country rock. According to this evidence, these structures are internal pre-Alpine structures. The layering of the ultramafites has been folded. This can be seen in all bodies. These folds were measured systematically only in the bodies at the Etang de Lers and the Forêt de Freychinède.

In the ultramafic body of the Etang de Lers the folds are usually small, asymmetrical, and isoclinal (Fig. 16 and Plate V, c), but exceptions are found. Without exception, these asymmetric folds are overturned, the axial plane, which usually coincides with the layering, dips to the southeast, and the southeastern limb overlies the northwestern limb. These folds could therefore be shear folds, caused by overthrusting of the southeastern limb over the northwestern. But it is also possible that the small ones are parasitic folds (de Sitter, 1958) of a larger fold of which only the southeastern limb is visible.

In Fig. 14, pole-diagrams of the layering are given for each of the nine subareas (see map, Fig. 12). The diagrams do not show contours because of the small number of measurements. Some fold axes and fold mullions, measured directly in the field, are also given. All the diagrams reveal a distinct point-maximum, and a weak girdle is generally present. This pattern is very normal for isoclinally-folded areas. A clockwise rotation from west to east is visible, not only of the π -maximum but also of the fold axes. The fold axes have wide variations in orientation. This is not abnormal for isoclinal folding of a non-homogeneous body.

To obtain a more detailed picture of the folding, β -diagrams were made for the nine subareas (Fig. 15). All the diagrams show a girdle pattern parallel to S_0 and S_L , which is in keeping with the isoclinal nature of the folds. The significant point-maxima of 7% or more are consistent with the fold axes. The clock-wise

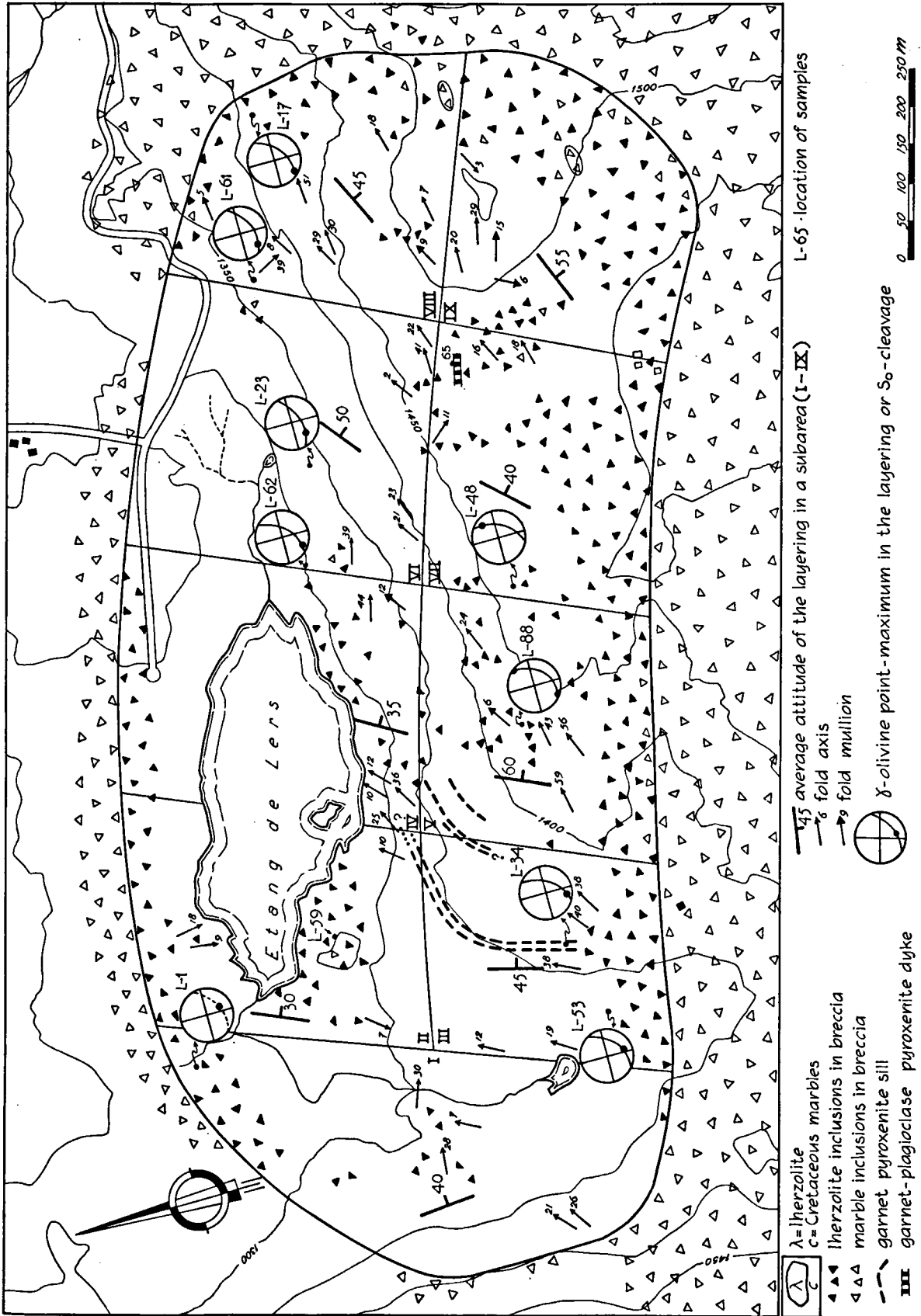


Fig. 12. Map of the Iherzolite of the Etang de Lers.

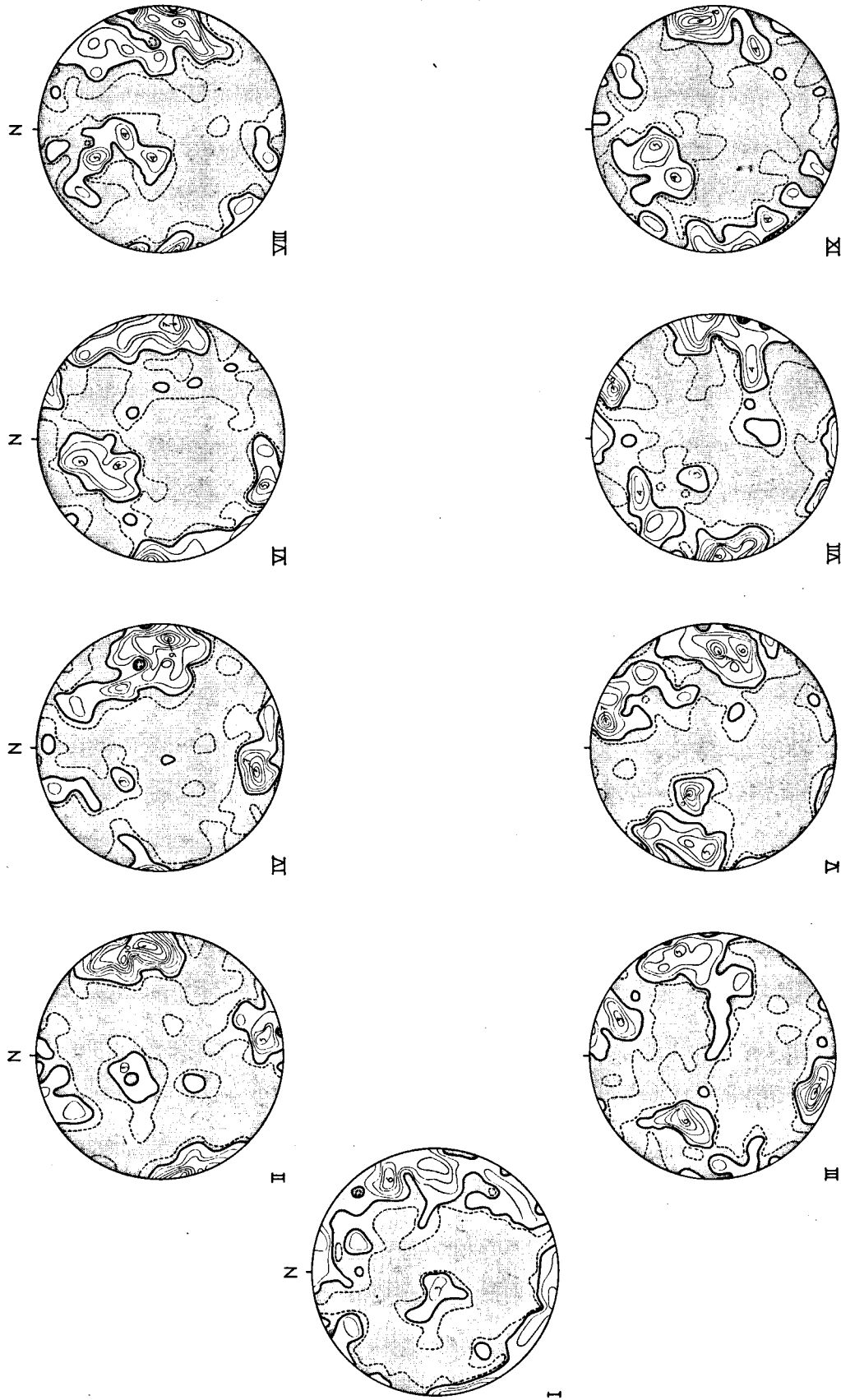


Fig. 13. π -diagrams of 100 cleavages for each of the nine subareas (see Fig. 12) of the lherzolite of the Etang de Lers. Contours at 1% (dashed lines), 2%, 3%, 4%, 5%, 6%, 7%, 8%, 9%, and 10% per 1% area.

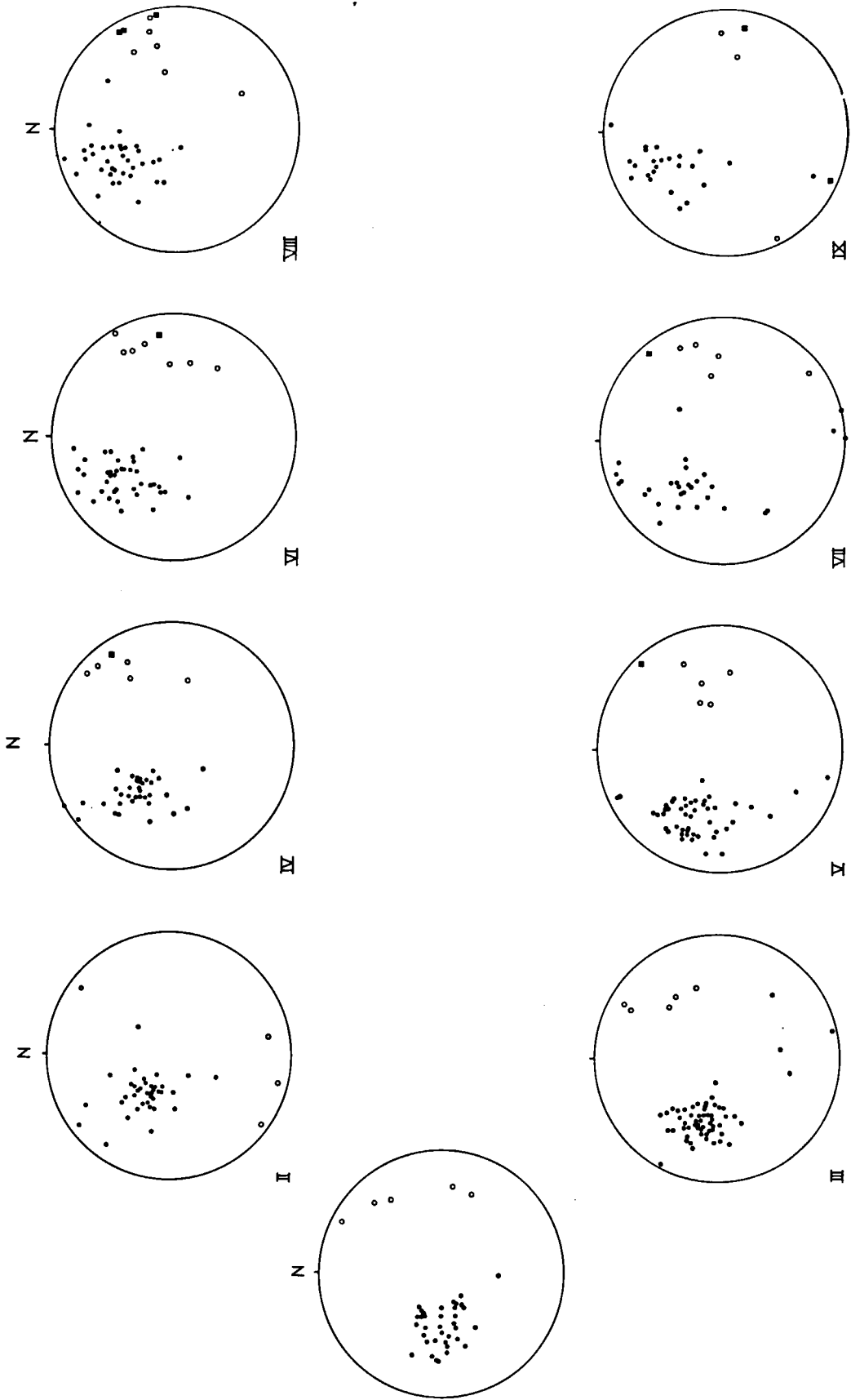


Fig. 14. π -diagrams of the layering (dots), with fold axes (squares), and fold mullions (circles) in the nine subareas (see Fig. 12) of the lherzolite of the Etang de Lers. In subarea I: 36 layering planes, 5 fold axes, no fold mullions: 36-5-0; II: 37-4-0; III: 59-5-0; IV: 48-5-1; V: 48-5-1; VI: 35-5-1; VII: 30-5-1; VIII: 36-6-3; and in subarea IX: 24-3-2.

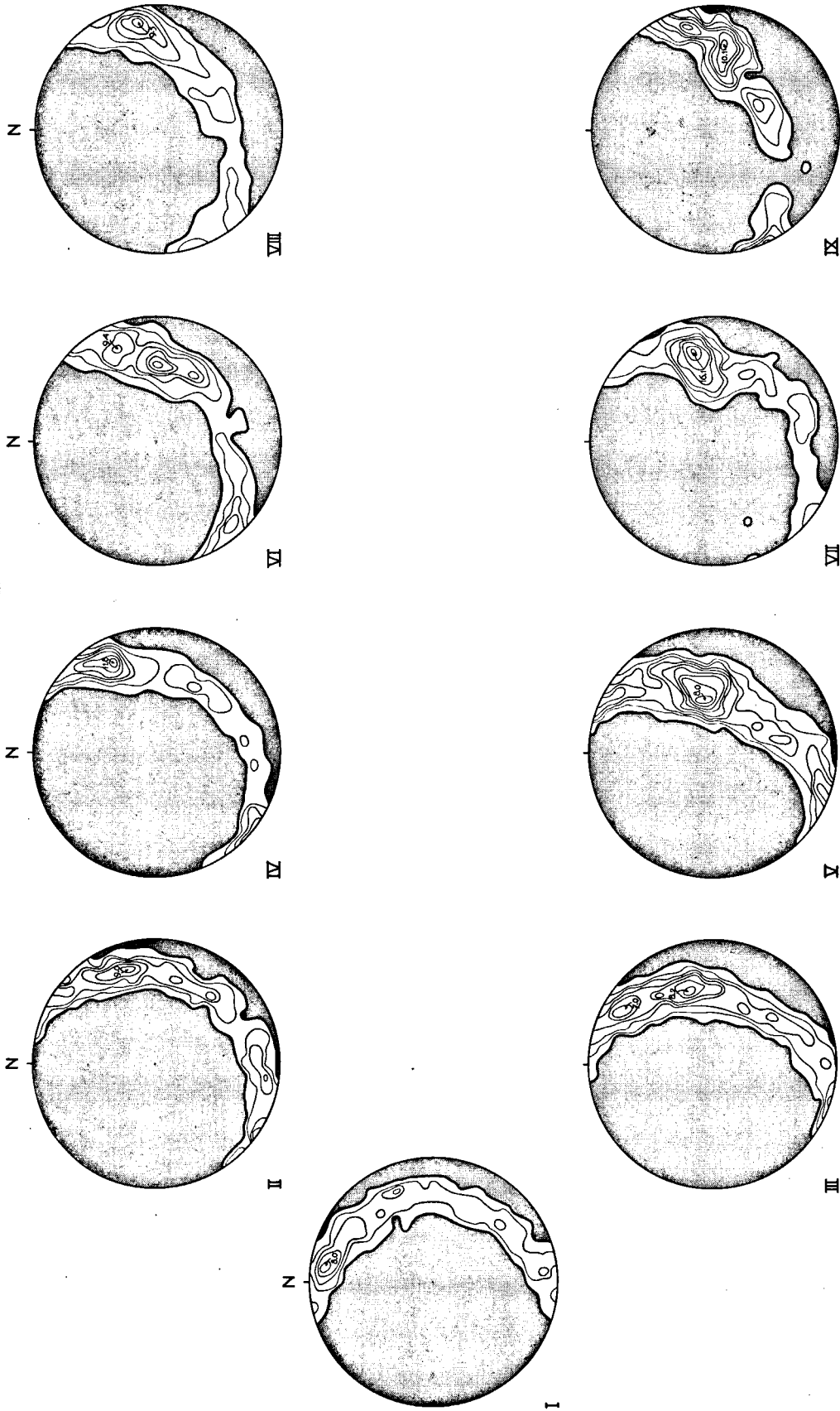


Fig. 15. β -diagrams of the layering planes in the nine subareas (see Fig. 12) of the lherzolite of the Etang de Lers. In subarea I: 630 β -intersections; contours at 1.6%, 3.2%, 4.8%, 6.4%, and 8.0% per 1% area. II: 666; 1.5%, 3.0%, 4.5%, 6.0%, 7.5%, and 9.0%. III: 1711; 1.2%, 2.4%, 3.5%, 4.7%, 5.9%, 7.0%, and 8.2%. IV: 595; 1.7%, 3.4%, 5.0%, 6.7%, 8.4%, 10.1%, and 11.8%. V: 1128; 0.9%, 1.8%, 2.7%, 3.5%, 4.4%, 5.3%, 6.2%, 7.1%, and 8.0%. VI: 741; 1.3%, 2.7%, 4.0%, 5.4%, 6.7%, 8.1%, and 9.4%. VII: 435; 1.1%, 2.3%, 4.6%, 6.9%, 9.2%, 11.5%, 13.8%, and 16.1%. VIII: 630; 1.6%, 3.2%, 4.8%, 6.3%, 7.9%, and 9.5%. IX: 276; 1.4%, 2.9%, 4.3%, 5.8%, 7.2%, 8.7%, and 10.1% per 1% area.

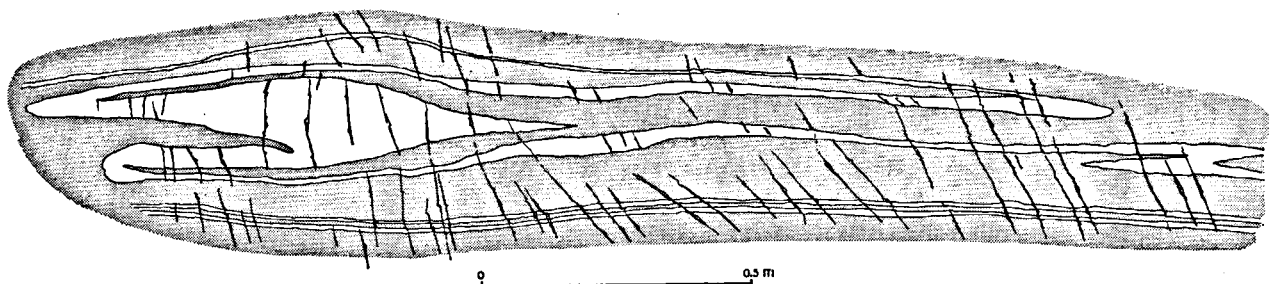


Fig. 16. Asymmetric isoclinal folds of spinel pyroxenite layers in lherzolite with Alpine S_0 -cleavages. South of the small island in the Etang de Lers, in subarea IV.

rotation from west to east (i.e. from subareas I to IX) is evident. Fig. 17, a gives all the 7% point-maxima from the nine diagrams; Fig. 17, b shows the axes of the nine girdles from the β -diagrams. These points coincide with the average position of the poles to the layering. In both diagrams (Fig. 17, a and b) rotation is evident, but always with a rather constant difference between the northern zone (subareas II, IV, VI, VIII) and the southern zone (subareas III, V, VII, IX). This is an indication that the isoclinal folding was the

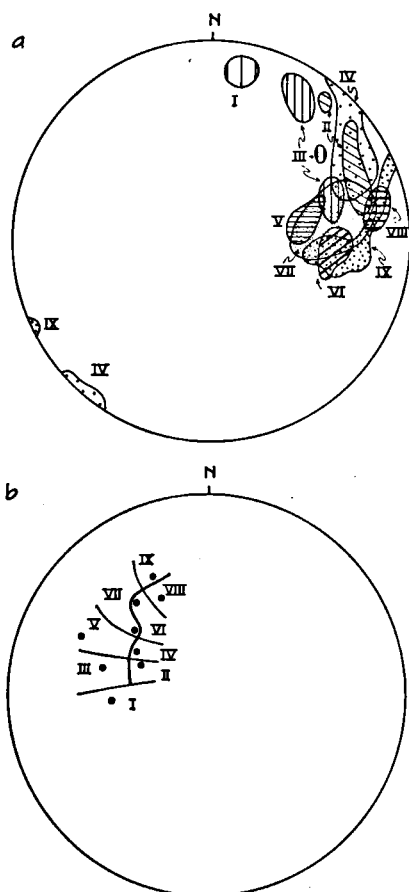


Fig. 17. a. A composite diagram of the 7% contours of all the β -diagrams of the nine subareas (Fig. 15). b. The penetration points of axes of the girdles from the nine β -diagrams, which represent the average layering plane of each subarea.

result of an older deformation phase than that which caused the clock-wise rotation from west to east.

The rotation occurred later. It is impossible to assume a fold axis to account for this rotation, because of the differences in structural orientation between the northern and the southern subareas, but the assumption of two fold axes would solve this problem: one of them an E-W-trending axis and the other a N-S-trending one. The plunge is impossible to reconstruct, however. The N-S-trending axis may plunge considerably.

These two phases can thus be compared with the Alpine F_1 - and F_2 -phases. The external shape of the lherzolite body is in contradiction with this concept, however. It therefore seems more likely that these phases, too, are pre-Alpine.

The S_0 -cleavage generally lies parallel to the layering or makes a very small angle with it. In fold hinges, however, the S_0 -cleavage cuts across the layering at right angles. Thus, it is evident that S_0 is an axial-plane cleavage of the S_L -folds. In the diagrams in Fig. 13 this cleavage has the same clock-wise rotation from west to east as the layering.

The bands of harzburgitic lherzolite are much more strongly deformed than the normal lherzolite. This can be seen at places where spinel pyroxenite layers are totally disrupted and form fold mullions. Folds are visible as ghost structures (Fig. 26). On the S_0 -cleavage plane, long streaks and lenses of spinel pyroxenite are visible. These fold mullions lie parallel or almost parallel to the fold axes.

Lherzolite of the Forêt de Freychinède

The lherzolite of the Forêt de Freychinède is poorly exposed. There is a possibility that it consists of two or even more separate bodies. However, the layering is rather uniform in all parts, usually showing a SE-NW-strike and a steep dip to the northeast (Fig. 18, A). The rock is isoclinally folded around a fold axis plunging to the northwest. The folds are tight in some places, in others open (Plate V, d). If these folds are shear folds, the northeastern part was thrust over the southwestern part. The β -diagram (Fig. 18, B) shows a girdle coinciding with the average layering and a main point-maximum coinciding with that of the fold axes.

One hundred cleavages were measured (Fig. 18, C).

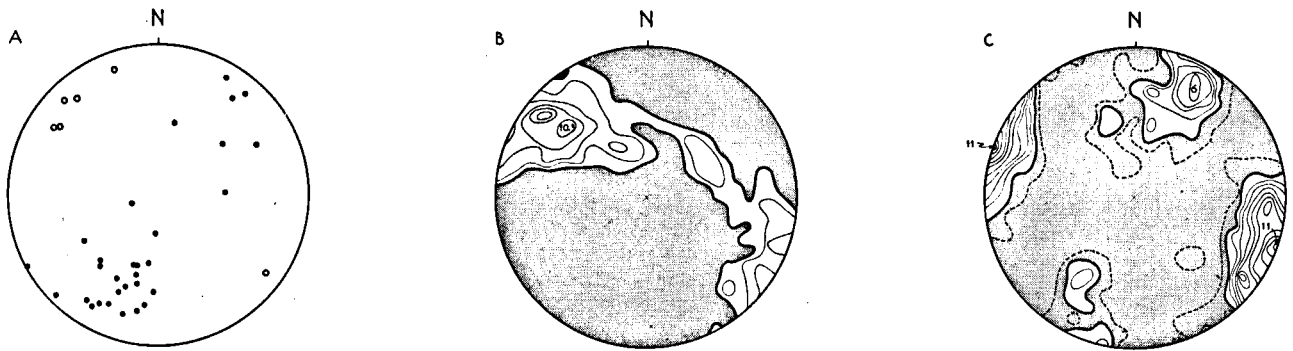


Fig. 18. The lherzolite of the Forêt de Freychinède. A. Poles to 30 layering planes (dots), and 6 fold axes (circles). B. β -diagram of the layering planes: 435 β -intersections; contours at 1.0%, 2.1%, 4.1%, 6.2%, 8.3%, and 10.3% per 1% area. C. π -diagram of 100 cleavage planes; contours at 1% (dashed lines), 2%, 3%, 4%, 5%, 6%, 7%, 8%, 9%, 10%, and 11% per 1% area.

The vertical NNE-SSW-striking S_3 -cleavage is very strongly developed. The WNW-ESE-striking, steeply southward-dipping S_1 -cleavage is less marked but clearly evident. There is also a WNW-ESE-striking cleavage which dips to the north and lies parallel to the layering. This is the pre-Alpine axial-plane cleavage S_0 . Although the general orientation of the layering is

totally different from that at the Etang de Lers, the two Alpine cleavages (S_1 and S_3) have corresponding attitudes. This is another indication of the Alpine age of these two cleavages, in contrast to the pre-Alpine age of the S_0 -cleavage. The lherzolite of the Forêt de Freychinède also appears to have an outer rim of lherzolitic breccia.

CHAPTER V

FABRIC ANALYSIS OF THE ULTRAMAFIC ROCKS

INTRODUCTION

Fabric analyses were carried out for olivine, enstatite, and diopside from samples of lherzolite, spinel pyroxenite, and one garnet pyroxenite. For olivine and enstatite, the orientation of the optic elasticity axes α , β , and γ in each grain was measured and in two cases the {110}-cleavages of enstatite as well; for diopside, the crystallographic directions [100] and [001] were also constructed, together with the {100}-cleavage. The optic directions of olivine α , β , and γ coincide with: $\alpha = X = [010]$, $\beta = Y = [001]$, $\gamma = Z = [100]$, and of enstatite: $\alpha = X = [010]$, $\beta = Y = [100]$, $\gamma = Z = [001]$.

In the lherzolite samples, 200 olivines were usually measured; Raleigh (1963, 1965) measured 50 grains, Collée (1962) 100 grains of one mineral per sample. The present author is of the opinion that measurement of 50 grains will give a general idea of the fabric, but that a more representative picture requires measurement of 200 or more grains, depending on the rate of preferred orientation. Comparison of the fabric pattern of 100 grains per sample with that of another set of 100 grains from the same sample shows that although the general picture is the same, some minor point-maxima in the first set do not always coincide with the point-maxima of the second — in fact they sometimes coincide with minima. The measurement of 200 grains reduces the chance of including fortuitous concentrations or minima. In one case (Fig. 23, L-59),

where only a general idea was needed, 100 olivine grains per thin section were measured. Depending on whether a detailed or a general picture was needed, 200 or 100 grains of enstatite were measured. Because measurement of the crystallographic axes of diopside is very time-consuming, 100 grains and once 150 were measured.

The lherzolites are sometimes so coarse-grained that two thin sections are needed to obtain 200 enstatites, whereas one slide always contains enough olivines. The pyroxenites are even coarser; in L-53³ (Fig. 31), three thin sections were needed to obtain 150 enstatites. In cases where more than one thin section were needed, the partial fabrics were generally so similar that it could be concluded that the lherzolites and pyroxenites are homogeneous from the fabric point of view. In finer-grained varieties, traverses of the thin section were made perpendicular to the mineral foliation. Microphotographs were used to locate the measured grains. In coarse-grained rocks almost all the grains in a thin section had to be measured to achieve the required number of 200. The thin sections were cut either perpendicular to the foliation or parallel to the horizontal plane. In the first case, the measurements were rotated into the horizontal plane; the direction N on the diagrams thus coincides with the geographic north. The measurements were plotted in an equal-area projection on the lower hemisphere of the Schmidt net.

The interlayering of lherzolite and pyroxenite is

represented in the diagrams by S_L , while the foliation — if distinctly visible — is indicated by S_0 . In some cases both were invisible and consequently do not appear in the diagram.

In all the lherzolite samples subjected to fabric analysis the average grain shape of the olivines was evaluated. However irregular and xenomorphic the olivine grains may be, they usually show a pronounced elongation parallel to the trace of the layering (S_L). In sections taken parallel to S_L there is in general a slight statistical elongation parallel to the γ -point-maximum. Having taken the pole to S_L as the fabric c -axis and the γ -point-maximum as the fabric b -axis, a being per definition perpendicular to the bc -plane, length-width measurements were carried out in three thin sections perpendicular to the a , b , and c fabric axes. The over-all shape of the olivine grains can be represented by a triaxial ellipsoid.

FABRICS

Collée (1962) added a chapter on the fabric of the lherzolite at the Etang de Lers to his study of lherzolitite

nodule fabrics in basalt. His preliminary conclusion was that the fabric of the lherzolites had been caused mostly by the Alpine orogeny, although the layering could be an older phenomenon. His three samples of the lherzolite from Lers all have a strong γ -olivine point-maximum, trending SSW-NNE and coinciding with the direction of major stress during the Alpine orogeny. On the basis of a comparison of the fabric diagrams of lherzolites from four different bodies (Sem, Bois de Soubrouque, Forêt de Freychinède, Etang de Lers), it is concluded here that the fabric is not of Alpine age.

Sample V-42: Lherzolite of Sem (Fig. 19)

This sample was taken from the lherzolite of Sem, about 2 km east of Vicdessos. This lherzolite is a pyroxene-rich variety. It contains approximately 45% olivine, 35% enstatite, 15% diopside, and 5% spinel. Some secondary hornblende and opaque ore minerals are present. Serpentinization is weak. The Alpine S_3 -cleavage has hardly influenced the texture. The pyroxenite layering dips very gently to the NNE.

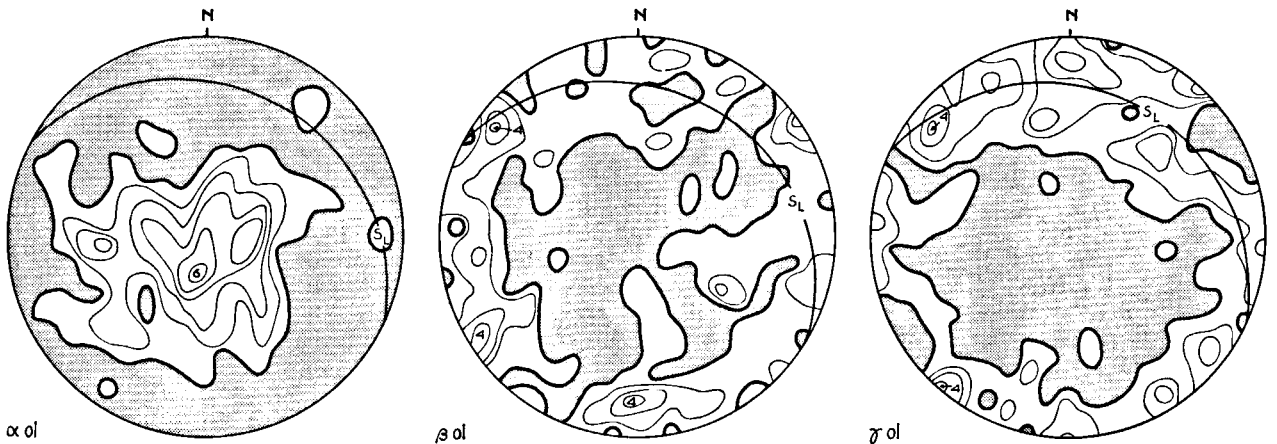


Fig. 19. Lherzolite of Sem (Sample V-42). 200 α -, β -, and γ -olivine. Contours at 1%, 2%, 3%, 4%, 5%, and 6% per 1% area. S_L = layering.

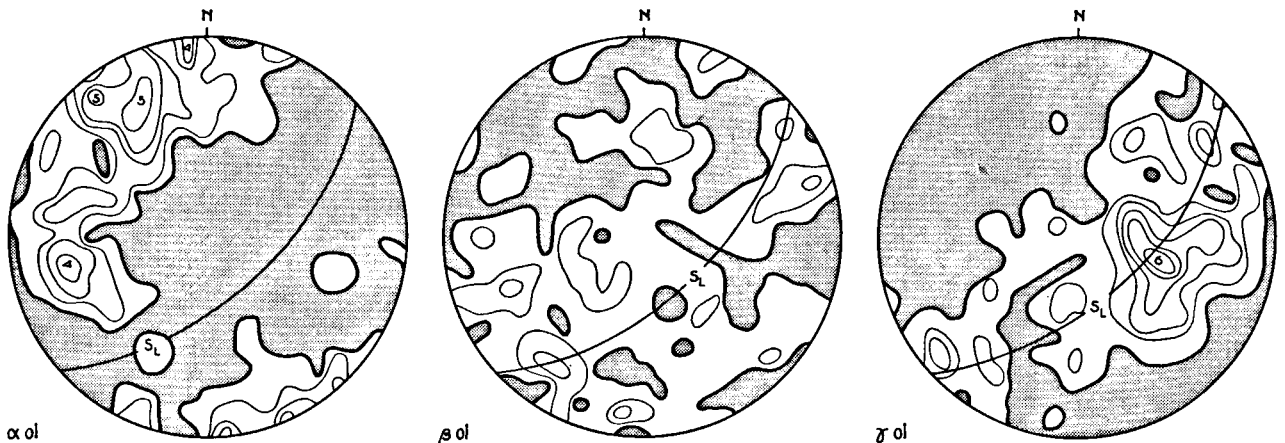


Fig. 20. Lherzolite of the Bois de Soubrouque (Sample V-75). 200 α -, β -, and γ -olivine. Contours at 1%, 2%, 3%, 4%, 5%, and 6% per 1% area. S_L = layering.

The α -olivine is concentrated in one broad point-maximum, with a peak of 6%; this maximum is slightly elongate, forming a partial WNW-ESE-striking, steeply SSW-dipping girdle. The β - and γ -patterns show girdles in the layering, the γ -girdle being better developed and showing stronger concentration in the northern quadrants. The grain shape is very irregular. However, the overall shape of the grains can be represented by a triaxial

ellipsoid whose axes are 2.0, 2.2, and 1.4 mm for a , b , and c , respectively.

Sample V-75: Lherzolite of the Bois de Soubrouque (Fig. 20)

This very small lherzolite body is located almost 4 km WNW of Vicdessos. It is a normal lherzolite containing approximately 75% olivine, 12% enstatite, 11% diopside, and 2% spinel. The Alpine S_1 - and

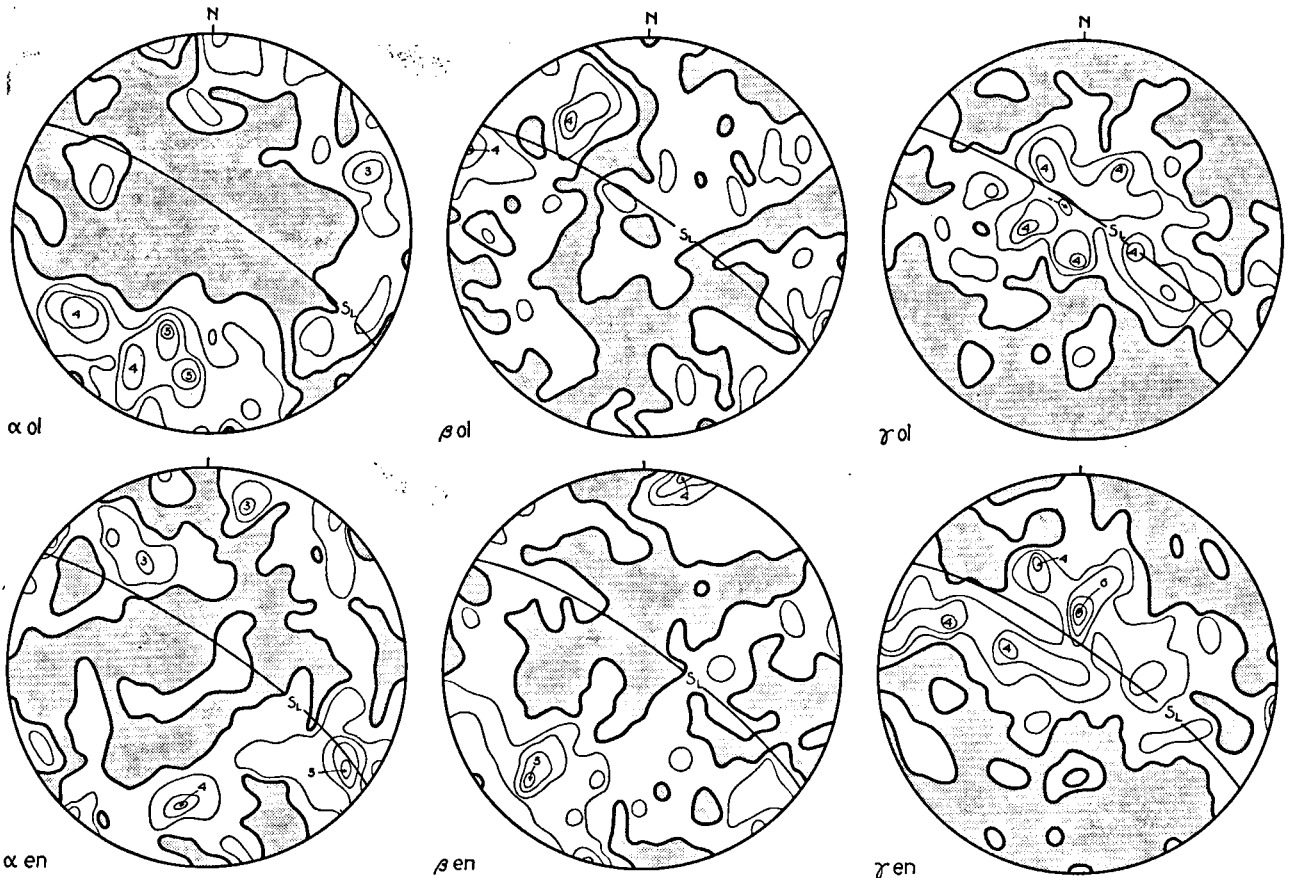


Fig. 21. Lherzolite of the Forêt de Freychinède (Sample L-76). 200 α -, β -, and γ -olivine, and 200 α -, β -, and γ -enstatite. Contours at 1%, 2%, 3%, 4%, 5%, and 6% per 1% area. S_L = layering.

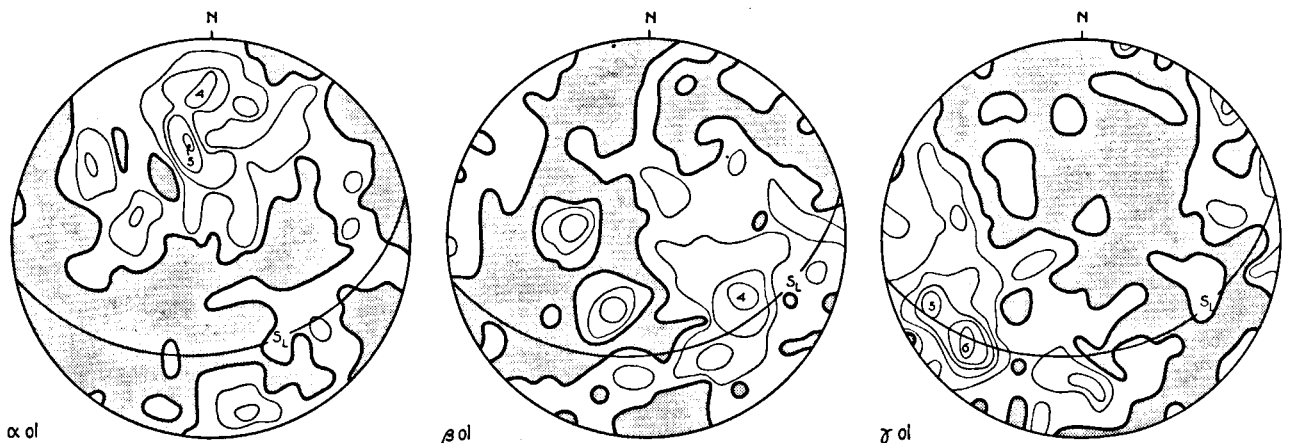


Fig. 22. Lherzolite of the Etang de Lers (Sample L-61). 200 α -, β -, and γ -olivine. Contours at 1%, 2%, 3%, 4%, 5%, and 6% per 1% area. S_L = layering.

S_3 -cleavages are rather strongly developed but do not appear to have influenced the fabric. Serpentinization is weak.

Again, the olivine fabric is in complete agreement with the layering, which strikes NE-SW and dips 65° to the SE. The α -olivine pattern shows a partial girdle, perpendicular to the layering, with a point-maximum concentration of up to 5%, also perpendicular to the layering. The β -pattern is irregular, having a minimum only in the region of the α -maximum. The γ -girdle parallel to the layering is very well developed, with a point-maximum of 6% nearly parallel to the dip direction.

The average grain shape conforms to a triaxial ellipsoid whose axes are 2.1, 2.5, and 1.3 mm for fabric a , b , and c , respectively.

Sample L-76: Lherzolite of the Forêt de Freychinède (Fig. 21)

The lherzolite body of the Forêt de Freychinède is larger than most of the other outcrops. It lies about 2 km ESE of Port de Lers (= Port de Massat, Port d'Erce). This lherzolite contains approximately 70% olivine, 20% enstatite, 5% diopside, 3% spinel, and 2% hornblende. In addition to the strong S_0 -cleavage

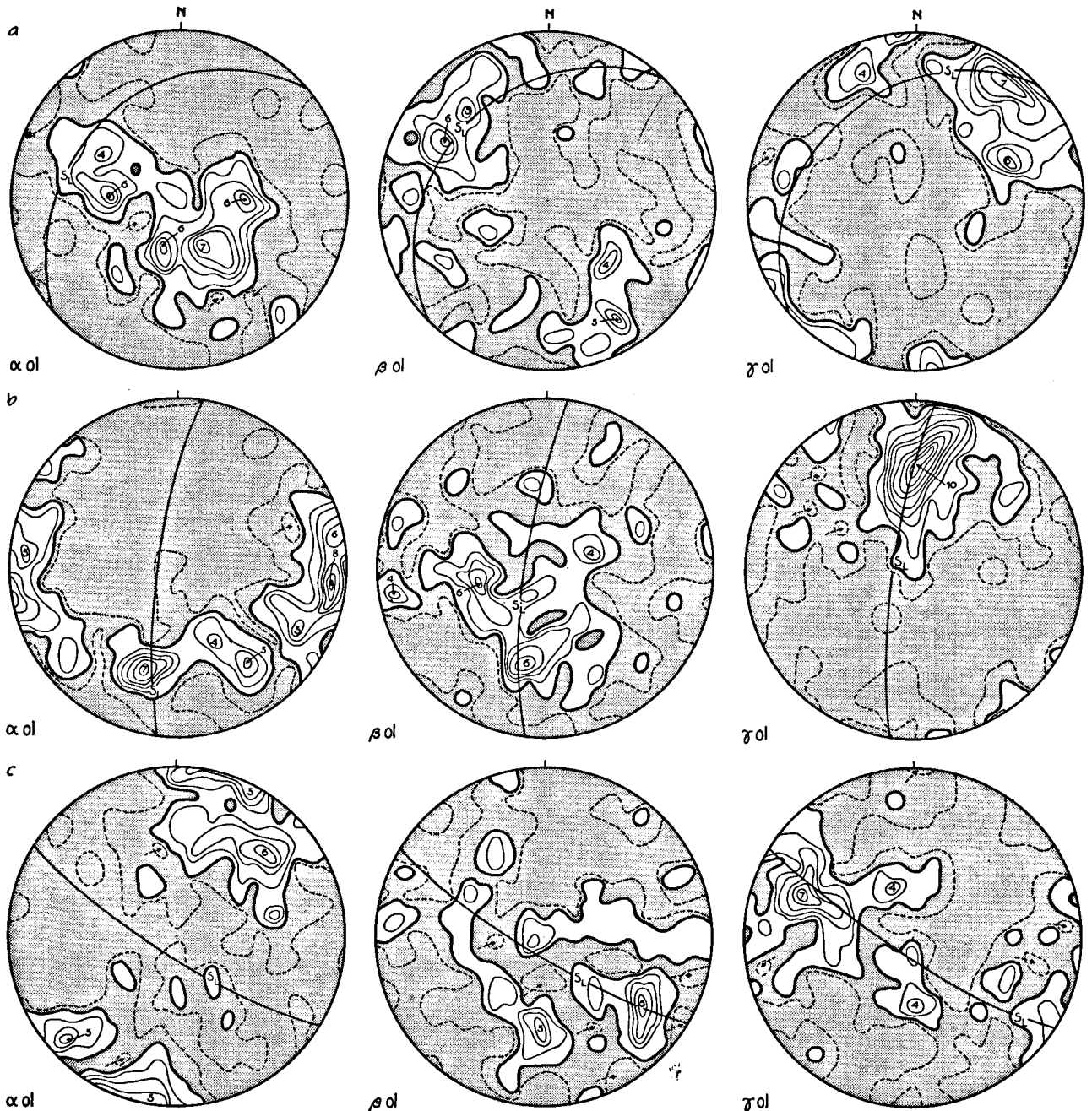


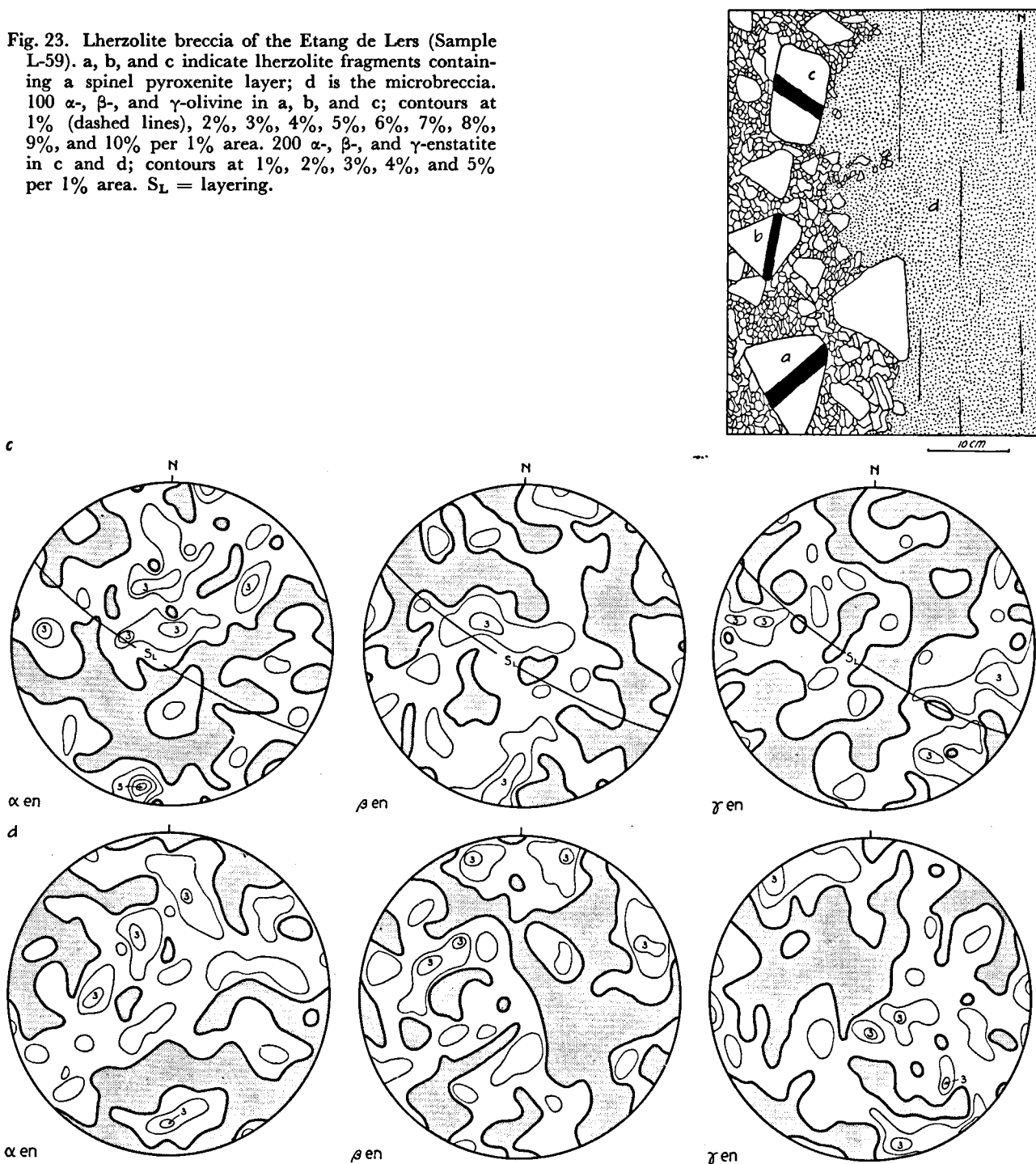
Fig. 23. See opposite page.

parallel to the layering S_L , the Alpine S_3 -cleavage is rather well developed. There are signs of some granulation along S_3 -planes. Serpentinization is weak. In this sample, 200 olivine and 200 enstatite grains were measured. The layering strikes NW-SE, and dips 80° to the NE. The α -olivine pattern shows a girdle containing a broad point-maximum of up to 5%, both

perpendicular to the layering. The β -olivine has an almost random orientation, whereas γ -olivine shows a girdle parallel to the layering with a broad point-maximum of up to 4% parallel to the direction of dip.

Enstatite gives a related pattern: α -enstatite is as weakly oriented as α -olivine; γ -enstatite and γ -

Fig. 23. Lherzolite breccia of the Etang de Lers (Sample L-59). a, b, and c indicate lherzolite fragments containing a spinel pyroxenite layer; d is the microbreccia. 100 α -, β -, and γ -olivine in a, b, and c; contours at 1% (dashed lines), 2%, 3%, 4%, 5%, 6%, 7%, 8%, 9%, and 10% per 1% area. 200 α -, β -, and γ -enstatite in c and d; contours at 1%, 2%, 3%, 4%, and 5% per 1% area. S_L = layering.



olivine are almost identical; and β -enstatite resembles the α -enstatite girdle.

The average grain shape is comparable to a triaxial ellipsoid with axial lengths of 1.4, 1.7, and 0.9 mm in the directions of a , b , and c , respectively.

Sample L-61: Lherzolite of the Etang de Lers (Fig. 22)

This sample contains approximately 60% olivine, 25% enstatite, 10% diopside, and 5% spinel; some secondary hornblende is present. The grains are much less tectonized than is normally found; kinking is scarce. The Alpine S_3 -cleavage is important, but does not contort the grains.

The layering in this sample strikes WSW-ENE and dips only 40° to the SSE. A total of 200 olivines were measured. The α -olivine shows an irregular girdle containing a rather broad point-maximum of 5%, both perpendicular to the layering. The β -olivine is distributed almost at random, showing two weak girdles, one parallel to the α -girdle, one parallel to the γ -girdle; γ -olivine has an incomplete girdle parallel to the layering with a point-maximum of 6% in the SW nearer to the strike than to the dip.

The average grain shape is once again a triaxial ellipsoid, with axial lengths of 1.6, 1.7, and 1.0 mm for a , b , and c , respectively.

The conclusions to be drawn from these four samples are evident:

1. Both the olivine and the enstatite patterns are related to the layering S_L , with α -olivine in a point-maximum perpendicular to the layering (fabric c -axis) and in a sometimes incomplete girdle, also perpendicular to S_L ; and with γ -olivine and γ -enstatite in a girdle parallel to S_L containing a point-maximum (which is taken as the fabric b -axis).
2. Since the layering has a different orientation in each of the lherzolite bodies as a consequence of randomization during their emplacement, the layering must be pre-Alpine (see Chapter IV). Since both the olivine and enstatite fabrics seem to be dependent on the layering, it is obvious that the fabric of the lherzolites is also pre-Alpine.
3. The grains, xenomorphic and irregular though they may be, have a general shape that is tabular parallel to S_L (=fabric ab) and elongate parallel to fabric b . In connection with the preferred lattice orientation of olivine, the grains are predominantly tabular or discoid parallel to $\{010\}$ and elongate parallel to $\gamma = [100]$. However, the longest axis of an olivine grain lying parallel to fabric b can make a considerable angle with the direction of γ (Plate VI, a and b), just as the shortest axis (fabric c) can also make an angle with the direction of α .

Samples L-59-a, b, c, and d: Lherzolite breccia of the Etang de Lers (Fig. 23)

An even better proof that the layering and fabric of the lherzolites are not of Alpine origin is shown in

Fig. 23 (L-59). The drawing shows a breccia with angular lherzolite inclusions in which layering is sometimes visible, lying in a matrix of microbreccia. In each of the three inclusions (a, b, and c) 100 olivine grains were measured, and in L-59-c 200 enstatite grains. It is again very clear that the fabric is closely related to the layering. An α -girdle is consistently present, sometimes with a definite point-maximum perpendicular to the layering, as well as a γ -girdle with a pronounced point-maximum parallel to the layering. The β -olivine gives girdles sometimes parallel to the α -girdle, sometimes parallel to the γ -girdle, depending on the relative strength of the α - or γ -point-maximum. In the outcrop the N-S-striking, subvertical S_3 -cleavage of Alpine age is not obvious but nevertheless visible. The major E-W- or ESE-WNW-striking cleavage of Alpine age can scarcely be seen. The fabric clearly has nothing to do with these Alpine cleavages.

Because of the fact that in the crushed, fine-grained matrix, i.e. the microbreccia, the olivine grains are almost all serpentinized but not the pyroxenes, measurements were made in this microbreccia of 200 enstatite grains (L-59-d) and, for purposes of comparison, also 200 enstatites in L-59-c. The preferred orientation of enstatite in the inclusion is very weak; in the α -diagram there is a deficiency near the plane of the layering, and the γ -diagram has some similarity to the γ -olivine diagram. The enstatite diagrams of the microbreccia are different, although the fabric is also very weak. It is possible that there is a steep ENE-WSW-striking α -girdle perpendicular to the Alpine S_3 -cleavage, whereas β - and γ -enstatite seem to have a random orientation. In any case, it is clear that the fabric of the lherzolite was not affected by the Alpine metamorphism and deformation. This is also clear from the thin sections. The Alpine cleavages S_1 and S_3 are both visible, showing very narrowly-spaced parallel fractures cutting through crystals without rotation.

A further demonstration that the fabric of the lherzolite is pre-Alpine is given by the other diagrams (Figs. 24, 26—33), all from the body at the Etang de Lers. In the west, the layering strikes N-S (Fig. 12), in the east ENE-WSW. In most cases the orientation patterns of olivine, as well as those of enstatite and diopside, depend upon the layering. They show the same clock-wise rotation from west to east as does the layering.

Samples L-48-A, B, and C: Lherzolite from the Etang de Lers (Fig. 24)

The pre-Alpine isoclinal folding phase, which caused an axial-plane cleavage S_0 , has been described in Chapter IV. To study the relation of this phase to the fabric in more detail, a single fold was selected for fabric analysis. The composition of the lherzolite in these samples is approximately 65% olivine, 20% enstatite, 10% diopside, the remainder being spinel

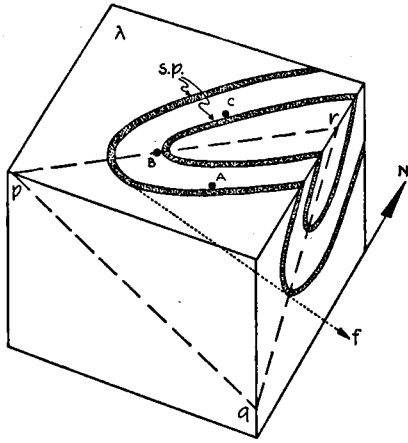
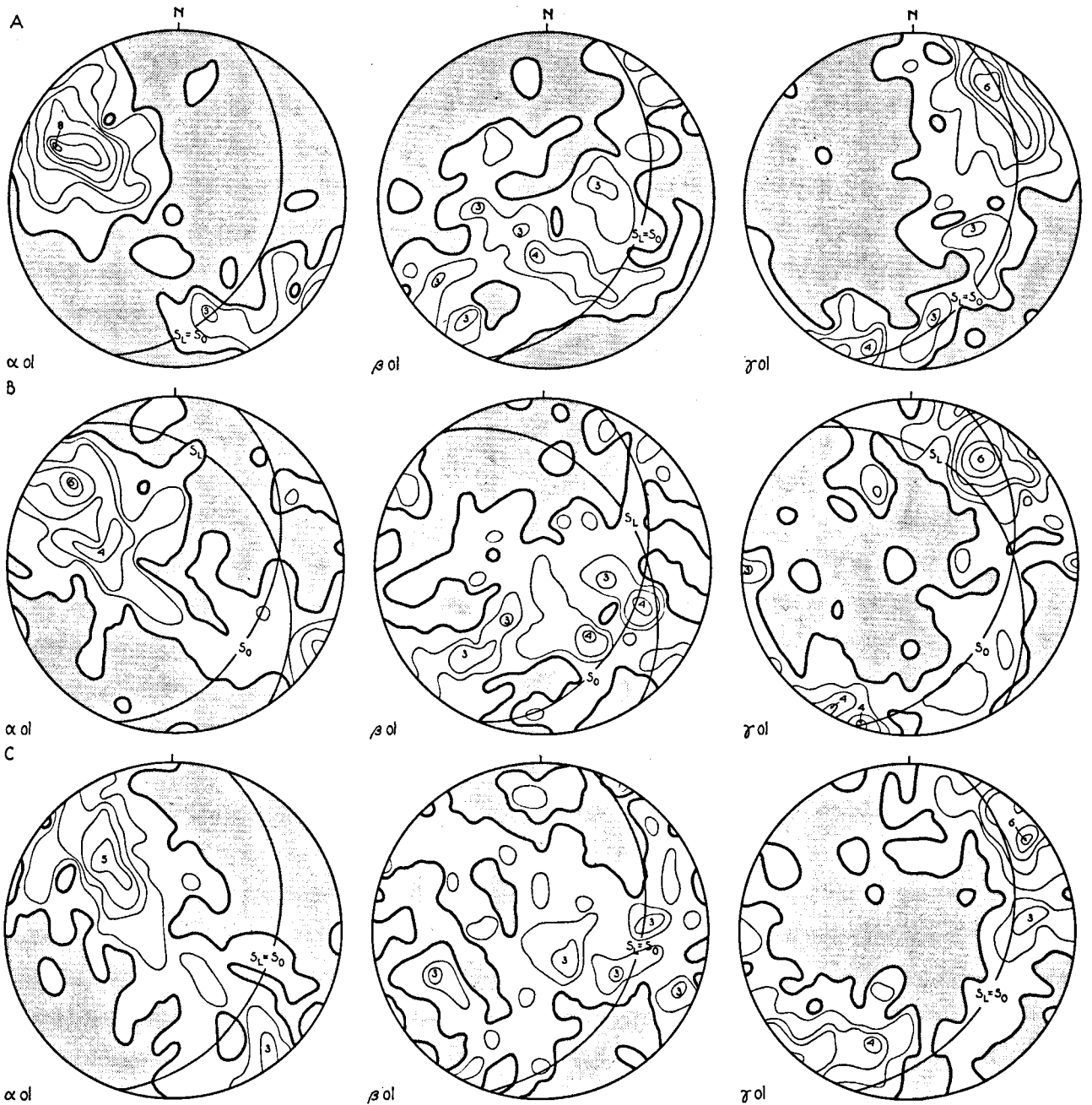


Fig. 24. Lherzolite of the Etang de Lers (Samples L-48-A, B, and C). Block diagram: the spinel pyroxenite layers (s.p.) in lherzolite (λ) are folded isoclinally; pqr = axial plane, f = fold axis, A, B, and C = location of samples. In each sample: 200 α -, β -, and γ -olivine. Contours at 1%, 2%, 3%, 4%, 5%, 6%, 7%, and 8% per 1% area. S_L = layering, S_0 = axial-plane cleavage.



and hornblende. The Alpine S_1 - and S_3 -cleavages are weakly developed.

Three samples of this isoclinal fold from Lers were analysed. For each of the three samples (two from the limbs and one from the hinge) 200 olivines were measured. The same orientation pattern is again present: in the flanks an α -girdle containing a point-maximum, both perpendicular to the layering, and a γ -girdle parallel to the layering with a definite point-maximum near the strike. The β -olivine pattern in

L-48-A has a girdle parallel to the γ -girdle as a result of the strong α -point-maximum. In L-48-C one girdle lying somewhat parallel to the γ -girdle and a second parallel to the α -girdle show once more that the β -pattern is dependent on the relative strength of α and γ . In the hinge (L-48-B), orientation patterns similar to those in the limbs are present for α , β , and γ . Here, however, the fabric is asymmetrical with respect to the layering but dependent on the axial plane cutting across it. As has been shown in

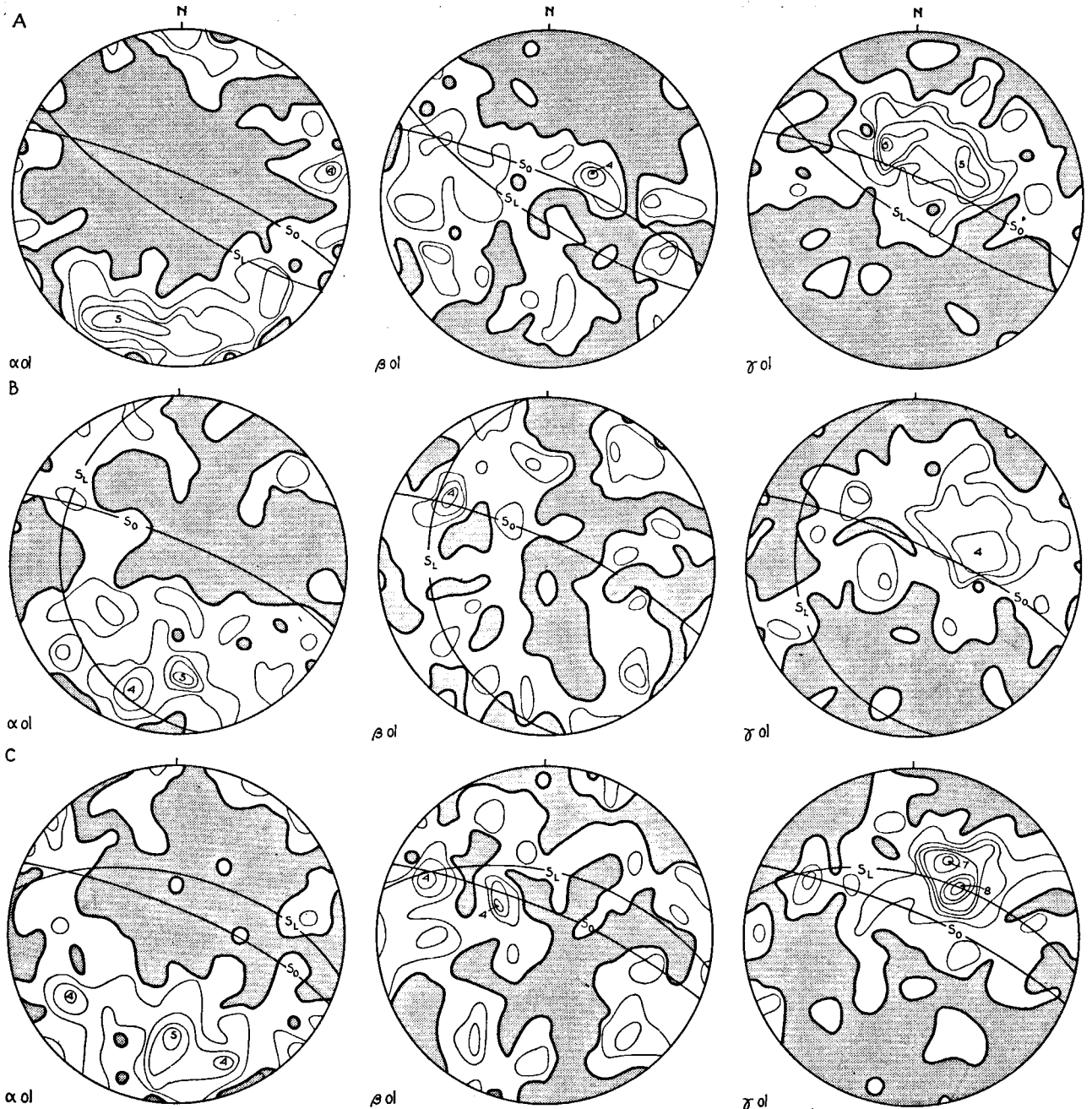


Fig. 25. Fold from the lherzolite of the Forêt de Freychinède (Sample L-102; Plate V, d). In each of the three hand specimens A, B, and C: 200 α -, β -, and γ -olivine. Contours at 1%, 2%, 3%, 4%, 5%, 6%, 7%, and 8% per 1% area. S_L = layering, S_0 = axial-plane cleavage.

Chapter IV, the axial-plane cleavage lies almost parallel to the layering, except in fold hinges. Thus, the layering is only indirectly related to the fabric. Since the layering is deformed by the axial-plane cleavage S_0 , it must be older than the fabric. The fabric must have originated during the pre-Alpine metamorphism and deformation, which folded the lherzolites isoclinally and gave them their pronounced cleavage, mostly parallel to the layering. The γ -point-maxima in the three cases strike NE-SW and plunge slightly to the NE. There is a small discrepancy between this direction and the fold axis.

In each of the three samples the average grain shape was evaluated. It is obvious that the definitions for the fabric axes must now be re-adjusted. The fabric a -axis coincides with the pole to S_0 (which is elsewhere parallel to S_L) or the α -point-maximum of olivines, while the b -axis coincides with the γ -point-maximum. The average grain shape is always a triaxial ellipsoid, the axes of which are 1.7, 1.9, and 1.0 mm in sample L-48-A, 1.3, 1.7, and 0.8 mm in sample L-48-B; and 1.4, 1.5, and 0.9 mm in sample L-48-C, for a , b , and c , respectively.

Sample L-102: Lherzolite of the Forêt de Freychinède (Fig. 25)

A more open fold from the lherzolite of the Forêt de Freychinède was examined. A photograph of this fold is shown in Plate V, d. The lherzolite is somewhat serpentinized. The pre-Alpine S_0 - and Alpine S_3 -

cleavages are strongly developed. The composition is the same as that of sample L-76.

In each of the thin sections (A being from the north flank, C from the south flank, and B from the fold hinge), 200 olivines were measured. In A there is a well-developed α -girdle containing a 5% point-maximum, both perpendicular to the axial-plane cleavage S_0 ; a definite γ -girdle subparallel to the cleavage S_0 with a wide point-maximum up to 6% along the dip; and a poorly-developed β -girdle, somewhat parallel to the γ -girdle. In C the γ -point-maximum close to the dip of S_0 is much stronger (8%), while the girdle parallel to S_0 is incomplete; the α -girdle is complete but broader, as is the point-maximum (up to 5%). In fold hinge B, where S_0 is virtually perpendicular to S_L , the rock has a fabric similar to that in A and C. The γ -point-maximum is very wide and less strong, being only 4%. The differences between the three fabrics are believed to be negligible; the small discrepancies are attributed to errors in the orientation performed in the field and in the preparation of the thin sections. The similarities in all three samples are evident. In fold hinge B the α -olivine girdle seems to lie parallel to the layering S_L , while the γ -girdle is perpendicular to S_L . But from a comparison of these patterns with the fold limbs A and C, it is obvious that they are related not to S_L but to the axial-plane cleavage S_0 . For this fold, too, it has been shown that the rocks have a tectonite fabric, caused by metamorphism during deformation.

The average grain shape of olivine is referable to a

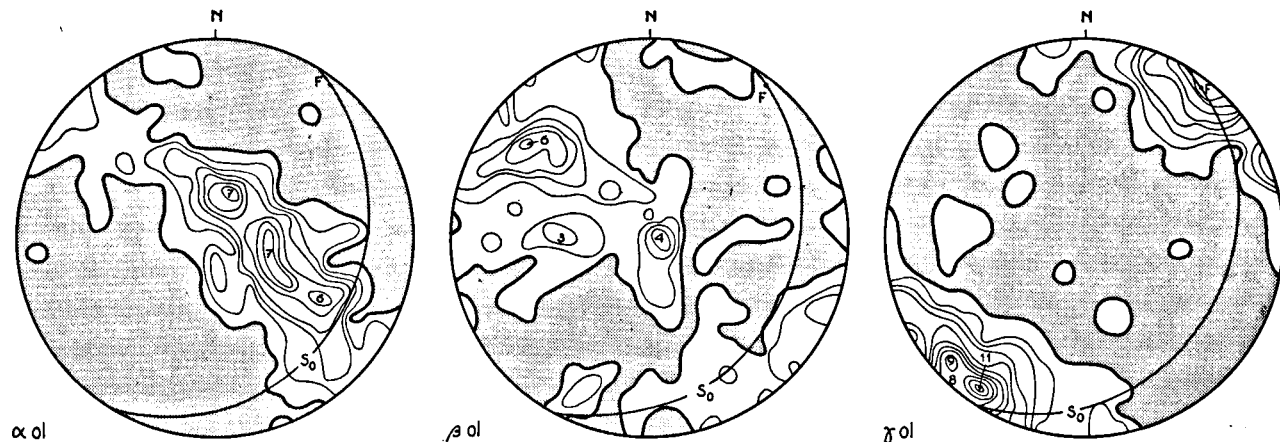
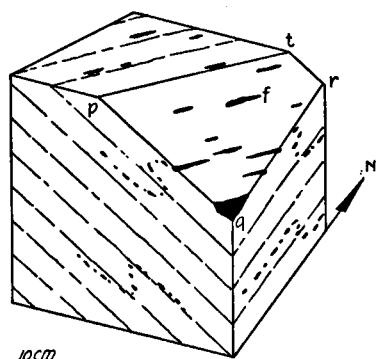


Fig. 26. Harzburgitic lherzolite of the Etang de Lers (Sample L-88). Block diagram: pqrt = axial-plane cleavage S_0 of some rudimentary folds; f = fold mullion. 200 α -, β -, and γ -olivine; contours at 1%, 2%, 3%, 4%, 5%, 6%, 7%, 8%, 9%, 10%, and 11% per 1% area. S_0 = axial-plane cleavage.

triaxial ellipsoid, the axes of which are 1.8, 2.3, and 1.0 mm in sample L-102-A, 1.4, 1.5, and 0.8 mm in sample L-102-B, 1.5, 2.0, and 0.9 mm in sample L-102-C for *a*, *b*, and *c*, respectively.

Sample L-88: Harzburgitic lherzolite of the Etang de Lers (Fig. 26)

The lherzolite body of the Etang de Lers contains bands, some twenty metres wide, lying parallel to the layering, which are harzburgitic in composition. Sample L-88 contains approximately 85% olivine, 12% enstatite, and diopside and spinel as accessories. The deformation here is far more pronounced than in the lherzolite. The rock is very fissile along the S_0 -cleavage. This harzburgitic variety also contains some narrow layers of spinel pyroxenite. Mostly, however, these layers are broken up and lensed out into streaks and fold mullions.

In a thin section taken perpendicular to one of these fold mullions, 200 olivines were measured; the results are shown in the diagrams in Fig. 26. The most striking element in the fabric is the high γ -point-maximum of 11%, which coincides with the direction of the fold mullion. The olivines are all elongate parallel to this

direction, their shortest diameter lying perpendicular to S_0 . The α -diagram shows a complete girdle perpendicular to S_0 with two 7% point-maxima, one perpendicular to S_0 , the other making an angle with S_0 . The β -diagram is more irregular; an incomplete girdle parallel to the α -girdle is necessarily present because of the high γ -point-maximum.

The average grain shape of the olivines is comparable to a triaxial ellipsoid whose axes are 1.9, 2.5, and 1.1 mm in the direction of *a*, *b*, and *c*, respectively.

The following fabric analyses deal with enstatite and diopside in lherzolites and spinel (-garnet) pyroxenites, all from the Etang de Lers area. For comparison, olivines were also measured.

In the lherzolite of the Forêt de Freychinède (L-76), 200 enstatites were measured; the diagrams (Fig. 21) have already been described (see page 28-30).

Sample L-62: Lherzolite of the Etang de Lers (Fig. 27)

In this sample of lherzolite, which contains about 60% olivine, 22% enstatite, 17% diopside, and a little spinel, 200 olivines and 100 enstatites were measured.

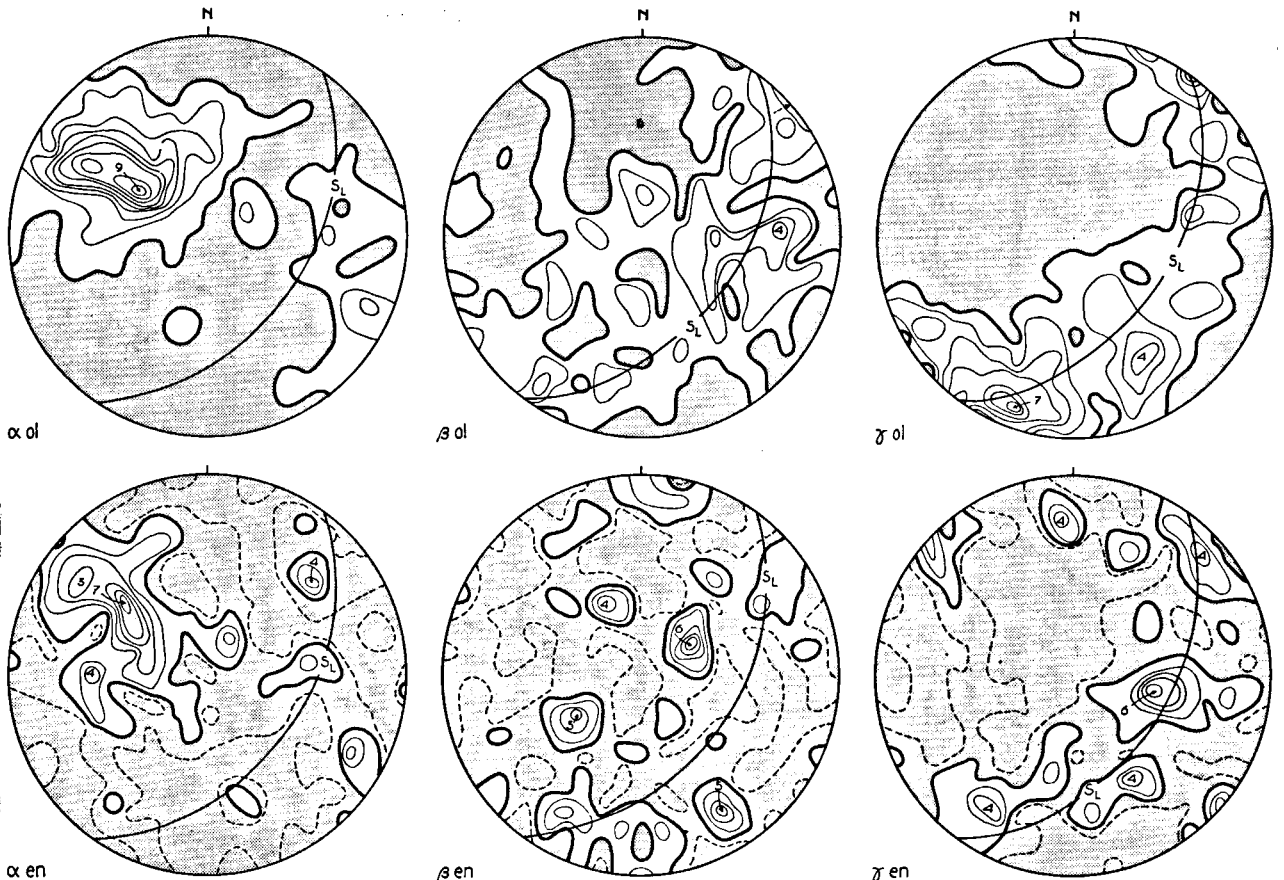


Fig. 27. Lherzolite of the Etang de Lers (Sample L-62). 200 α -, β -, and γ -olivine; contours at 1%, 2%, 3%, 4%, 5%, 6%, 7%, 8%, and 9% per 1% area. 100 α -, β -, and γ -enstatite; contours at 1% (dashed lines), 2%, 3%, 4%, 5%, 6%, and 7% per 1% area. S_L = layering.

The pre-Alpine cleavage S_0 is almost parallel to the layering. The grains show little influence of deformation. Zones of granulation and mylonitization appear to be of later age than the S_0 -cleavage.

Olivine. — The very definite α -olivine point-maximum of 9% is perpendicular to the layering S_L ; a weak and incomplete girdle is present. The β -olivine lies in a wide inconspicuous girdle in the S_L -plane. The γ -girdle parallel to S_L is complete and contains a point-maximum of 7% lying almost horizontal and striking NE-SW.

The average grain shape is that of a triaxial ellipsoid whose axes are 1.4, 1.8, and 1.0 mm for the fabric axes a , b , and c , respectively.

Enstatite. — The orientation of α -enstatite has a broad point-maximum of up to 7% perpendicular to S_L . The α -girdle is very weak and incomplete, and lies parallel to the α -olivine girdle. The β -enstatite is somewhat concentrated near the layering S_L . The γ -enstatite girdle is parallel to S_L but very irregular; some 4% and 6% point-maxima are dispersed over this girdle.

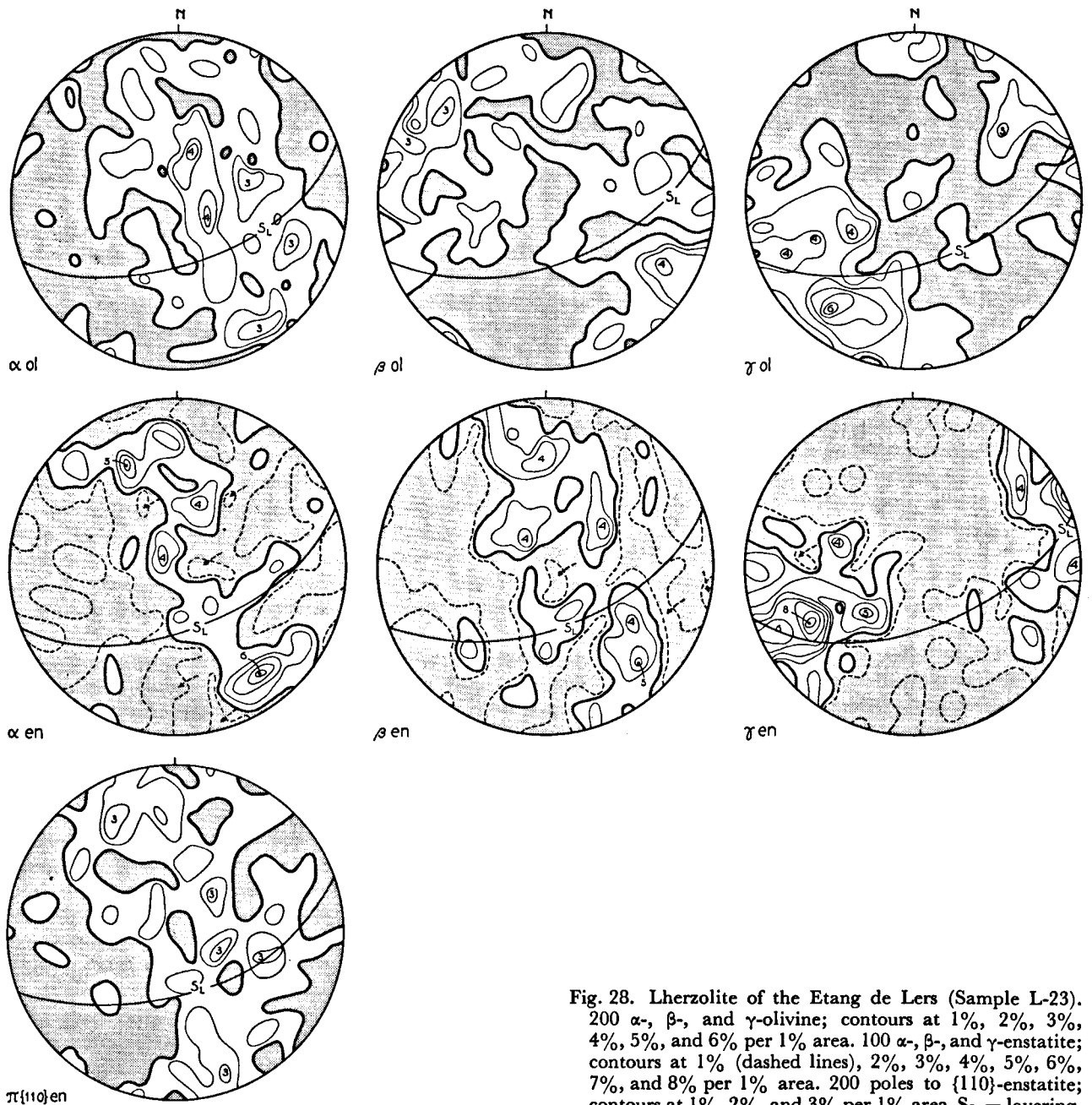
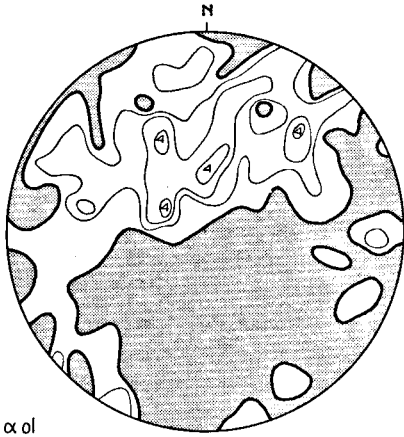
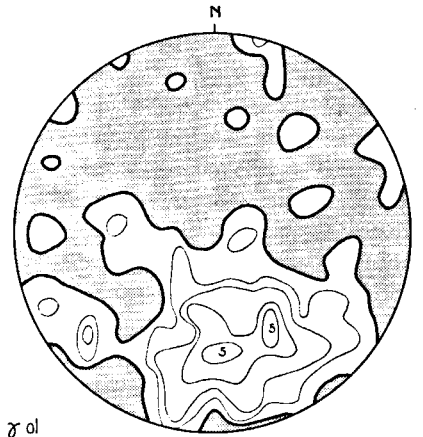
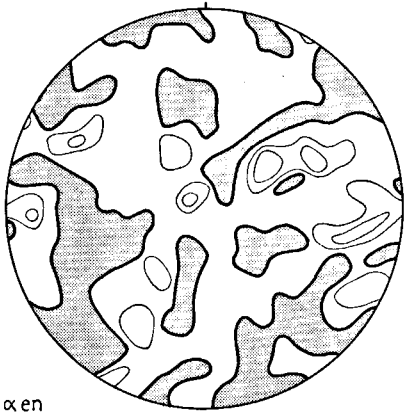
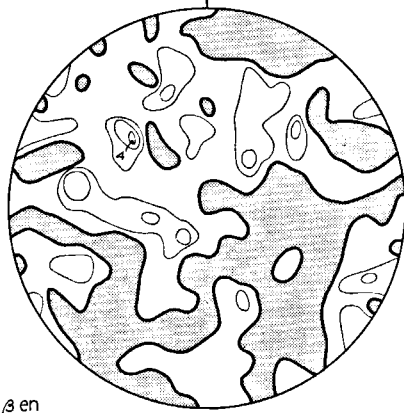
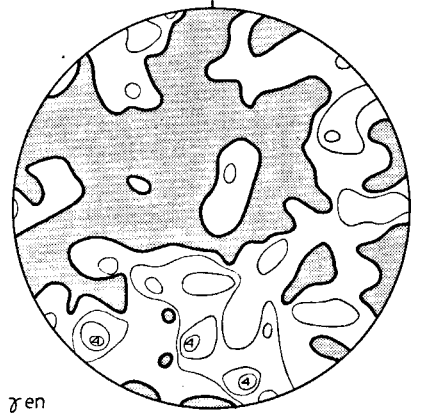
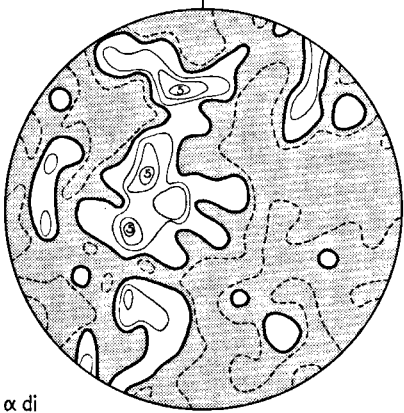
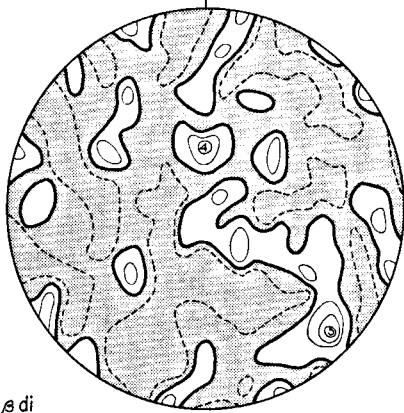
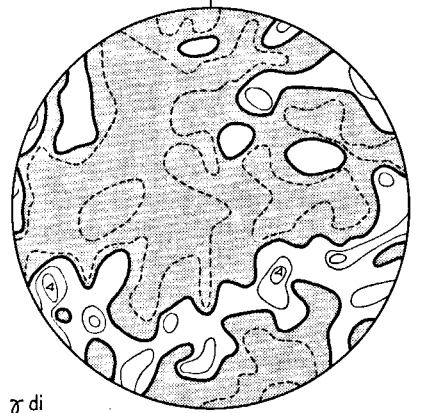
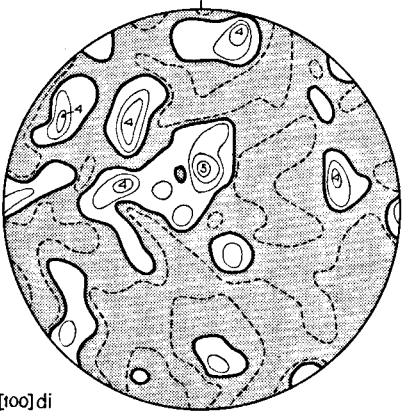
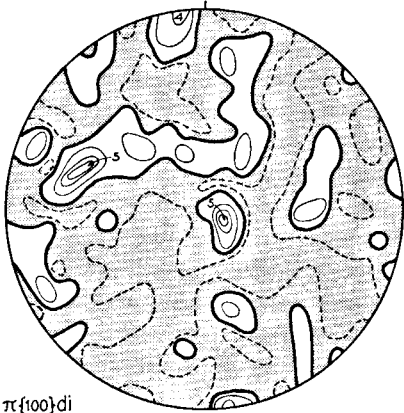
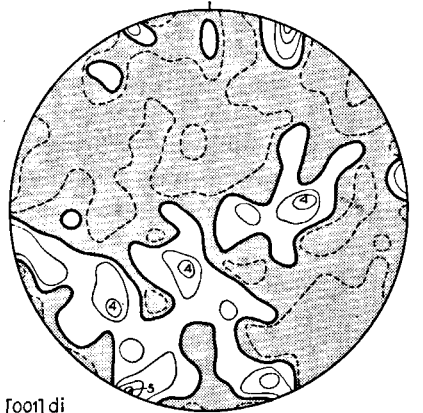


Fig. 28. Lherzolite of the Etang de Lers (Sample L-23). 200 α -, β -, and γ -olivine; contours at 1%, 2%, 3%, 4%, 5%, and 6% per 1% area. 100 α -, β -, and γ -enstatite; contours at 1% (dashed lines), 2%, 3%, 4%, 5%, 6%, 7%, and 8% per 1% area. 200 poles to $\{110\}$ -enstatite; contours at 1%, 2%, and 3% per 1% area. S_L = layering.

 α ol β ol γ ol α en β en γ en α di β di γ di $[100]$ di $\pi \{100\}$ di $[001]$ di

Sample L-23: Lherzolite of the Etang de Lers (Fig. 28)

This lherzolite, containing about 70% olivine, 15% enstatite, 10% diopside, and some spinel, is rather serpentized. Finely-granulated zones cut across the S_0 -cleavages and lie parallel to the Alpine S_1 -cleavage. In this sample 200 olivines and 100 enstatites were measured.

Olivine. — The α -olivine girdle perpendicular to S_L has no pronounced point-maximum. The γ -olivine orientation consists of a broad point-maximum in the SW quadrant with a peak of 6%; a γ -girdle in S_L is not very well defined.

The axes of the triaxial ellipsoid, representing the average grain shape, are 1.6, 1.9, and 1.1 mm in the fabric directions a , b , and c , respectively.

Enstatite. — The α -enstatite girdle is rather irregular but complete, having point-maxima of 5% and 6%, which are not convincingly significant. The β -girdle is parallel to the α -girdle, but is wider and therefore incomplete. The γ has a definite point-maximum of 8% coinciding with the γ -olivine point-maximum. A γ -girdle, although incomplete, is better developed than the γ -olivine girdle. Because of the fact that there are two α -point-maxima, the {110}-cleavages of enstatite were measured and plotted. Any preference shown by the {110}-cleavages to lie in the S_L - or S_0 -plane would have resulted in one or two definite point-maxima of π {110} within the $\alpha\beta$ -girdle. This is not the case. The girdle is wide and irregular, having many 3% point-maxima scattered over it.

Sample L-1: Lherzolite of the Etang de Lers (Fig. 29)

This sample was taken from a large block situated near the outlet of the Etang de Lers. Measurement of 200 olivines, 200 enstatites, and 100 diopsides (for the enstatites and diopsides two thin sections were needed) showed that this block was not in its original position. During the last ice age a glacier passed through a narrow gorge just here. It is therefore possible that this block was overturned, which would explain why the S_0 -plane parallel to the γ -girdles of olivine and enstatite strikes ENE-WSW instead of N-S as it does in the nearby region (Fig. 12).

Nevertheless, this sample is dealt with here because of its relative richness in diopsides, which provided an opportunity to measure them in the lherzolite itself. The composition is about 55% olivine, 20% enstatite, 18% diopside, some spinel, and a little hornblende.

Fig. 29. Lherzolite of the Etang de Lers (Sample L-1). 200 α -, β -, and γ -olivine, and 200 α -, β -, and γ -enstatite; contours at 1%, 2%, 3%, 4%, 5%, and 6% per 1% area. 100 α -, β -, γ -, [100]-, poles to {100}, and [001]-diopside; contours at 1% (dashed lines), 2%, 3%, 4%, and 5% per 1% area.

Olivine. — A well-defined α -girdle contains a weak point-maximum, reaching only 4%. The β -pattern shows a very irregular girdle roughly parallel to the α -girdle. The γ -olivine has a weak and incomplete girdle, whose pole coincides with the α -point-maximum, containing a broad point-maximum of up to 5% within it.

The average grain shape is a triaxial ellipsoid with axes of 1.2, 1.8, and 1.0 mm in the direction of a , b , and c , respectively.

Enstatite. — The α - and β -diagrams show random orientations. The γ -pattern has a rather well-developed girdle parallel to the γ -olivine girdle; a point-maximum concentration of up to 4% coincides with the γ -olivine point-maximum.

Diopside. — The α -pattern resembles a girdle parallel to the α -olivine girdle. The maximum concentration of up to 5% also coincides with the α -olivine point-maximum. The β -orientation seems to be random, whereas γ has a conspicuous girdle parallel to that of γ -olivine, although there is no pronounced point-maximum.

From measurements of {110}- or {100}-cleavages the crystallographic axes were constructed. When impossible to measure, the {100}-cleavages of the diopsides were constructed to examine whether the orientation of diopside was determined by its crystallographic axes, its optic elasticity axes, or its {100}-cleavages. Although the angle between [100] and α is only 26°, the [100]-orientation is less pronounced than the α -orientation. The poles to {100}-cleavages also seem to have a random orientation. The [001] of diopside are concentrated in a girdle parallel to the γ -diopside girdle, although the [001]-girdle is much wider. If it were as narrow as the γ -girdle, there would be a pronounced β -point-maximum, γ and [001] lying in the plane normal to β . This is not the case. Therefore, the optic elasticity axes must have been much more directly involved in the orienting mechanism that caused this fabric than the crystallographic axes or the {100}-cleavages.

Sample L-53¹: Lherzolite of the Etang de Lers (Fig. 30)

This sample contains about 75% olivine, 15% enstatite, 7% diopside, and little spinel and hornblende. Serpentinization is rather strong along S_0 - and S_1 -cleavage planes. The S_3 -cleavage is less evident. Two hundred olivines and 200 enstatites were measured.

Olivine. — A well-developed α -girdle perpendicular to both the layering S_L and the S_0 -cleavage has maximum concentrations of up to 5% lying perpendicular to S_L and S_0 . According to the results of the fabric analyses of the two folds (Figs. 24 and 25), it may be concluded that the fabric is dependent on the axial-plane cleavage S_0 rather than on the layering S_L . The split maximum of α must therefore be an accidental phenomenon. The β -pattern is irregular,

but somewhat resembles the α -girdle. The γ -girdle more parallel to S_0 than to S_L is weak and complete, whereas a strong 8% point-maximum almost coincides with the intersection of cleavage S_0 and layering S_L , which strikes N-S, dipping some 30° to the east. The axes of the triaxial ellipsoid representative of the average grain shape are 1.7, 2.4, and 1.2 mm long, in the fabric direction a , b , and c , respectively.

Enstatite. — Of the two similar α - and β -girdles, the α -girdle is better developed, showing no definite maxima. The γ -girdle is very similar to the γ -olivine girdle, except that the peak near the intersection of

S_L and S_0 is not so high. However, in the south there is a stronger concentration (up to 4%) than is found in the eastern quadrants of the diagram. The diagram, constructed from 400 poles to the $\{110\}$ -cleavages, shows an irregular girdle, parallel to the α -enstatite girdle without maxima.

Sample L-53²: Spinel pyroxenite of the Etang de Lers (Fig. 31)

In the preceding hand specimen the lherzolite has a 2 cm wide layer of spinel pyroxenite in which 150 enstatites and 150 diopsides were measured. This rock is so coarsely-grained that three thin sections were needed to complete the measurements.

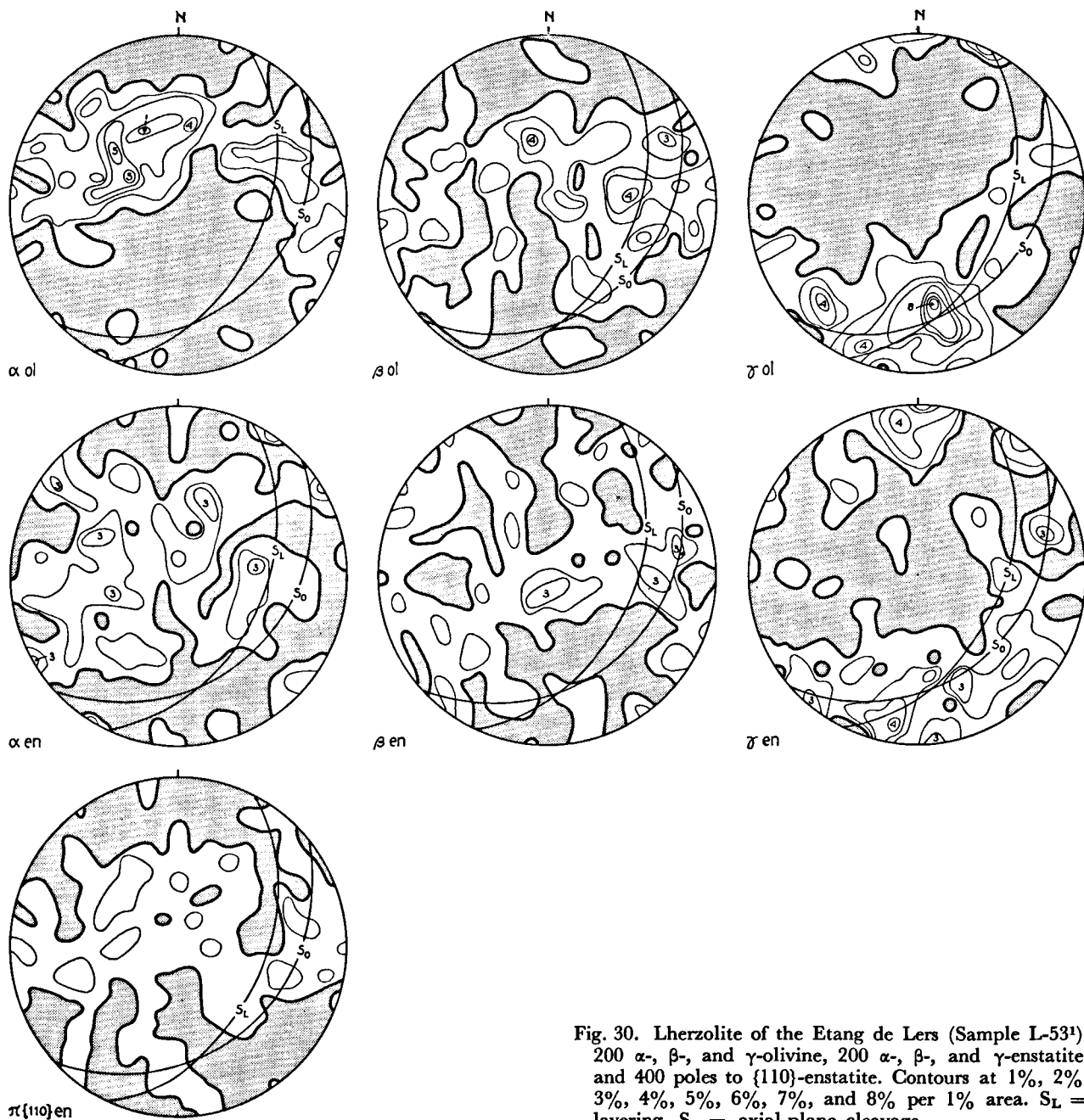


Fig. 30. Lherzolite of the Etang de Lers (Sample L-53¹). 200 α -, β -, and γ -olivine, 200 α -, β -, and γ -enstatite, and 400 poles to $\{110\}$ -enstatite. Contours at 1%, 2%, 3%, 4%, 5%, 6%, 7%, and 8% per 1% area. S_L = layering, S_0 = axial-plane cleavage.

The spinel pyroxenites seem to be far less tectonized than the lherzolites. No granulation zones occur. The Alpine cleavages cut across the grains without contorting them. The grains are barely tabular or elongate, being almost equidimensional. This rock contains about 40% enstatite, 55% diopside, and 5% spinel.

Enstatite. — The α -orientation forms a very irregular girdle perpendicular to S_0 without pronounced point-maxima. The β -pattern seems to consist of an in-

complete girdle perpendicular to S_0 and to the α -girdle. However, this could be a chance orientation. The γ -orientation is the best developed, showing a complete, rather regular girdle in the cleavage plane S_0 and layering S_L . Some 4% point-maxima occur but deviate considerably from the cleavage-layering intersection.

Diopside. — Measurement of 150 grains does not seem sufficient to give a clear picture of the fabric. The α

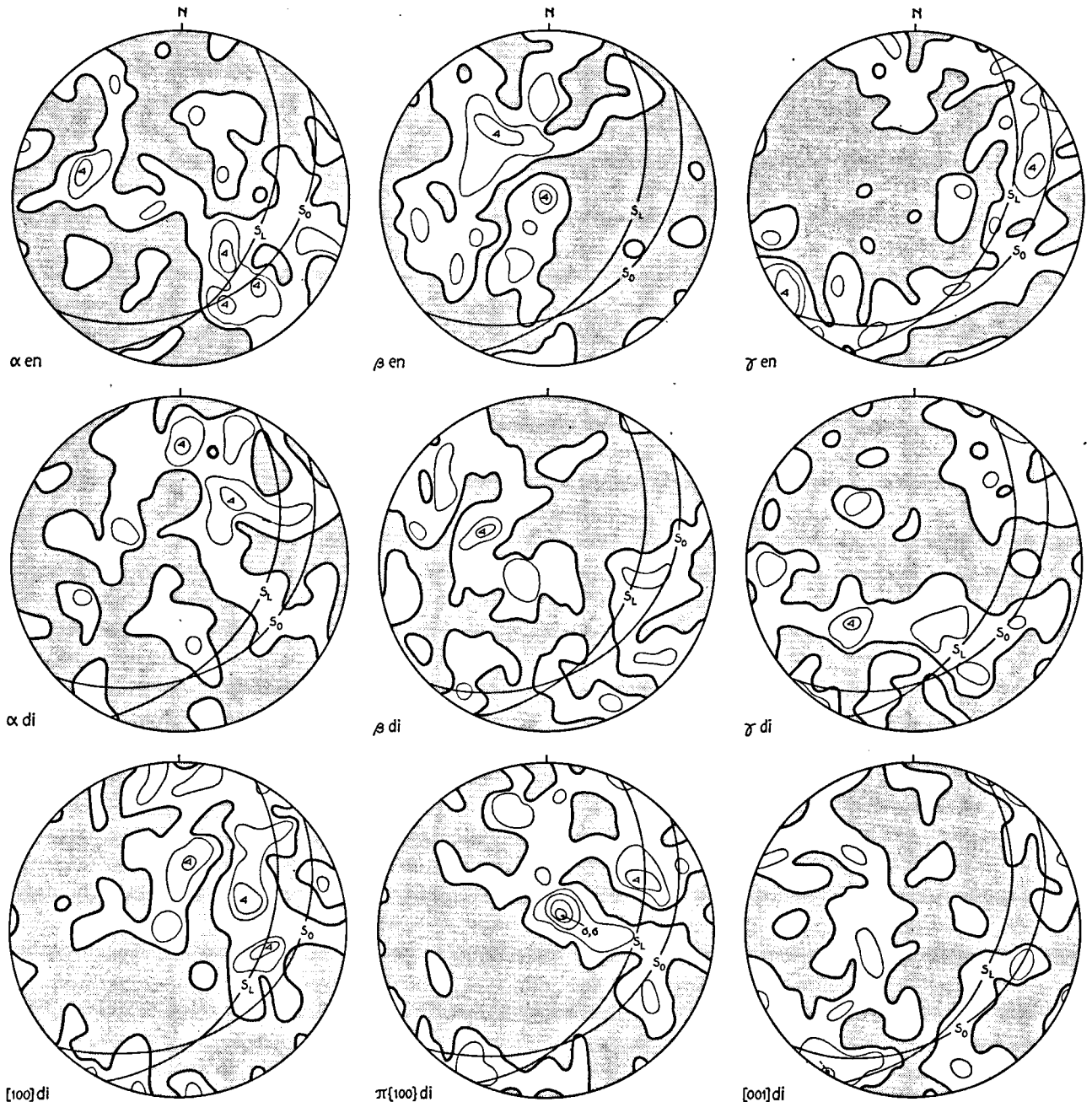
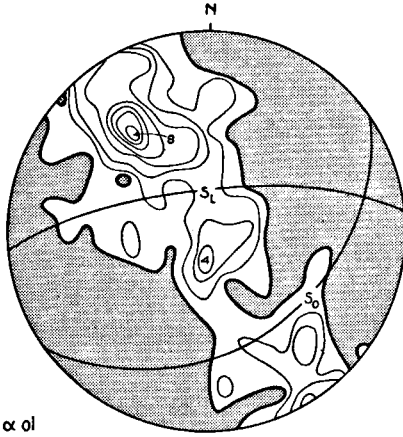
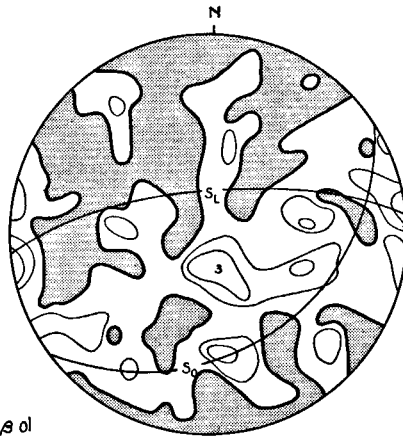


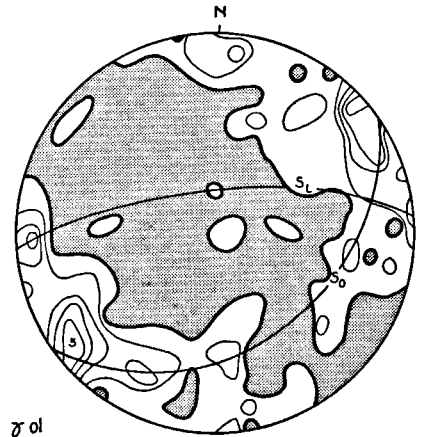
Fig. 31. Spinel pyroxenite of the Etang de Lers (Sample L-53^a). 150 α -, β -, and γ -enstatite and 150 α -, β -, γ -, [100]-, poles to {100}, and [001]-diopside. Contours at 1.3%, 2.6%, 4.0%, 5.3%, and 6.6% per 1% area. S_L = layering, S_0 = axial-plane cleavage.



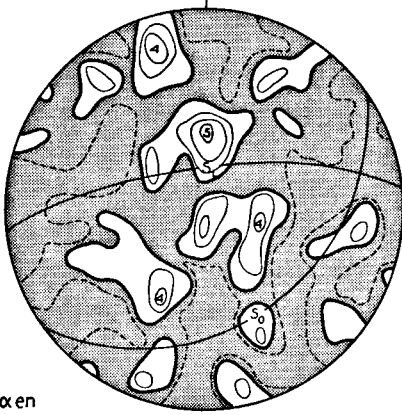
α ol



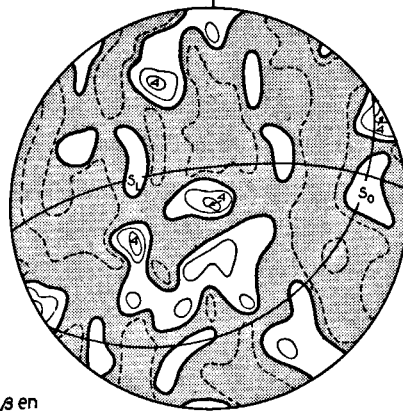
β ol



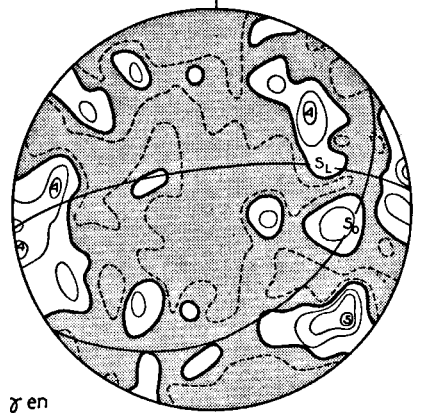
γ ol



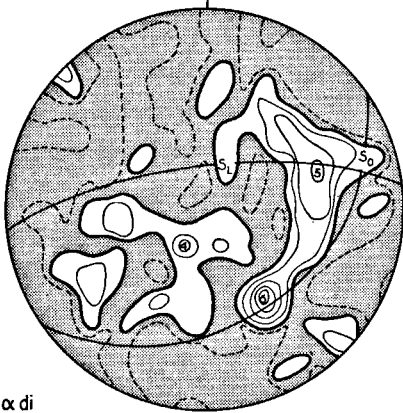
α en



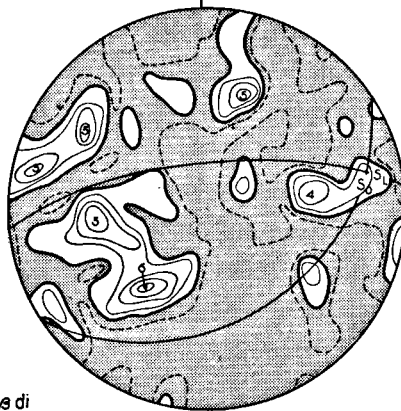
β en



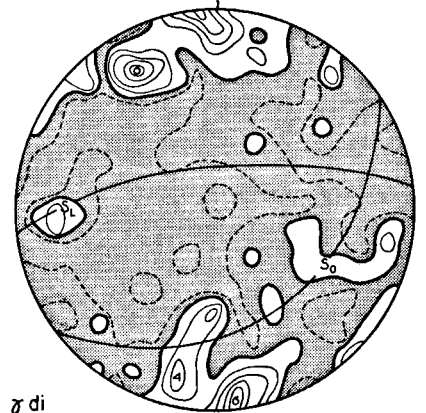
γ en



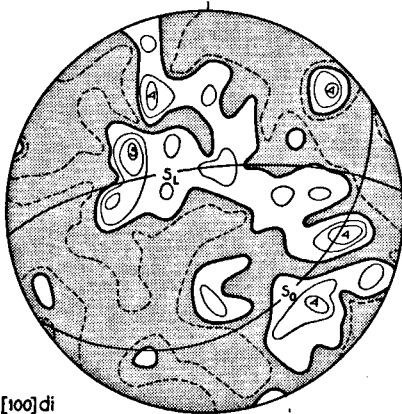
α di



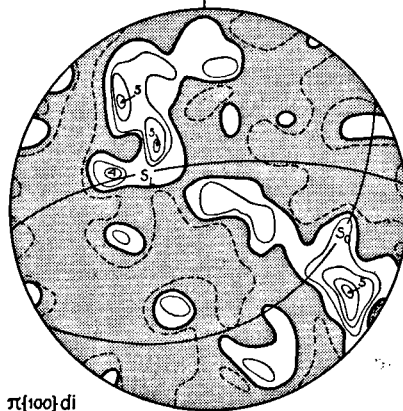
β di



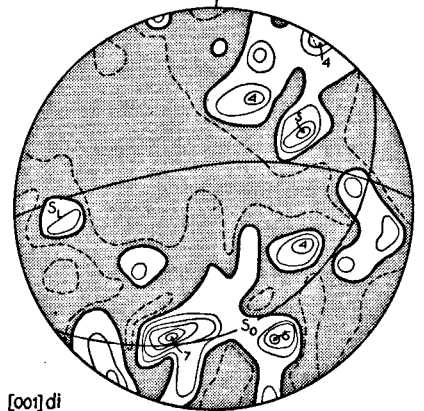
γ di



[100] di



$\pi\{100\}$ di



[001] di

and β are too randomly oriented to permit description. Only γ seems to have a girdle orientation parallel to the γ -enstatite girdle, but it is a very incomplete one. The diagrams of [100] and the poles to {100} have irregular concentrations in the northern and north-eastern quadrants. Although the [001] could have a cleft-girdle orientation, it is believed that this is also a random orientation.

Sample L-17: Lherzolite with spinel pyroxenite of the Etang de Lers (Fig. 32)

This sample of lherzolite contains about 60% olivine, 20% enstatite, 13% diopside, 5% spinel, and some hornblende. Apart from the S_0 -cleavages, only the S_3 has been developed. The influence of the latter is very weak. Two hundred olivines were measured. In this sample a 10 cm wide layer of spinel pyroxenite occurs. The layering strikes almost E-W, dipping 73° to the N; the S_0 -cleavage strikes ENE-WSW and dips 40° to the SSE. In the pyroxenite, 100 enstatites and 100 diopsides were measured.

Olivine. — An 8% point-maximum of α , lying in a perfect girdle, tends to be perpendicular to the S_0 -cleavage. The β -pattern is irregular, but has a weak preferred girdle orientation in the S_0 -cleavage plane. The γ -olivine has an almost perfect girdle orientation in the cleavage plane, with a 5% point-maximum not far from the cleavage-layering intersection.

The average grain shape of the olivines is a triaxial ellipsoid, whose axes are 1.1, 1.5, and 0.9 mm long in the fabric directions a , b , and c , respectively.

The pyroxenes in the pyroxenite have an almost equidimensional shape. This rock has a composition similar to that of the other spinel pyroxenite.

Enstatite. — The enstatite fabric of the spinel pyroxenite has an almost random orientation, although a very weak concentration of α near the α -girdle of olivine and of γ near the γ -girdle of olivine, can be distinguished. There are no pronounced maxima.

Diopside. — In the diopside, the crystallographic axes are better oriented than the optic elasticity axes. Thus, [100] tends to lie in a girdle parallel to the α -olivine girdle. Because of the fact that the poles to {100} make only a small angle (16°) with [100], the {100} diagram shows the same girdle. The degree of preferred orientation in a girdle lying in the cleavage plane is almost the same for γ and [001].

Fig. 32. Lherzolite and spinel pyroxenite of the Etang de Lers (Sample L-17). 200 α -, β -, and γ -olivine from the lherzolite; contours at 1%, 2%, 3%, 4%, 5%, 6%, 7%, and 8% per 1% area. 100 α -, β -, and γ -enstatite and 100 α -, β -, γ -, [100]-, poles to {100}, and [001]-diopside from the spinel pyroxenite; contours at 1% (dashed lines), 2%, 3%, 4%, 5%, 6%, and 7% per 1% area. S_L = layering, S_0 = axial-plane cleavage.

Sample L-34: Lherzolite and garnet pyroxenite of the Etang de Lers (Fig. 33)

These are in fact two samples from one outcrop, one from a lherzolite, the other from a 40 cm wide layer of garnet pyroxenite. In both, the layering makes a very small angle with the cleavage S_0 ; the Alpine E-W-striking cleavage S_1 is very distinct and the N-S-cleavage S_3 is visible. In the lherzolite, which contains about 75% olivine, 15% enstatite, 5% diopside, and 5% spinel, 200 olivines and 200 enstatites, and in the garnet pyroxenite, which contains about 60% diopside and 40% garnet, 100 diopsides were measured.

Olivine. — A distinct girdle of α lies perpendicular to S_L and the S_0 -cleavage. The higher concentrations in this girdle tend to lie near the poles to layering and cleavage plane. The γ -olivine is concentrated in one large point-maximum with a peak of 7% coinciding with the cleavage-layering intersection. The β -olivine tends to lie in two girdles, one parallel to the α -girdle, the other parallel to the S_0 -cleavage plane. The average dimensions of the olivines are 1.9, 2.5, and 1.2 mm in the directions of fabric a , b , and c , respectively.

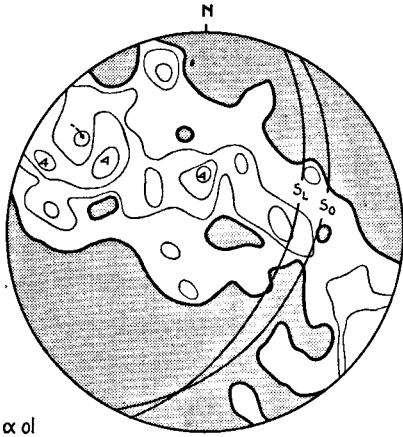
Enstatite. — The enstatite fabric of the lherzolite has a very weak preferred orientation, although it shows some similarity to the olivine fabric: very wide and poorly-developed α - and β -girdles parallel to the α -olivine girdle, γ having something of a girdle parallel to S_L and S_0 showing a point-maximum of only 3% parallel to the γ -olivine point-maximum.

Diopside. — The diopsides in the garnet pyroxenite show a very peculiar fabric. The optic elasticity axes have much stronger preferred orientations than the crystallographic axes. The α , β , and γ have distinct point-maxima of up to 7%, 7%, and 10%, respectively, without definite girdle patterns except for β . The conspicuous γ -point-maximum is parallel to the γ -olivine point-maximum. The α -point-maximum, however, makes an angle with the α -olivine point-maximum and with the poles to the layering and S_0 -cleavage plane. In the β diagram a very incomplete girdle can be distinguished, lying parallel to the α -olivine girdle. Since α , β , and γ have such pronounced maxima, the diagrams for [100], [001], and the poles to {100} cannot have a random orientation. The [100]-pattern shows a cleft-girdle around the α -point-maximum, and the poles to {100} lie in a great-circle girdle whose pole coincides with the β -point-maximum. The [001]-pattern is very irregular, showing an imperfect girdle parallel to the {100}-girdle.

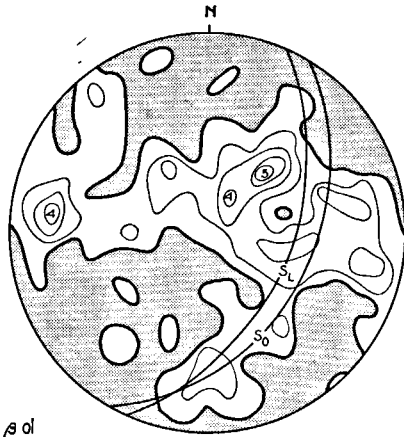
CONCLUSIONS BASED ON THE FABRICS

Olivine

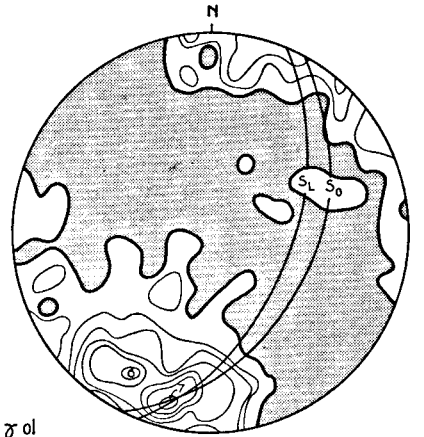
The results show conclusively that the orientation of olivine is directly dependent on the pre-Alpine axial-plane cleavage S_0 and is only indirectly related to the



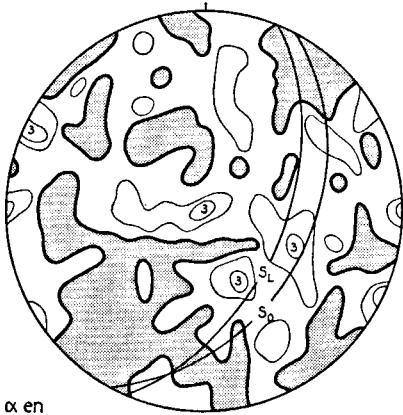
α ol



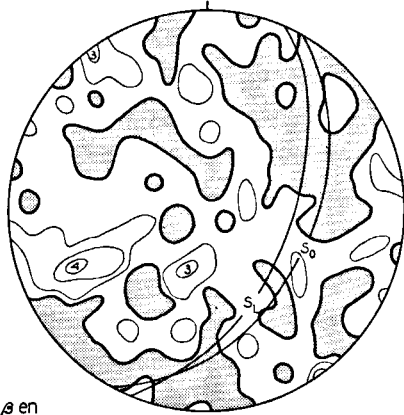
β ol



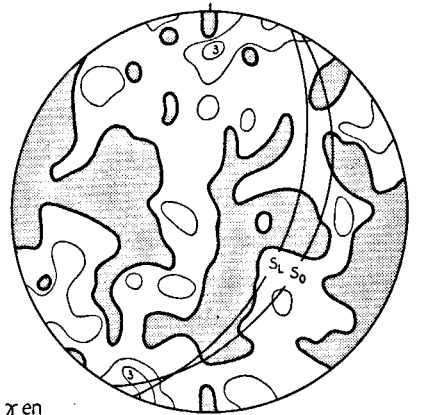
γ ol



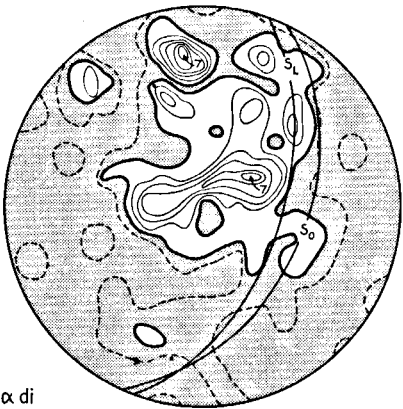
α en



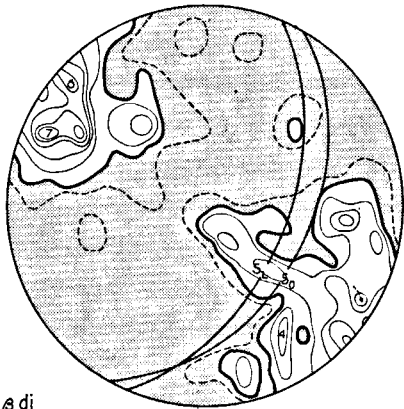
β en



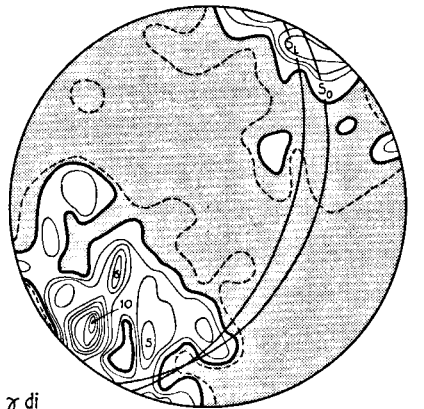
γ en



α di



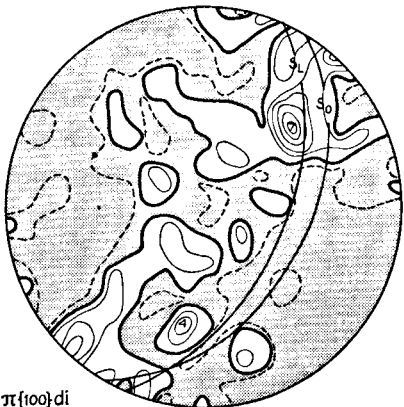
β di



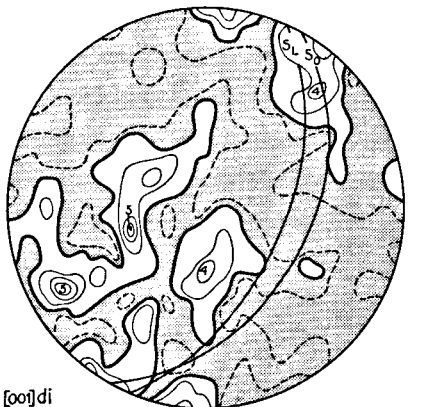
γ di



[100] di



π {100} di



[001] di

layering S_L . Because the lherzolites were folded isoclinally, the axial-plane cleavage is almost always parallel to the layering, but in the two examples of fold hinges (Fig. 24: L-48 and Fig. 25: L-102) it is evident that the fabric is asymmetrical with respect to the layering and follows the cleavage.

There are two types of preferred orientations of olivine, with a series of transitions. The first type shows an excellent α -point-maximum perpendicular to the cleavage and β - and γ -girdles in the plane of the cleavage; α has no girdle, and β and γ have no pronounced point-maxima (Fig. 19: V-42): The second type has a definite γ -point-maximum, without a girdle, lying in the cleavage plane and making no angle or only a small one with the fold axis, the cleavage-layering intersection, or the fold mullions, and has α - and β -girdles whose axes coincide with the γ -point-maximum. In these two girdles there are no pronounced point-maxima (Fig. 23: L-59-b, Fig. 26: L-88, Fig. 33: L-34).

All forms of transition between these two types are present (Fig. 20: V-75, Fig. 21: V-76, Fig. 22: L-61, Fig. 23: L-59-a, c, Fig. 24: L-48, Fig. 25: L-102, Fig. 27: L-62, Fig. 28: L-23, Fig. 29: L-1, Fig. 30: L-53¹, Fig. 32: L-17). In most cases there are α -girdles with distinct point-maxima, perpendicular to the cleavage, and γ -girdles in the cleavage plane with a point-maximum near the cleavage-layering intersection. The β -pattern is mostly irregular and sometimes shows two girdles, one parallel to the α -girdle, the other parallel to the γ -girdle; at the intersection of these two girdles there is sometimes a relative point-maximum.

The most pronounced γ -point-maximum occurs in the harzburgitic variety (L-88, Fig. 26). This rock was much more strongly deformed than the other rocks, as judged from the marked fissility along the S_0 -cleavage planes and the breaking up of the pyroxenite layers into mullions. Conceivably, the harzburgitic variety was less competent and therefore more susceptible to penetrative deformation.

The equally pronounced γ -point-maximum of L-34 (Fig. 33) in the lherzolite could have originated from a stronger deformation in a narrow zone. The lherzolites in which the S_0 -cleavage is weakest usually have a pronounced α -point-maximum, without a girdle, whereas the γ -girdle does not show much of a point-maximum.

Some instances suggest a negative correlation between the strength of the γ - and α -point-maxima, or that the γ -point-maximum becomes stronger with decreasing strength of the α -point-maximum. A graph was

constructed to investigate this possibility (Fig. 34, a). The following procedure was applied: in a stereographic projection of the α - and γ -axes of olivine, small-circles with an angular radius of 20° were drawn around the fabric c -axis (or the pole to S_0) and the fabric b -axis (or the point-maximum of γ), respectively; the percentage of points lying inside of these small-circles is a measure of the strength of the α - or of the γ -point-maximum. On the ordinate (y) of the graph the percentages of α -olivine within the small-circle around c are plotted, and on the abscissa (x) the percentages of γ -olivine within the small-circle around b . However, none of the statistical tests gave a correlation factor, so α and γ may be independent.

Enstatite

Enstatites were measured in eight samples: Fig. 21: L-76, Fig. 27: L-62, Fig. 28: L-23, Fig. 29: L-1, Fig. 30: L-53¹, Fig. 31: L-53², Fig. 32: L-17, Fig. 33: L-34. The fabric diagrams of enstatite are a weak reflection of the olivine fabrics. The most persistent character of enstatite orientations is the γ -girdle always lying parallel to the γ -olivine girdle. Often, there is a point-maximum in the girdle, also parallel to the γ -olivine point-maximum or cleavage-layering intersection. The enstatite orientations in the spinel pyroxenite layers are much weaker; they have no pronounced point-maximum in their γ -girdle. The α -enstatite usually has a girdle parallel to the α -olivine girdle, nearly always without a pronounced point-maximum; only in Fig. 27 (L-62) there is a strong point-maximum near the α -olivine maximum. The β has in general a random orientation, although in some cases a weak girdle parallel to the α -girdle is distinguishable. In one case (Fig. 31: L-53²) in a spinel pyroxenite, β -enstatite seems to have a girdle perpendicular to both the α - and the γ -girdle, but this is probably an accidental phenomenon.

In two cases the $\{110\}$ -cleavages were measured. There are no signs that $\{110\}$ -cleavages of enstatite are important elements of the orientational mechanism that gave rise to the fabric. Because of the strong γ -concentration of enstatite, there is a well-developed girdle of the poles to the $\{110\}$ -cleavages, perpendicular to the γ -point-maximum. If one or both of the orthogonal $\{110\}$ -cleavages tended to lie in the S_0 -cleavage plane, the girdle would show two point-maxima, one perpendicular to and one lying in the plane of the S_0 -cleavage. If the $\{110\}$ -cleavages lay symmetrical with respect to this plane, there would be two point-maxima in the girdle, each making an angle of 45° to the pole to S_0 . This not being the case here, i.e. the girdle having no definite point-maxima, rotation of the $\{110\}$ -cleavages by recrystallization or by flow gliding cannot be held responsible for the observed fabric of enstatite. This is corroborated by the fact that α and β have girdles lacking definite point-maxima.

The orientation patterns of enstatite in the lherzolite are in complete accordance with the orientation of

Fig. 33. Lherzolite and garnet pyroxenite of the Etang de Lers (Sample L-34). 200 α -, β -, and γ -olivine and 200 α -, β -, and γ -enstatite from the lherzolite; contours at 1%, 2%, 3%, 4%, 5%, 6%, and 7% per 1% area. 100 α -, β -, γ -, $[100]$ -, poles to $\{100\}$, and $[001]$ -diopside from the garnet pyroxenite; contours at 1% (dashed lines), 2%, 3%, 4%, 5%, 6%, 7%, 8%, 9%, and 10% per 1% area. S_L = layering, S_0 = axial-plane cleavage.

olivine, except that the enstatite fabrics are weaker. Collée (1962) found agreement between β -enstatite and α -olivine in his samples. The present study does not support this. The α - and γ -enstatite orientations coincide with the α - and γ -olivine orientations, respectively. The orientation patterns of enstatite in the spinel pyroxenite layers are also the same, but even weaker. The pyroxenites appear to have been far more competent and less susceptible to deformation and metamorphism than the lherzolites.

Diopside

Diopsides were measured in four samples, one from a lherzolite (Fig. 29: L-1), two from spinel pyroxenites (Fig. 31: L-53^a and Fig. 32: L-17), and one from a garnet pyroxenite (Fig. 33: L-34). In most cases the orientation of the optic elasticity axes of diopside is better than of the crystallographic axes. The former lie parallel to the olivine and enstatite orientations. Therefore, γ -diopside in general shows girdles parallel to the γ -olivine and γ -enstatite girdles, although without a point-maximum. L-34 is an exception; here only a very pronounced γ -point-maximum occurs, parallel to and having the same shape as the γ -olivine point-maximum. The α -diopside also shows a girdle orientation parallel to the α -olivine orientation, sometimes with a point-maximum in the same direction as the α -olivine point-maximum within the girdle. The orientation pattern of α in the garnet pyroxenite is again extreme: a point-maximum lying somewhat asymmetrically disposed with respect to the cleavage plane. It is believed that the deformation in this locality was much stronger than elsewhere, resulting also in the extreme γ -olivine point-maximum. The orientation of β -diopside is often random, once again with the exception of the diopside in the garnet pyroxenite.

In L-17 (Fig. 32) the crystallographic axes [100] and [001] seem to show a preferred orientation more strongly than α and γ . The [001]-girdle lies parallel to the γ -olivine girdle, and [100] and the poles to {100} show girdles parallel to α -olivine.

GRAIN SHAPE

In all samples of lherzolite subjected to fabric analysis, the average shape of the olivine grains was evaluated. The olivines are never idiomorphic. Their boundaries are often irregular and ragged, but they always have approximately the same shape; they are tabular parallel to the pre-Alpine S_0 -cleavage (fabric *ab*), and somewhat elongate parallel to the γ -point-maximum (fabric *b*). An important fact is that the elongation in *b* increases with increasing strength of the γ -point-maximum. This is shown clearly by the graph in Fig. 34, b. The average length-width ratio (*b/c*) of olivine grains in the S_0 -plane is plotted along the ordinate (*y*); on the abscissa (*x*) the strength of the γ -point-maximum. The resulting graph shows a strongly positive correlation, according to Kendall's

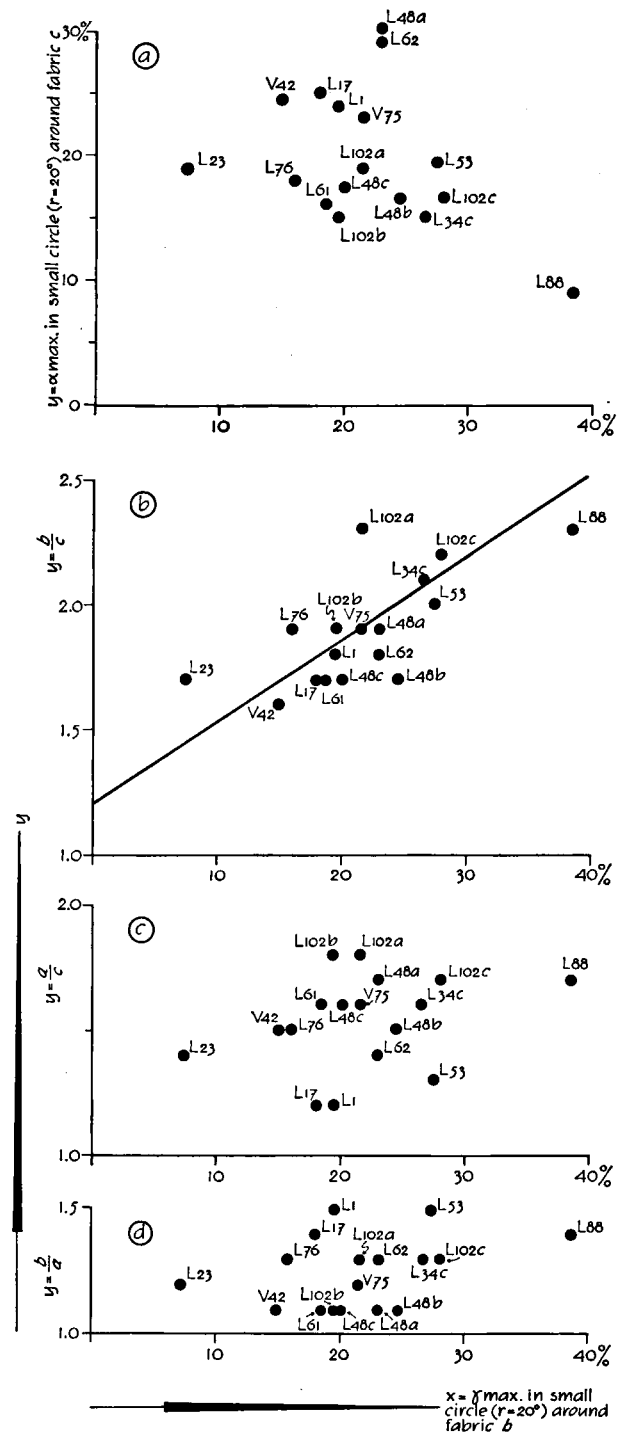


Fig. 34. a. Relative strength of the α - and γ -concentrations near the directions of *c* and *b*, respectively. b. *b/c*-ratio against the strength of the γ -point-maxima. c. *a/c*-ratio against the strength of the γ -point-maxima. d. *b/a*-ratio against the strength of the γ -point-maxima. (See page 43.)

test. There is no such correlation between the *a/c*-ratio and the strength of the γ -point-maximum (Fig. 34, c), or the *b/a*-ratio (Fig. 34, d).

GRANULATION AND MYLONITIZATION

The lherzolites sometimes contain very finely granulated zones composed of grains so small (0.01 mm) that it is almost impossible to determine them. Recrystallization seems to have taken place in these zones, giving rise to some sort of mosaic texture, but the minuteness of the grains made it impossible to measure the direction of their optic elasticity axes with the universal stage. These zones are almost never serpentinized; serpentinization occurred only along cracks and Alpine cleavages, but then much more weakly than in the larger neighbouring olivine grains. Recrystallization probably changed these zones into well-knit masses (Bowen and Tuttle, 1949) without channels offering access to serpentinizing agents. An occasional fine-grained granulated zone has a central aphanitic zone containing some large eyes, mostly of clinopyroxene, orthopyroxene, and spinel, but sometimes even with olivine, surrounded by flow lines (Plate VI, c and d). The aphanitic part, according to an X-ray powder diagram, contains only olivine with some orthopyroxene. Such zones are clearly mylonitic. Photographs of mylonites from the Totalp serpentinite (Peters, 1963) and from the dunite of St. Paul's Rocks (Tilley, 1947) closely resemble those found at Lers. A pronounced preferred orientation of olivine (and possibly of enstatite) is visible under the microscope upon insertion of the gypsum plate. Inspection of several thin sections, all of them taken perpendicular to the cleavage plane of these mylonites, suggests a strong α -point-maximum perpendicular to this plane, a result similar to that recorded by Tilley (1947).

The granulated and mylonitized zones cut across the lherzolites, contorting and rotating the pre-existing grains. Mylonitization is therefore considered to have taken place after the deformational phase that caused the over-all fabric of the rock, but before the Alpine phases. The Alpine S_1 - and S_3 -cleavages are indeed observed to cut across the mylonite zones.

GEOLOGICAL EVIDENCE DERIVED FROM THE FABRIC ANALYSES

Collée (1962) supposed that the fabric of the lherzolites was originated by the Alpine orogeny. His interpretation was based on the fact that in most parts of the Etang de Lers locality, the γ -point-maxima for olivine show a NE-SW orientation parallel to the F_1 -direction of Alpine major stress. For other localities and the eastern and western part of the lherzolite of the Etang de Lers, it has now been demonstrated that the γ -point-maxima are unrelated to the Alpine directions. The fact that almost all the lherzolites have a border zone of lherzolititic breccia points to a relation between the intrusion of the lherzolite and the origin of this breccia. Fig. 23 shows the results of fabric analyses of some inclusions from the breccia. It is evident that the fabric is older than the brecciation, because of the totally different orientation of the fabric patterns and the layering. It may there-

fore be concluded that both the fabric and the layering are older, pre-Alpine features. From Figs. 24 and 25, in which fabrics of lherzolite samples from different places in a fold are shown, it is evident that the layering is even older than the fabric. There are no traces of an older fabric showing a correlation with the layering. The fabric of the lherzolites was caused by the same orogenic phase that folded and metamorphosed the lherzolites.

It has already been mentioned (Chapter IV) that from the structural evidence it seems impossible to find any other explanation for the emplacement of the lherzolites than solid intrusion. The fabric data of the lherzolites make this conclusion even more definite.

A peculiar structural feature is the northward or eastward plunge direction of the fold axes in the lherzolites of the Etang de Lers; the γ -point-maxima of olivine either plunge mainly to the south or west or are horizontal, creating a constant discrepancy between the fold axes and the γ -point-maxima. In the lherzolite of the Forêt de Freychinède (Fig. 25) the difference is even much greater. There are two possible explanations for this discrepancy: 1. the stress field causing the folding was slightly modified after the folding to create the S_0 -cleavage and the fabrics; 2. the fold axes were contemporaneous with but not parallel to the deformation axis, i.e. the layering was already tilted before the folding. The second alternative seems more probable. An illustration of how this situation could have originated is shown in Fig. 35, which is a simplified drawing after Ramsay (1960). The deformation axis would then be parallel to the γ -point-maxima, and this is demonstrated convincingly by sample L-88 (Fig. 26), where

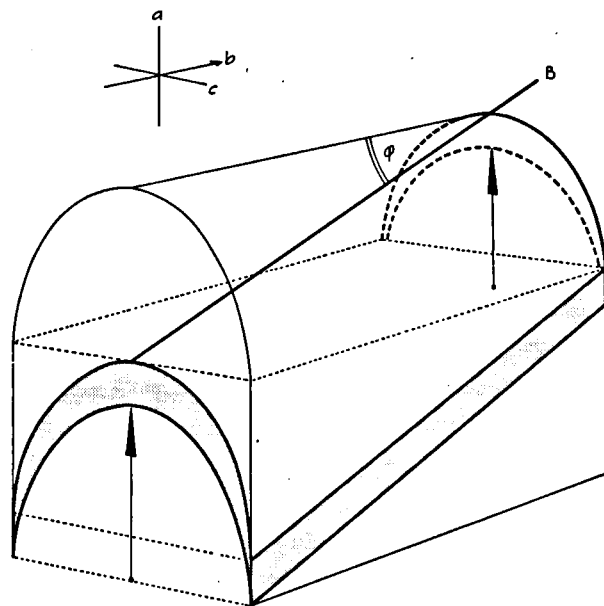


Fig. 35. A similar fold whose axis (B) makes an angle (ϕ) with the fabric b or deformation axis because of tilting before folding (after Ramsay, 1960).

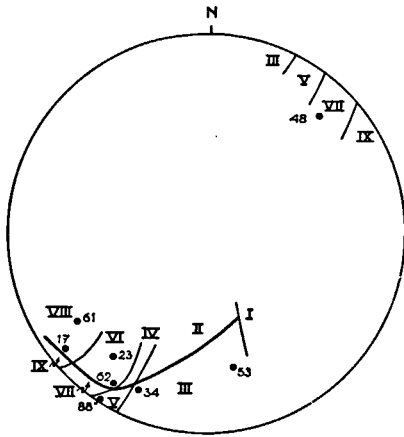


Fig. 36. A composite diagram of the γ -olivine point-maxima of all the samples from the Iherzolite of the Etang de Lers.

a strong γ -olivine point-maximum is almost exactly parallel to the fold nullions.

The slight clock-wise rotation from west to east of the Iherzolite fabric of the Etang de Lers originated after the pre-Alpine metamorphism. This is demonstrated by Fig. 36, where all γ -point-maxima of olivine from the fabric subareas are shown in one diagram, and by the map in Fig. 12. The clock-wise rotation from west to east is the same as in the diagrams containing the poles to β -girdles (Fig. 17, b) and the β -point-maxima (Fig. 17, a) of the layering for each of the nine sectors of the Iherzolite of the Etang de Lers.

COMPARISON WITH OTHER FABRICS FROM THE LITERATURE

Olivine

There is an extensive literature on the petrofabrics of olivine arising from gravitational accumulation in magmatic intrusions, intrusion of a crystal mush lubricated by interstitial liquid, metamorphism and deformation, as well as on the fabrics of ultramafic inclusions in basalts. Numerous fabric patterns have been recorded, many of them susceptible to more than one explanation. A short review of the previous work will be useful.

Gravitational accumulation. — For many definitely proved magmatic intrusions it has been recorded that olivines have preferred orientations only in the case of a pronounced anisotropic habit. Most olivines have a tabular form parallel to $\{010\}$, from which an α -point-maximum perpendicular to the bedding plane results. In a troctolite from the Wichita Mts. (U.S.A.), Huang and Merrit (1952) found such a pattern, but a sample with equidimensional olivine grains showed no preferred orientation. A slight obliquity and a small deviation of α into a partial girdle could be explained by laminar or turbulent flow during deposition. In basalt dykes and flows, Brothers (1959) found weak α -point-maxima subperpendicular to the

plane of laminar flow, and in 1964 he recorded the same pattern in peridotites and allivalites of Rhum and in a hortonolite ferrogabbro of Skaergaard. The β and γ generally have girdles without definite point-maxima. When there is also a prominent zone-axis $[100]$ or $[001]$ of olivine, a point-maximum of β or γ indicates flow during deposition. Thus, in the Skaergaard sample Brothers recorded a γ -point-maximum parallel to the direction of flow. A β -point-maximum occurs in the diagrams of Huang and Merrit. The habit of olivines in the ultramafic zone of the Stillwater complex is prismatic parallel to $[001]$. Jackson (1961) found β -girdles parallel to the bedding plane (a pronounced γ -point-maximum in one of his samples was attributed to later deformation).

Crystal-mush intrusion. — Many of the intrusions on record cannot have been formed by gravitational accumulation *in situ* but nevertheless contain olivine with a distinct preferred orientation. This orientation could have been caused by intrusion of a crystal mush having some lubricating liquid in the pores. Phillips (1938) thus explained strong α -point-maxima perpendicular to a fissility in certain olivine-rich rocks from Rhum and Skye. In a peridotite from Rhum, Turner (1942) recorded a β -point-maximum parallel to a megascopic lineation, which he thought to be perpendicular to the direction of flow. This mechanism clearly gives rise to fabric patterns with the same symmetry as those derived from laminar flow in a gravity field. In both cases the dimensional habit of the olivines is the controlling factor. This mechanism has been put forward to explain the existence of fissile olivine-rich rocks showing signs of post-crystalline strain and a marked preferred orientation of the minerals, while their country rock lacks any trace of either strain or contact metamorphism, which would have occurred with gravitational accumulation from either a stagnant or a convecting magma. When examination in the field shows that a dyke has intruded into the country rock, the crystal-mush hypothesis seems acceptable. This hypothesis, however, has often been applied to "Alpine-type" peridotites without exact knowledge of the field relations.

Olivine tectonites. — The first to describe tectonite fabrics of olivine were Andreatta (1934) and Ernst (1935), who recorded strong α -point-maxima perpendicular to a schistosity plane, often accompanied by partial or complete girdles. Usually, however, the α -girdles were caused by the development of point-maxima, normal to the α -girdle, of β or γ . Yoshino (1961, 1964), in studying non-fissile dunites of Higashiakaishiyama in Japan, found distinct α -point-maxima perpendicular to schistosity planes in nearby amphibolites which he thought to be related to the dunites. In general, α -girdles are also present, whereas β -girdles lie parallel to the schistosity planes, often with a distinct β -point-maximum parallel to the fold axes in the amphibolites. Ladurner (1956) reported that a pyroxene-olivine rock from Seefeldler Alpe

(Austria) showed a β -point-maximum of olivine parallel to a lineation. Turner (1942) and Battey (1960) described olivine fabrics from the dunite of Dun Mountain in New Zealand, in which strong γ -point-maxima seem to lie parallel to the regional fold axis. Paulitsch (1953) observed in a dunite from Greece a γ -point-maximum of olivine parallel to the cleavage-bedding intersection, while β forms a point-maximum within a partial girdle perpendicular to the cleavage. Raleigh (1963, 1965) studied a harzburgite from Cypress Island (Washington State, U.S.A.) and found a γ -point-maximum parallel to fold axes of some asymmetrical, isoclinal folds, whereas α -girdles and α -point-maxima lay perpendicular to the axial plane.

The lherzolites from the Pyrenees. — The preceding review of the literature on fabric patterns and their supposed modes of origin, makes it possible to discard various possibilities in attempting to deduce the probable mode of origin of the lherzolite fabrics. The question may now be asked: Did the fabric of the lherzolites originate by gravitational accumulation, from a crystal-mush intrusion, or is it a tectonite fabric?

The fabric of olivine has been shown to consist of an α -point-maximum within a partial or complete girdle perpendicular to the axial-plane cleavage of small asymmetrical, isoclinal folds, and a γ -girdle parallel to the cleavage, often with a point-maximum parallel to the fold axis or the longest diameter of the olivine grains. In zones where deformation appears to have been stronger, the γ -point-maximum is more pronounced.

Comparison of these fabrics with depositional and appositional fabrics reveals many points of agreement. An α -point-maximum has been recorded in several instances for which gravitational accumulation is evident. The axial-plane cleavage resembles the foliation due to the tabular habit prevailing in certain olivine accumulations. The asymmetrical folds could be explained as slump structures. The fabric in the fold hinges could be explained by gliding of the tabular grains over each other, with the result that even in fold hinges the tablets remained parallel. The γ -point-maximum parallel to the fold axis could be explained by the elongate habit of the olivines in this direction. In sediments where pebbles were rolled over the deposition surface, the longest axis may lie perpendicular to the direction of the flow.

But there are even more arguments against this mode of origin. The very tight isoclinal folds shown in Fig. 16 are not consistent with true slump structures. The axial plane of normal slump structures is irregular, which is not the case in the lherzolites. Shear folding in loosely packed material seems improbable. The existence of fold mullions, the strong axial-plane cleavage, and the deformed state of all grains point strongly to a tectonic origin of the fabric. The average grain shape is a triaxial ellipsoid having a strongly pronounced preferred orientation, while the axes of

this ellipsoid never lie exactly parallel to the crystallographic axes of the grains concerned (Plate VI, a and b). Furthermore, the clinopyroxenes are not oriented parallel to their morphological forms or crystallographic habit, as in Skaergaard (Brothers, 1964), but parallel to their optic elasticity axes. This, too, supports a tectonic or metamorphic origin of the fabric.

Comparison of the fabric of lherzolites with the fabrics of rocks caused by crystal-mush intrusion again reveals many similarities but even more dissimilarities. Again, the α - and γ -point-maxima are recorded for rocks presumed to be crystal-mush intrusions. But these, too, are primary dimensional fabrics, and the fabric of the lherzolites is not a primary dimensional fabric, as has already been stated. The structures, fissility, and even the folds, should be parallel to the wall rock. This is not the case in the lherzolites.

Consequently, there seems only one possible mode of origin, and that is the metamorphic — not, however, caused by the Alpine orogeny. The grade of the Alpine metamorphism is not sufficiently high and, as has been shown in the preceding paragraphs, the fabric is older.

The origin of the layering is another matter. The fabric of the lherzolites is younger than the layering. No traces of an older fabric that could be related to the layering have been found. So again, all modes of origin could be applied to the formation of the layering, but only in a level differing considerably from the present one.

Orthopyroxene

In rocks formed by gravitational accumulation, the same relation holds for the orthopyroxenes as for the olivines: the fabric pattern depends on the crystal habit (Jackson, 1961). It is very probable that the fabrics in rocks originated by crystal-mush intrusion depend on the dimensional habit of the orthopyroxenes. Because it has been concluded that lherzolites are tectonites, the enstatite fabrics given here represent tectonite fabrics. It has been shown that enstatite reacts to stress in the same way as olivines, but that the fabrics of enstatite are much weaker. The orientations of α - and γ -enstatite coincide with those of α - and γ -olivine, while β rarely shows preferred orientation and when it does is always dependent on the relative strength of the α - and γ -point-maxima. Raleigh (1963, 1965) described some enstatite fabrics from Cypress Island (U.S.A.). The γ -enstatite shows a tendency to lie parallel to γ -olivine. Raleigh explained the γ -enstatite point-maximum in a pyroxenite vein, normal to the vein boundary, as a growth fabric; however, this maximum also lies parallel to the γ -olivine point-maximum in the harzburgite, which could point to a tectonite fabric for the vein as well. Collée (1962) described many enstatite fabrics from peridotite inclusions in basalt, and concluded that the inclusions had a tectonite fabric: γ -enstatite shows the same tendencies as γ -olivine, but here the β -

enstatite (= [100]) shows more resemblance to the α -olivine orientation; in some samples, however, the reverse seems true. Perhaps small changes in the physical conditions of the deformation can reverse the relative optic elasticity of α - and β -enstatite.

Clinopyroxene

A depositional or appositional fabric of clinopyroxenes has been reported by Brothers (1964). It is apparent that the orientation of clinopyroxenes is dependent on the crystal habit. Yoshino (1961, 1964) measured only the optic elasticity axes of clinopyroxene. He found a rather wide γ -point-maximum coinciding with the β -olivine point-maximum parallel to the fold axis. Because of the width of the γ -point-maximum, Yoshino thought that a definite [001]-point-maximum existed parallel to the fold axis. The β (= [010]) clinopyroxene seems to be preferentially oriented parallel to the α -olivine point-maximum, perpendicular to a statistical S-plane. It is a pity that no crystallographic axes were constructed. In the present work the directions of the optic elasticity axes seem more important than those of the crystallographic axes during tectonic action. In the Iherzolites γ -diopside seems to be oriented parallel to γ -olivine or the fold axis, while α -diopside has affinities with α -olivine.

MECHANISM CAUSING THE OBSERVED FABRICS

Turner (1942), in describing olivine fabrics from New Zealand, concluded that kink bands parallel to {100} were of deformational origin. The process most likely to have formed them is translation gliding on {010} in the direction of [100] = γ . Another possible glide direction is [001] = β , but this would of course result in {001} kink bands.

Chuboda and Frechen (1950) also described {100} kink bands in olivine due to translation gliding on {010} in the [100] = γ direction, the rotation axis being [001] = β . Deviations in β = [001] directions in different kink bands could have originated from gliding on {010} in the [001] direction, in some places giving rise to a chess-board undulatory extinction pattern.

Because they occur in olivines found in many different rocks (in olivine nodules in basalt, in "Alpine-type" peridotites, and in truly magmatic peridotites), a tectonic origin of the kink bands has been denied by many authors. During gravitational accumulation at high temperatures, small forces, such as load pressure, were thought to be sufficient to produce the kink bands (Frechen, 1963).

Other authors, however, have thought that kink bands result from the same process that produced the whole fabric. Collée (1962) interpreted the fabric of the Pyrenean Iherzolites as having originated by translation gliding in {010} in the direction of γ = [100] and rotation of the {010}-planes into two distinct shear planes. His interpretation, however, rests on the assumption that γ -olivine point-maxima lie parallel

to the axis of major compression of the Alpine orogeny, which is not the case, as has been demonstrated in the present paper.

Griggs *et al.* (1960) carried out deformation experiments on dunites under high pressures and temperatures. After these exposures, olivine grains oriented with γ subparallel to the axis of compression showed strong undulatory extinction caused, according to these authors, by translation gliding on irrational planes.

Continuing these experiments on dunites and on olivine sands, Raleigh (1963) reproduced straight bands of undulatory extinction, kink bands, and thin lamellae, caused by three systems of translation gliding: glide planes (T) = {010}, glide direction (t) = [100]; T = {100}, t = [001]; and T = {100}, t = [010]. The last of these has never been observed in naturally deformed olivines. The system with T = {001} and t = [100] which in natural olivines could operate together with T = {010} and t = [100], giving irrational rotation axes, has not been established clearly in the experimentally deformed olivines. Raleigh thought it possible that even higher temperatures (1400°–1500° C) than he used would be needed for this system to operate. In one olivine crystal more than one system of translation gliding could be responsible for the kinking, although in one kink band a single system predominates.

After comparing his results with glide systems causing preferred orientations in polycrystalline aggregates produced experimentally in cold-worked metals, Raleigh concluded that in uniaxial compression [100] = γ -olivine rotates away from the compression axis, causing γ -girdles normal to the compression axis or a γ -point-maximum near the major axis of extension in a triaxial stress field, i.e. the fold axis. Since in experiments the translation on {010} in the [100] direction appears not to require such extremely high temperatures as does translation gliding on {001} in the [100] direction, rotation of {010} could result in strong [010] = α concentrations parallel to the compression axis and normal to the schistosity plane.

The olivines in the Iherzolites show a distinct elongation parallel to the γ -point-maximum. This preferred dimensional orientation could be caused by external rotation of the grains along translation glide planes. The fact that in extremely deformed areas, for instance near the fold mullions, the *b/c*-ratio (see Fig. 34) is highest and the γ -point-maximum strongest, might be taken to indicate that the fabric resulted from translation gliding during plastic deformation. In general, however, the elongation of the grains deviates more or less significantly from γ (Plate VI, a and b), and observations in other regions have demonstrated the same lattice orientations for olivine grains showing no dimensional orientation. It must therefore be concluded, as Raleigh has tentatively suggested, that translation gliding with rotation cannot be the sole cause of the fabric.

Because olivine is orthorhombic, Raleigh could not establish with certainty which of the two mechanisms — rotation with translation gliding or syntectonic

recrystallization — had been responsible for the observed fabric. However, the fabric pattern of monoclinic crystals such as diopsides should give a more satisfactory answer to this question.

According to deformation experiments done by Griggs and his co-workers (1960), {001}-twinning in diopside could have originated by translation gliding on {001} in the [100] direction. They found this mechanism only in experimentally deformed diopsides and never in nature. Another type of translation gliding occurs parallel to {100} in the [001] direction.

If this latter form is adapted for the assumption of translation gliding as the mechanism responsible for the orientational process, the {100}-planes of diopside would be oriented parallel to the schistosity planes and the [001]-axis parallel to the axis of major extension: in this case the fold axis. However, since in diopside γ shows more orientation parallel to the fold axis than [001] and α has a stronger orientation normal to the schistosity than the poles to {100}, it is evident that rotation and translation gliding during plastic deformation form a highly improbable mechanism to have caused the observed fabrics of the lherzolites.

Furthermore, there is another argument against translation gliding. Following the suggestions of Mügge (1898), Griggs *et al.* (1960) and Turner *et al.* (1960) have shown experimentally that translation gliding in enstatite occurs parallel to {100} in the [001] direction. If rotation and translation gliding had been the orienting mechanism, then β -enstatite (= [100]) would be preferentially oriented normal to the schistosity, as Collée (1962) has recorded for lherzolic inclusions in basalts. The present study, however, has shown that α -enstatite (= [010]) rather than β (= [100]) is oriented normal to the schistosity.

Although more experimental work must be done to provide conclusive evidence, it is highly probable that the only possible mechanism responsible for the fabric is syntectonic recrystallization. The development of kink bands has nothing to do with the primary fabric but is caused by a later post-crystallization deformation that disturbed and disoriented this primary fabric.

In 1959 and 1961 Kamb proposed a thermodynamic theory of preferred lattice orientation produced by crystallization under non-hydrostatic stress. Later, Hartman and den Tex (in press) applied this theory to orthorhombic crystals, more especially to olivine. They calculated the equilibrium shape of olivine grains under uniaxial compression with intergranular liquid, and also under uniaxial compression the thermodynamic equilibrium orientations of the olivine lattice with or without intergranular liquid. According to them, olivine grains dissolved to saturation in an intergranular liquid acquire a fabric habit causing tabular olivines to develop perpendicular to the compression axis, whereas the thermodynamically most stable lattice orientation of olivine is that with α parallel to the unique compression axis. However, α -olivine need not be precisely normal to the tabular shape. The two processes (flattening of the grains and orientation of α) are in fact not immediately

interdependent. This picture is in full agreement with the fabrics and textures of the lherzolites showing only an α -point-maximum of olivine with β - and γ -girdles containing no point-maxima. In the case of uniaxial tension, Hartman and den Tex concluded that growth would occur preferentially in this direction and that a γ -girdle would develop perpendicular to it. Since the long axis of the olivine grains in the lherzolites is parallel to the fold axis or fabric *b*, it may be concluded for the lherzolites that tension took place along this fold axis. Since, however, the stress field was not uniaxial but triaxial, the calculations of Hartman and den Tex are not wholly applicable to the lherzolites. In triaxial stress systems, conceivably, γ -olivine may be preferentially oriented parallel to the least stress deviator.

According to Hartman and den Tex, recrystallization of olivine rocks without intergranular liquid under uniaxial compression or tension would give rise to a γ -point-maximum parallel to this axis, and the grains would more or less retain the same shape. This clearly does not apply to any of the fabric patterns observed in the lherzolites.

Much as further experiments are required to resolve these problems, the present results seem to indicate that syntectonic recrystallization was mainly responsible for the observed fabric and texture of the lherzolites.

OPHITES

Ophitic intrusions occur throughout the Pyrenees. They are not restricted to the narrow Mesozoic belt north of the North-Pyrenean fault. Ophites contain as major components an idiomorphic calcic plagioclase often showing scapolitization, clinopyroxene, and as minor components hornblende, epidote, apatite, and some ore minerals. Other mafic intrusives occur, among them syenites and olivine-basalt dykes. These are very scarce, however.

Many authors, including Lacroix (1901), Zwart (1954), and Ravier (1959), have considered these mafic rocks to be closely related to the lherzolites. Zwart divided the ophites into two groups, one of Triassic, the other of Cretaceous age. He suggested that only the latter were closely related to the lherzolites and that all chemical transitions between ophites and lherzolites exist. He thought that the Cretaceous ophites were the residual gabbroic liquids from a differentiating lherzolic magma.

Petrofabric analyses of these rocks have not been carried out, but it is evident that they have an ophitic texture. The ophites are true magmatic intrusive bodies, and have caused contact metamorphism in the Mesozoic limestones (Monchoux, 1965).

Scapolitization of the plagioclases was believed by Lacroix (1916) to be caused by weathering. It seems most likely that it happened by a pneumatolytic, autometamorphic process. Epidotization of plagioclases has also been attributed to pneumatolytic processes (Riotte and Thiébaud, 1965).

Because the lherzolites underwent an older pre-Alpine deformation and the ophites did not, the relation between them, if any, must be indirect or, in

other words, a common origin could only have taken place deep in the crust or the upper mantle.

CHAPTER VI

ORIGIN AND EMPLACEMENT OF THE LHERZOLITES

The foregoing has shown the lherzolite bodies to contain all the Alpine structures found in the Mesozoic country rocks, but even more older structures than the latter because the Alpine structures cut across them. These older structures in the lherzolites are the layering, isoclinal folding, and axial-plane cleavage. The clock-wise rotation from W to E of all the pre-Alpine structures in the body at the Etang de Lers was probably caused by two other pre-Alpine phases of deformation. The fabric of the lherzolite (and some other associated ultramafic members) is that of a metamorphic tectonite, its orientation depending on the axial-plane cleavage of the pre-Alpine isoclinal folds.

A structural theory of the origin and emplacement of the lherzolites must take into account the pre-Alpine structures of the lherzolites as well as the three factors of brecciation, metamorphism, and lherzolite occurrence.

Emplacement of the lherzolites

Sedimentary origin. — The theory of Longchambon (1912) that the lherzolites are metamorphosed Jurassic dolomites is contradicted by the occurrence of pre-Alpine structures. Furthermore, the Alpine metamorphism was too weak to create such rocks. Elsewhere, lherzolites occur in unmetamorphosed terrains (Monchoux, 1965). Many other objections to this theory have also been put forward (c.f. Ravier, 1959).

Peridotitic magma. — Lacroix (1894, 1894/95) thought that the lherzolites were of igneous origin. The presence of pre-Alpine structures invalidates his theory, as does the occurrence of lherzolites lacking contact aureoles. The fact that the Alpine metamorphism, though definitely dynamo-thermal, is of a very low-pressure type, led Lacroix to think that it was caused by a lherzolithic magma.

Most of these arguments can also be invoked against Hess's theory (1938, 1955) of an intrusion of a more or less hydrous primary peridotitic magma. The Pyrenean lherzolites show little serpentinization and then always along Alpine cleavages. Recently, Hess (1966) withdrew his theory.

Semi-solid or crystal-mush intrusion. — One of the more widely accepted theories concerning the emplacement of "Alpine-type" peridotites explains them as a crystal-mush intrusion (Bowen and Schairer, 1933; 1935;

Bowen and Tuttle, 1949). Ultramafic accumulations differentiated from a basaltic magma could intrude into higher levels, lubricated by intergranular liquids. This would explain the lack of contact metamorphism. Phillips (1938) and Turner (1942) accepted this view. According to them, pronounced fabrics of olivine could originate in this manner and the layered appearance could have been caused by laminar flow. But in that case the layering should be parallel to the contact with the country rock. The strongly discordant nature of all pre-Alpine structures of the lherzolites with respect to the country rock boundary precludes a crystal-mush intrusion, however. There is no indication of later tectonic movement of the lherzolite bodies along faults, the mechanism often brought forward to explain discordancies. The tectonite fabric in folds and the fabric of the lherzolite breccia both point to another mode of origin and emplacement.

Despite these theories, all the features observed in the lherzolite bodies indicate an exclusively solid intrusion. Two agents can cause solid intrusion: tectonic forces and gaseous forces.

Tectonic intrusion. — As already shown, the lherzolite bodies occur only in the northern zone of the narrow E-W-striking Mesozoic belt. This belt is bordered in the south by the North-Pyrenean fault and in the north probably by a detachment plane. There has been a general tendency among geologists to suppose faults along lherzolite occurrences, but it seems unlikely that they are indeed bounded by faults, because the Mesozoic strata are not displaced.

The theory that the lherzolites are tectonic intrusions brought upward along faults (de Roever, 1957) does not apply. The fragments in the breccia rims around the lherzolites are angular, sometimes somewhat rounded, but never elongate or tabular or disposed in a parallel manner. The funnel-shaped brecciated bodies are also incompatible with this theory. Typical sheared contact zones are entirely lacking.

Emplacement caused by gaseous explosions. — The results of the present study support the theory advanced by Ravier (1959). There are many arguments in favour of an emplacement of the lherzolites caused by gaseous explosions. The internal structure of the lherzolites indicates a completely solid intrusion, probably without any intergranular liquid. All ultramafic bodies have an outer rim of breccia or

are totally brecciated. The inner contact between non-brecciated lherzolite and lherzolite breccia is very irregular, but the outer contact between the lherzolite breccia and the marble breccia is very distinct.

Fabric analyses of lherzolite fragments in the breccia show that each fragment has the same fabric, determined by the layering or pre-Alpine cleavage. Their mutual orientations, however, are completely random. Consequently, the fragmentation or brecciation must have taken place after the development of the tectonite fabric. It is clear that the brecciation is causally linked to the emplacement of the lherzolites, because the brecciated zone in the country rocks coincides with the zone containing the lherzolite and each lherzolite body contains a brecciated rim. It is definitely proved in these instances that the lherzolites were emplaced as solid blocks. There are no traces of any intergranular liquid crystallized during the Alpine orogeny.

Therefore, the most likely agent of solid emplacement is gaseous explosions, which would explain all the features described for the lherzolites.

De Cizancourt (1948) summarized the results of a gravity investigation carried out in the French Pyrenees during exploration for oil and gas. He found a relatively strong, positive Bouguer anomaly in the E-W-striking zone coinciding with the zone containing lherzolite, and suggested that a horizontal E-W-trending cylinder, with a radius of about 7 km, lying at a depth of 10 to 20 km and containing lherzolites or other rocks of density 3.3, could be responsible for this anomaly. Since the presence and shape of this structure are inferred from indirect evidence, any hypothesis on its nature, emplacement, and origin would be highly speculative.

Other "Alpine-type" peridotites

Since the lherzolite bodies of the Pyrenees have been proven to be solid intrusions, they should be compared to other "Alpine-type" peridotites. In many instances, the same mode of emplacement is indicated.

In describing the Totalpserpentinite (Switzerland), Peters (1963) concluded that the internal structures of this body, in origin a lherzolite, were not caused by the Alpine orogeny. He suggested that this mass intruded as a hot but solid body into wet sediments, causing it to become strongly serpentinized, more so peripherally than in the centre. The resemblance of this case to the Pyrenean lherzolites is striking. In both instances, no mixing with older gneisses occurred. Mixing with adjacent limestones, however, occurred frequently. The Swiss body is much more strongly serpentinized, however; so the ophicalcite rim between the serpentinite and the limestones could once have been the same as the mixed lherzolite-limestone breccia in the Pyrenees. Bailey and McCallien (1960), in describing a Ligurian ophicalcite (Italy), supposed that it could have originated from a serpentinite shattered by gaseous explosions, after which the cracks and voids were cementated with carbonates.

Wolfe (1965) found internal structures in the Blue River ultramafic intrusion (Canada) which are also discordant with respect to the country rocks, showing a thin zone of metamorphic alterations in the amphibolite facies. Notwithstanding the discordant nature, Wolfe concluded that a crystal-mush intrusion was the most likely mode of intrusion.

Raleigh (1963, 1965) also observed discordant structures and fabrics in the peridotite of Cypress Island (U.S.A.). He attributed the layering to crystal settling in a deep-seated magma reservoir, and the folding and fabric to a crystal-mush intrusion.

Yoshino (1964) suggested a solid intrusion for the peridotites of Higashiakaishiyama (Japan). Structures in some amphibolites, which he thought to be closely related to the generally massive peridotite, were discordant to the country rock.

Burch (1965) suggested a tectonic emplacement of the Burro Mountain ultramafic intrusion (U.S.A.) because of disconformity between internal and external structures as well as the low-grade of metamorphism in the country rocks.

To explain the intrusion of the ultramafic rocks of New Zealand, Challis (1965a) referred to a concept offered by Eaton (1962). There is geophysical evidence that basaltic magma in Hawaii was derived from a 60 km-deep source. Eaton suggested that its extrusion took place in two stages: an intrusion into magma reservoirs at a depth of 4 km, followed by extrusion. In these reservoirs, gravitational differentiation could have taken place. At intervals, extrusion of basaltic lavas occurred. Filter pressing could have given rise to monomineralic rocks such as dunite. These Hawaiian reservoirs coincide with strongly positive gravity anomalies. Although a similar anomaly has been found underneath the line of lherzolitic bodies in the Pyrenees, Eaton's concept is not applicable to them. O'Hara and Mercy (1963, 1966) assumed the lherzolites to be differentiation products of a basaltic magma that originated by fusion or partial fusion of upper mantle material. If the body postulated by de Cizancourt is a gravity-differentiated or stratiform intrusion, and if the lherzolites are fragments of this body, the whole stratiform body, i.e. the lower-lying lherzolites and the higher-lying gabbroic rocks, should have the same structures and fabric. Since the structures and fabric of the lherzolites are pre-Alpine, the deep-seated body would have been emplaced in pre-Alpine, perhaps Hercynian times. If this had been the case, large amounts of foliated basaltic or gabbroic rock would be expected. In the Pyrenees, however, there are few gabbroic bodies (the ophites) and none with tectonite fabrics. Therefore, this hypothesis seems highly improbable. The origin and emplacement of the dunites of New Zealand, however, has given rise to disagreement. Lauder (1965a, b) has reported some fabrics of olivines of Dun Mountain, but since he gave only the β -olivine concentrations, no critical examination of his hypothesis of a volcanic pipe is possible. Battey's (1960) diagrams suggest a tectonite fabric very similar to the fabric of the Pyrenean

lherzolites, but he attributed it to regional metamorphism. Comparison of his diagrams with the picture derived from the Pyrenean lherzolites, shows some definite discordance with respect to the country rock. A border zone of serpentinite obscures the contact. The grade of metamorphism of the country rock is variable (Turner and Verhoogen, 1960; Challis, 1965b). Some microstructural data would settle this point.

A totally different kind of peridotites are those described by Taylor and Noble (1960) and Noble and Taylor (1960). In the southeastern part of Alaska there is a very long, narrow belt containing many ultramafic rocks. This occurrence greatly resembles the normal "Alpine-type" intrusions but here they seem truly magmatic, in contrast to the Pyrenean lherzolites. These bodies intruded into probably genetically related gabbroic rocks. They are composed of concentric shells of hornblende pyroxenite, olivine pyroxenite, peridotite, and dunite, in that order, going from the periphery to the centre and from old to young. Gabbroic pegmatites cut across all these rocks. The ultramafics appear to be of late Jurassic or early Cretaceous age. Layering, graded bedding, and cross-bedding are frequent. Contamination with country rock has been found. All the bodies have contact-metamorphic aureoles. Taylor and Noble's hypothesis attributed these phenomena to a process of multiple intrusion by fractional fusion within the upper mantle.

Origin of the lherzolites

Thus, many hypotheses have been offered to explain such peculiar aspects of "Alpine-type" peridotites as their tectonite fabric, discordant internal structures, lack of contact metamorphism, their constant composition and occurrence near large fault structures. For many cases, only solid intrusion would explain all these features.

The occurrence of ultramafic inclusions in basalt should also be taken into account. In general, they have the same mineralogical compositions as "Alpine-type" peridotites, containing olivine, enstatite, chromium diopside, and spinel (Ross, Foster, and Myers, 1954; Forbes and Kuno, 1964). These minerals themselves seldom vary in composition. Frechen (1948, 1963) studied some nodules from Dreiser Weiher (Germany), and found a complete series of chemical transitions from dunitic nodules to the surrounding basalt. He therefore concluded that all the nodules were autoliths, on which de Roever (1963) commented that the olivine-poor nodules could be autoliths — early segregations of the basaltic magma — but that most of the nodules, i.e. the olivine-rich, enstatite-bearing ones, seemed to be true xenoliths showing a tectonite fabric (Collée, 1962; den Tex, 1963). In a magnificent paper, White (1966) suggested the same: nodules of lherzolite, dunite, and harzburgite are xenoliths; nodules of other peridotites, pyroxenites, and gabbros, autoliths. His conclusions are based on many features typical for lherzolitic

nodules and lacking in other types, such as remarkably restricted ranges of composition of the major constituents olivine and pyroxenes; lack of zoning, except sometimes in enstatite porphyroblasts; the presence of recrystallization phenomena; disequilibrium between the minerals of the lherzolite nodules and their basaltic host; occurrence of glass in fissures or interstices; lack of plagioclase and poikilitic pyroxenes.

In oceanic regions, where the earth's crust is rather thin or absent, basaltic magmas have been proved to originate in the upper mantle. Geophysical data show that the rocks constituting the upper mantle should have an average density of 3.3. Two rock types approach this density: eclogite and peridotite. At present, there is fairly general agreement that a chemical transition from the crust to the upper mantle is more probable than a physical phase transition. Consequently, the hypothesis of a peridotitic upper mantle (Turner and Verhoogen, 1960; Yoder and Tilley, 1962) has become the more likely one.

The many constant and highly characteristic features of the "Alpine-type" peridotites suggest a common source. The hypothesis of a peridotitic upper mantle therefore seems very attractive.

Nature of the upper mantle

Yoder and Tilley (1962), O'Hara and Yoder (1963), and O'Hara and Mercy (1963, 1966) have suggested that the upper mantle consists of garnet peridotite, and that beneath orogenic areas lherzolite is unstable. According to Rost (1963), garnet peridotite is a higher-grade metamorphic rock than the chemically equivalent lherzolite. Ringwood, MacGregor, and Boyd (1964) and MacGregor (1964, 1965) assumed that garnet peridotites and lherzolites are both present in the upper mantle as shells depending on differences in the temperature-pressure regime. In continental regions lherzolite would be unstable, while in oceanic regions with their much steeper geothermal gradients, a relatively thick layer of lherzolite could exist. It is unfortunate that the thickness of the crust beneath the Pyrenees is not known. The development of the Mesozoic sedimentary rocks of the Northern Pyrenees suggest a more or less geosynclinal basin. A thin crust due to supracrustal erosion (Hsu, 1965) or subcrustal erosion (Gilluly, 1955) has recently been suggested for geosynclinal areas, so that the crust might be relatively thin beneath the Pyrenees. Furthermore, the Alpine metamorphism points to an extremely steep geothermal gradient. It is therefore possible that the upper mantle beneath the Pyrenees consists of lherzolite.

Orogenic interpretation of the lherzolites

It has been shown that the hypothesis of O'Hara and Mercy (1963, 1966) concerning the origin of the Pyrenean lherzolites is highly improbable. Because the lherzolites are pre-Alpine metamorphic tectonites and there are no basaltic or gabbroic rocks with the same fabric, their differentiation from a basaltic magma seems impossible. It is probable, however, that the

ophites are somehow genetically related to the lherzolites, as Miyashiro (1966) has shown for many orogenic peridotites in Japan.

There are two important hypotheses to explain the generation of magmas from a peridotitic upper mantle. The first (O'Hara and Mercy, 1963; 1966) suggests that a partial fusion of the upper mantle gave rise to magmas; in the Pyrenees these could be the gabbroic, dioritic, and syenitic intrusions, the so-called ophites that intruded during the whole of the Mesozoicum; the residue — the lherzolites — intruded shortly before the first Alpine deformation phase, as solid blocks. According to an alternative hypothesis put forward by de Roever (1961) and Verschure (1966), convection currents brought high-pressure Mg/Si-spinels from lower parts of the mantle into the upper mantle, where these spinels became unstable and were transformed into olivine, pyroxenes, and a lower-pressure spinel (Ringwood, 1956; 1958a, b, c). Some of this material could not be incorporated by any of the newly-formed minerals, and gave rise to intergranular liquid drops that were squeezed out by the plastic deformation caused by the convection current.

The mantle model, as derived from seismic data and experimental work carried out at the Geophysical Laboratory, Washington (Boyd and MacGregor, 1964), shows that the mantle could consist of different shells. This model is consistent with both hypotheses for the generation of basaltic magmas. Convection currents are also consistent with both hypotheses. In the former, such a convection current could bring heat upward to cause partial fusion; in the latter, the decrease in pressure would cause exsolution from the high-pressure Mg/Si-spinels. It is even possible that both processes took place.

The theory of convection currents implies the development of new convection cells after a major orogeny; the convection currents disappear the moment a new major orogeny starts. In the mantle beneath the Northern Pyrenees such currents could have been moved upward and outward directly beneath the crust after the Hercynian orogeny, giving rise to a N-S stress-relaxation in the crust, which caused it to become thinner (Gilluly, 1955). Or the influx of mantle material toward the axial zone of the Hercynian Pyrenees could have caused block faulting and a subsiding basin (Bott, 1965). Both cases could have led to the formation of a sedimentary basin.

During the upward movement of the convection currents, in the "building-up" time of the Alpine diastrophism, the peridotitic mantle material was plastically deformed. The layering of spinel pyroxenites could have originated in this manner as sheets between lherzolitic material, parallel to the flow planes. Therefore, at these elevated temperatures and pressures the layering was probably both a tectonic and a flow banding. This could have been facilitated by intergranular liquids: partial fusion products or exsolution material from the high-pressure Mg/Si-spinels.

The intergranular liquid could be squeezed out to in-

trude into the host lherzolite and form sills and dykes of garnet pyroxenite; or it could intrude directly into the crust as the post-Hercynian, but pre-Alpine ophites. O'Hara and Yoder (1963) do not agree with this view because of chemical differences between garnet pyroxenites and basaltic partial fusion products of peridotites. Zwart (1954) has shown, however, that the differences between the ultramafic dyke rocks in the lherzolites and the ophites are not very great.

During a later stage of the orogenic cycle, when the intergranular liquids had already been squeezed out, the physical differences between the lherzolites and the pyroxenites could have become so important that shear folding occurred, producing asymmetrical isoclinal folds with a definite axial-plane cleavage and a fabric that is dependent only on this cleavage, while older patterns were totally destroyed.

At the end of the convection cycle, the rate of relaxation was at its highest and some faults of the old fundamental North-Pyrenean fault zone at last reached the upper mantle. It is probable that during partial fusion in the upper mantle the volatiles were concentrated in the liquid such that release of pressure and separation of a gas phase could cause considerable explosions. Solid slabs and fragments of gas-soaked lherzolite were thus fired upward like canon balls. Most of this material may only have been propelled half-way (the hypothetical lherzolite body of de Cizancourt), but some relatively small slabs reached the presently exposed level immediately or after a short interval, when a second series of explosions of freshly liberated and accumulated gas brought them further upward, which would explain the complete absence in some cases of metamorphic minerals in the country rock (Monchoux, 1965). These explosions shattered the country rock without greatly displacing them. During the explosive expulsion some mixing occurred, leaving lherzolite fragments in the limestone breccia and some limestone fragments in the lherzolite breccia. Funnel-shaped breccia bodies are easily explained as explosion pipes. After the explosion, gas must have kept streaming upward, causing fluidization (Reynolds, 1954). The breccias lying in the Alpine E-W or N-S direction could be later fluidization products, like the dykes of lherzolitic microbreccia both inside and outside the massifs, which show some sort of graded bedding parallel to the dyke wall.

After the solid intrusion of the lherzolites, extreme heat flow continued for a while in some parts during the next phase: the first Alpine compressional phase.

After the Alpine orogeny, ophitic magmas again intruded. Although ubiquitous in the Pyrenees, they occur more frequently near the North-Pyrenean fault zone and may represent a last remnant of the squeezed-out basaltic magma.

The upheaval of the Pyrenees in Miocene times (de Sitter and Zwart, 1962) was probably caused by epeirogenetic movements after the Alpine orogeny.

Intrusions of "Alpine-type" peridotites are often accompanied by amphibolite bodies explained as

lower crust material (de Roever, 1957; MacKenzie, 1960; Yoshino, 1964). It is an astonishing fact that no metamorphic crustal material was brought upward into the lherzolite-containing Mesozoic belt, not even in the lherzolite breccia. One reason for this might be that only the lherzolites contained enough gas for such a long ascent. Or, is it possible that subcrustal erosion beneath orogenic regions is a much more important process than has ever been envisaged? If so, the Mesozoic strata in the studied area would have lain directly on a lherzolite basement, so that there was no material other than the Mesozoic and lherzolithic to blast upward.

The emplacement of the lherzolites took place just before the Alpine orogeny; of this there is no doubt. But the pre-Alpine structures and fabrics could have resulted from the Hercynian orogeny, perhaps even in the upper mantle. These structures in the lherzolites show resemblances to some of the Hercynian rocks, but there are arguments against this assumption. In the first place, there are no lherzolites anywhere in the Pyrenean Hercynian basement; they occur exclusively in the Alpine orogenic belt. Secondly, there are almost no Hercynian basaltic or gabbroic rocks in the Pyrenees. The third argument is derived from the general picture of "Alpine-type" peridotites; it has often been suggested that these peridotites in orogenic zones were emplaced in an early stage of the orogeny. The present author is therefore of the opinion that a completely Alpine history of the lherzolites is more likely. Isotopic age determinations could settle this problem¹).

Although this story is to a great extent based on rather flimsy evidence and on data and ideas of other in-

¹) A K-Ar age determination of hornblende of a hornblendite vein in the lherzolite of the Etang de Lers, has been carried out at the "Laboratorium voor Isotopen-Geologie" at Amsterdam, resulting in an age of 116 ± 5 m.y. As the hornblendes are not affected by the Alpine metamorphism *in situ*, it is possible that the age represents the moment of secondary crystallization in the upper mantle, just before the ejection of the ultramafites into the present level (Verschure, R. H., Hebeda, E. H., Boelrijk, N.A.I.M., Priem, H. N. A., and Avé Lallemand, H. G., 1967. K-Ar age of hornblende from a hornblendite vein in the "Alpine-type" ultramafic mass of the Etang de Lers, Ariège, French Pyrenees. *Leidse Geol. Med.*, vol. 42, in press).

vestigators, some facts have been added by the present structural and petrofabric study. The author believes that comparative studies of other localities would provide many similar data. It is most fortunate that serpentinization of the lherzolites was weak in the Pyrenees, so that important relations were preserved, and that the structures are rather simple. In many instances in other regions serpentinization was strong, the structures are very complicated, and tectonic transport is often clearly visible. This could be explained by temperatures of 500° C or higher, which would have caused dehydration of the serpentine. A slight increase in dehydration gives a disproportionately large decrease in shear strength (Raleigh and Paterson, 1965; Riecker and Rooney, 1966). In these cases it seems possible that in response to relatively small tectonic forces, "solid serpentine bodies may move into overlying sediments in much the same way that a watermelon seed moves when squeezed between one's fingers" (Hess, 1955). But these are probably late phenomena in the orogenic history of a mountain range.

Although the present writer supports the solid intrusion hypothesis for the Pyrenean lherzolites, he can not deny that long, narrow belts with truly magmatic peridotites are known (southeastern Alaska). Perhaps the condition of crustal thickness is an important factor in the genesis of peridotites, the Alaskan peridotite belt lying at the continental margin while the Pyrenean belt is enclosed between continents. Although the lherzolites seem to have yielded little basaltic magma as a result of subordinate partial fusion, the Alaskan ultramafics appear to be products of complete, though fractional fusion of the upper mantle. (Between the non-magmatic "Alpine-type" peridotites there are, as has already been mentioned, also different types, not only with respect to the relative quantities of constituent minerals but also to the fabric patterns.)

In between these two — little partial fusion (lherzolites) and total fusion (Alaskan peridotites) — there may have also been intermediate partial fusion, giving rise to basaltic or gabbroic magmas that supplied the stratiform peridotites and the autolithitic peridotite nodules caused by crystallization differentiation. Therefore, all peridotites could be related genetically, as Thayer (1960) has already suggested.

REFERENCES

- Andreatta, C., 1934. Analisi strutturali di rocce metamorfiche, V. Oliviniti. *Per. Min.*, 5, pp. 237—253.
- Babkine, J., Conquéré, F., and Vilminot, J. C., 1966. Données préliminaires sur les minéraux opaques dans les roches ultrabasiques des Pyrénées. *C. R. Acad. Sci., Paris*, 263, pp. 453—456.
- Bailey, E. B. and MacCallien, W. J., 1960. Some aspects of the Steinmann Trinity, mainly chemical. *Quart. Jour. Geol. Soc. London*, 116, pp. 365—395.
- Bathey, M. H., 1960. The relationship between preferred orientation of olivine in dunite and the tectonic environment. *Am. Jour. Sci.*, 258, pp. 716—727.
- Bondesen, E., 1964. An intrusion breccia with associated ultrabasics from Sermersût, South-West Greenland. *Grönland Geol. Unders.*, 41, 36 pp.
- Bott, M. H. P., 1965. The upper mantle in relation to the origin of vertical movements at the earth's surface. *The Upper Mantle Symposium, New Delhi, 1964. Intern. Union Geol. Sci.*, pp. 20—28.

- Bowen, N. L. and Schairer, J. F., 1933. The problem of the intrusion of dunite in the light of the olivine diagram. *Rep. Intern. Geol. Congr.*, 16th Sess., Washington, pp. 391—396.
- 1935. The system $MgO-FeO-SiO_2$. *Am. Jour. Sci.* (5th ser.), 29, pp. 151—217.
- Bowen, N. L. and Tuttle, O. F., 1949. The system $MgO-SiO_2-H_2O$. *Bull. Geol. Soc. Am.*, 60, pp. 439—460.
- Boyd, F. R. and MacGregor, I. D., 1964. Ultramafic rocks. *Carnegie Inst. Wash. Yearb.*, 63, pp. 152—156.
- Brothers, R. N., 1959. Flow orientation of olivine. *Am. Jour. Sci.*, 257, pp. 574—585.
- 1964. Petrofabric analysis of Rhum and Skaergaard layered rocks. *Jour. Petr.*, 5, pp. 255—274.
- Burch, S.H., 1965. Tectonic emplacement of the Burro Mountain ultramafic body, Southern Santa Lucia Range, California. Ph. D. Thesis, Stanford Univ. (Abstr. in *Diss. Abstr.*, U.S.A., 1966, 26, p. 3860).
- Casteras, M., 1933. Recherches sur la structure du versant nord des Pyrénées centrales et orientales. *Bull. Serv. Carte Géol. France*, 37/189, 525 pp.
- Cayeux, L., 1931. Origine épigénique des dolomies jurassiques des Pyrénées. *C. R. Acad. Sci.*, Paris, 192, pp. 645—648.
- Challis, G. A., 1965a. The origin of New Zealand ultramafic intrusions. *Jour. Petr.*, 6, pp. 322—364.
- 1965b. High-temperature contact metamorphism at the Red Hills ultramafic intrusion — Wairau Valley — New Zealand. *Jour. Petr.*, 6, pp. 395—419.
- Chuboda, K. F. and Frechen, J., 1950. Über die plastische Verformung von Olivin. *N. Jahrb. Min. Abh. Abt. A*, 81, pp. 183—200.
- Cizancourt, H. de, 1948. Essai d'interprétation de la tectonique profonde des Pyrénées. *Bull. Soc. Géol. France* (5th ser.), 18, pp. 271—284.
- Collée, A. L. G., 1962. A fabric study of lherzolites with special reference to ultrabasic nodular inclusions in the lavas of Auvergne (France). *Leidse Geol. Med.*, 28, pp. 1—102.
- Deer, W. A., Howie, R. A., and Zussman, J., 1962. Rock-forming minerals. 1. Ortho- and ring silicates. Longmans, London, 333 pp.
- Eaton, J. P., 1962. Crustal structure and volcanism in Hawaii, in *The crust of the Pacific Basin*. *Am. Geophys. Union, Geophys. Mon.*, 6, pp. 13—29.
- Ernst, Th., 1935. Olivinknollen der Basalte als Bruchstücke alter Olivinfelse. *Nachr. Ges. Wiss. Göttingen (math.-phys. Kl., N. F., Fachgr. 4)*, 1, pp. 147—154.
- Eskola, P., 1939. Teil III: Die metamorphen Gesteine, in: Barth, T. F. W., Correns, C. W., and Eskola, P.: *Die Entstehung der Gesteine*. Springer-Verlag, Berlin, pp. 263—407.
- Forbes, R. B. and Kuno, H., 1964. The regional petrology of peridotite inclusions and basaltic host rocks. *The Upper Mantle Symposium*, New Delhi, 1964. *Intern. Union Geol. Sci.*, pp. 161—179.
- Frechen, J., 1948. Die Genese der Olivinausscheidungen vom Dreiser Weiher (Eifel) und Finkenbergr (Siebengebirge). *N. Jahrb. Min. Geol. Paläont. Abh. Abt. A*, 79, pp. 317—406.
- 1963. Kristallisation, Mineralbestand, Mineralchemismus und Förderfolge der Mafite vom Dreiser Weiher in der Eifel. *N. Jahrb. Min., Mon. h.*, pp. 205—225.
- Gilluly, J., 1955. Geological contrasts between continents and ocean basins. *Geol. Soc. Am., Spec. Paper* 62, pp. 7—18.
- Green, D. H., 1961. Ultramafic breccias from the Musa Valley, Eastern Papua. *Geol. Mag.*, 98, pp. 1—26.
- Griggs, D. T., Turner, F. J., and Heard, H. C., 1960. Deformation of rocks at 500° to 800° C. *Geol. Soc. Am., Mem.* 79, pp. 39—104.
- Hartman, P. and Tex, E. den, (in press). Piezocrystalline fabrics of olivine in theory and nature.
- Hess, H. H., 1938. A primary peridotite magma. *Am. Jour. Sci.* (5th ser.), 35, pp. 321—344.
- 1955. Serpentine, orogeny and epeirogeny. *Geol. Soc. Am., Spec. Paper* 62, pp. 391—408.
- 1966. Caribbean research project, 1965, and bathymetric chart. *Geol. Soc. Am., Mem.* 98, pp. 1—10.
- Hsu, K. J., 1965. Isostasy, crustal thinning, mantle changes, and the disappearance of ancient land masses. *Am. Jour. Sci.*, 263, pp. 97—109.
- Huang, W. T. and Merritt, C. A., 1952. Preferred orientation of olivine crystals in troctolite of the Wichita Mountains, Oklahoma. *Am. Min.*, 37, pp. 865—868.
- Jackson, E. D., 1961. Primary textures and mineral associations in the ultramafic zone of the Stillwater Complex, Montana. *Geol. Surv. Prof. Paper* 358, 106 pp.
- Kalsbeek, F., 1963. A hexagonal net for the counting-out and testing of fabric diagrams. *N. Jahrb. Min., Mon. h.*, pp. 173—176.
- Kamb, W. B., 1959. Theory of preferred crystal orientation developed by crystallization under stress. *Jour. Geol.*, 67, pp. 153—171.
- 1961. The thermodynamic theory of nonhydrostatically stressed solids. *Jour. Geophys. Res.*, 66, pp. 259—271.
- Kennedy, G. F., 1947. Charts for correlation of optical properties with chemical composition of some common rock-forming minerals. *Am. Min.*, 32, pp. 561—573.
- Lacroix, A., 1891. Sur la transformation des feldspaths en dipyre. *Bull. Soc. Franç. Min.*, 14, pp. 16—30.
- 1894. Etude minéralogique de la lherzolite des Pyrénées et de ses phénomènes de contact. *Nouv. Arch. Mus. Hist. Nat.* (3d ser.), 6, pp. 209—308.
- 1894/1895. Les phénomènes de contact de la lherzolite et de quelques ophites des Pyrénées. *Bull. Serv. Carte Géol. France*, 42/6, pp. 307—446.
- 1901. Les roches basiques accompagnant les lherzolites et les ophites des Pyrénées. *C. R. 8^e Congr. Géol. Intern.*, Paris, 2, pp. 806—838.
- 1916. Sur la caractéristique chimique de la dipyrisation des plagioclases des ophites des Pyrénées. *Bull. Soc. Franç. Min.*, 39, pp. 74—77.
- Ladurner, J., 1956. Das Verhalten des Olivins als Gefügekorn in einigen Olivingesteinen. *Tschermaks Min. Petr. Mitt.* (3d ser.), 5, pp. 21—36.
- Lauder, W. R., 1965a. The geology of Dun Mountain, Nelson, New Zealand. Part 1 — The petrology and structure of the sedimentary and volcanic rocks of the Te Anau and Maitai groups. *New Zealand Jour. Geol. Geophys.*, 8, pp. 3—34.
- 1965b. The geology of Dun Mountain, Nelson, New Zealand. Part 2 — The petrology, structure, and origin of the ultrabasic rocks. *New Zealand Jour. Geol. Geophys.*, 8, pp. 475—504.
- Longchambon, M., 1912. Contribution à l'étude du métamorphisme des terrains secondaires dans les Pyrénées orientales et ariégeoises. *Bull. Serv. Carte Géol. France*, 21, pp. 323—391.
- MacGregor, I. D., 1964. The reaction $4 \text{ Enstatite} + \text{Spinel} \rightleftharpoons \text{Forsterite} + \text{Pyrope}$. *Carnegie Inst. Wash. Yearb.*, 63, p. 157.

- 1965. Stability fields of spinel and garnet peridotites in the synthetic system $MgO-CaO-Al_2O_3-SiO_2$. Carnegie Inst. Wash. Yearb., 64, pp. 126—134.
- MacKenzie, D. B., 1960. High-temperature alpine-type peridotite from Venezuela. Bull. Geol. Soc. Am., 71, pp. 303—317.
- Mattauer, M., Proust, F., and Ravier, J., 1964. Remarques sur l'âge du métamorphisme pyrénéen. C. R. Soc. Géol. France, pp. 129—131.
- Miyashiro, A., 1966. Some aspects of peridotite and serpentinite in orogenic belts. Jap. Jour. Geol. Geog., 37, pp. 45—61.
- Monchoux, P., 1965. Nouvelles observations sur les lherzolites et les ophites de Moncaup (Haute-Garonne). Bull. Soc. Hist. Nat. Toulouse, 100, pp. 325—329.
- Mügge, O., 1898. Ueber Translationen und verwandte Erscheinungen in Krystallen. N. Jahrb. Min. Geol. Paläont., 1, pp. 71—159.
- Noble, J. A. and Taylor, H. P., 1960. Correlation of the ultramafic complexes of Southeastern Alaska with those of other parts of North America and the world. Rep. Intern. Geol. Congr., 21th Sess., Norden, 13, pp. 188—197.
- O'Hara, M. J. and Mercy, E. L. P., 1963. Petrology and petrogenesis of some garnetiferous peridotites. Trans. Roy. Soc. Edinburgh, 65, pp. 251—314.
- 1966. Garnet-peridotite and eclogite from Bellinzona, Switzerland. Earth Planet. Sci. Lett., 1, pp. 295—300.
- O'Hara, M. J. and Yoder, H. S., 1963. Partial melting of the mantle. Carnegie Inst. Wash. Yearb., 62, pp. 66—71.
- Paulitsch, P., 1953. Olivinkornregelung und Genese des Chromitführenden Dunits von Anghida auf der Chalkidike. Tschermaks Min. Petr. Mitt. (3d ser.), 3, pp. 158—166.
- Peters, Tj., 1963. Mineralogie und Petrographie des Totalserpentins bei Davos. Schweiz. Min. Petr. Mitt., 43, pp. 529—685.
- Phillips, F. C., 1938. Mineral orientation in some olivine-rich rocks from Rum and Skye. Geol. Mag., 75, pp. 130—135.
- Raleigh, C. B., 1963. Fabrics of naturally and experimentally deformed olivine. Ph. D. Thesis, Univ. California, Los Angeles, 215 pp.
- 1965. Structure and petrology of an Alpine peridotite on Cypress Island, Washington, U.S.A. Beitr. Min. Petr., 11, pp. 719—741.
- Raleigh, C. B. and Paterson, M. S., 1965. Experimental deformation of serpentinite and its tectonic implications. Jour. Geophys. Res., 70, pp. 3965—3985.
- Ramsay, J. G., 1960. The deformation of early linear structures in areas of repeated folding. Jour. Geol., 68, pp. 75—93.
- Ravier, J., 1959. Le métamorphisme des terrains secondaires des Pyrénées. Mém. Soc. Geol. France (N.S.), 38/86, 250 pp.
- Reynolds, D. L., 1954. Fluidization as a geological process, and its bearing on the problem of intrusive granites. Am. Jour. Sci., 252, pp. 577—613.
- Riecker, R. E. and Rooney, T. P., 1966. Weakening of dunite by serpentine dehydration. Science, 152, pp. 196—198.
- Ringwood, A. E., 1956. The olivine-spinel transition in the earth's mantle. Nature, 178, pp. 1303—1304.
- 1958a. The constitution of the mantle — I. Thermodynamics of the olivine-spinel transition. Geoch. Cosmoch. A., 13, pp. 303—321.
- 1958b. The constitution of the mantle — II. Further data on the olivine-spinel transition. Geoch. Cosmoch. A., 15, pp. 18—29.
- 1958c. The constitution of the mantle — III. Consequences of the olivine-spinel transition. Geoch. Cosmoch. A., 15, pp. 195—212.
- Ringwood, A. E., MacGregor, I. D., and Boyd, F. R., 1964. Petrological constitution of the upper mantle. Carnegie Inst. Wash. Yearb., 63, pp. 147—152.
- Rio, M., 1966. Observation sur deux gisements de lherzolite des Basses-Pyrénées. Lab. Pétr. Fac. Sci., Paris, 43 pp.
- Riotte, Ch. and Thiébaud, J., 1965. Caractères pétrographiques de l'ophite de Vèbre (Ariège). Bull. Soc. Géol. France (7th ser.), 7, pp. 168—171.
- Roeber, W. P. de, 1957. Sind die Alpinotypen Peridotitmassen vielleicht tektonisch verfrachtete Bruckstücke der Peridotitschale? Geol. Rundschau, 46, pp. 137—146.
- 1961. Mantelgesteine und Magmen tiefer Herkunft. Fortschr. Min., 39, pp. 96—107.
- 1963. Ein Versuch zur Synthese der verschiedenen Ansichten zur Herkunft der Mafititknollen vom Maarvulkan Dreiser Weiher in der Eifel. N. Jahrb. Min., Mon. h., pp. 243—250.
- Ross, C. S., Foster, M. D., and Myers, A. T., 1954. Origin of dunites and of olivine-rich inclusions in basaltic rocks. Am. Min., 39, pp. 693—737.
- Rost, F., 1963. Ultrabasite der Kruste und ihr Mineralbestand. N. Jahrb. Min., Mon. h., pp. 263—272.
- Sander, B., 1930. Gefügekunde der Gesteine. Springer-Verlag, Wien, 352 pp.
- 1948. Einführung in die Gefügekunde der geologischen Körper. 1, Springer-Verlag, Wien, 215 pp.
- Shaw, D. M., 1960. The geochemistry of scapolite. Jour. Petr., 1, pp. 218—285.
- Sitter, L. U. de, 1953. La faille Nord-Pyrénéenne dans l'Ariège et la Haute-Garonne. Leidse Geol. Med., 18, pp. 287—291.
- 1958. Boudins and parasitic folds in relation to cleavage and folding. Geol. Mijnb. (n. ser.), 20, pp. 277—286.
- Sitter, L. U. de and Zwart, H. J., 1959. Geological map of the Paleozoic of the Central Pyrenees. Sheet 3, Ariège, France. Leidse Geol. Med., 22, pp. 351—418.
- 1962. Geological map of the Paleozoic of the Central Pyrenees. Sheet 1, Garonne, 2 Salat, France. Leidse Geol. Med., 27, pp. 191—236.
- Taylor, H. P. and Noble, J. A., 1960. Origin of the ultramafic complexes in Southeastern Alaska. Rep. Intern. Geol. Congr., 21th Sess., Norden, 13, pp. 175—187.
- Tex, E. den, 1963. Gefügekundliche und geothermometrische Hinweise auf die tiefe, exogene Herkunft lherzolitischer Knollen aus Basaltlaven. N. Jahrb. Min., Mon. h., pp. 225—236.
- Thayer, T. P., 1960. Some critical differences between Alpine-type and stratiform peridotite-gabbro complexes. Rep. Intern. Geol. Congr., 21th Sess., Norden, 13, pp. 247—259.
- Tilley, C. E., 1947. The dunite-mylonites of St. Paul's Rocks (Atlantic). Am. Jour. Sci., 245, pp. 483—491.
- Turner, F. J., 1942. Preferred orientation of olivine crystals in peridotites, with special reference to New Zealand examples. Trans. Proc. Roy. Soc. New Zealand, 72, pp. 280—300.
- Turner, F. J., Heard, H., and Griggs, D. T., 1960. Experimental deformation of enstatite and accompanying inversion to clinoenstatite. Rep. Intern. Geol. Congr., 21th Sess., Norden, 18, pp. 399—408.
- Turner, F. J. and Verhoogen, J., 1960. Igneous and metamorphic petrology. McGraw-Hill, New York, 694 pp.
- Turner, F. J. and Weiss, L. E., 1963. Structural analysis of metamorphic tectonites. McGraw-Hill, New York, 545 pp.

- Verschure, R. H., 1966. Possible relationships between continental and oceanic basalt and kimberlite. *Nature*, 211, pp. 1387—1389.
- White, R. W., 1966. Ultramafic inclusions in basaltic rocks from Hawaii. *Contr. Min. Petr.*, 12, pp. 245—314.
- Winkler, H. G. F., 1965. *Petrogenesis of metamorphic rocks*. Springer-Verlag, Berlin, 220 pp.
- Wolfe, W. J., 1965. The Blue River ultramafic intrusion, Cassiar District, British Columbia. *Geol. Surv. Canada, Paper 64—48*, 15 pp.
- Yoder, H. S. and Eugster, H. P., 1954. Phlogopite synthesis and stability range. *Geoch. Cosmoch. A.*, 6, pp. 157—185.
- Yoder, H. S. and Tilley, C. E., 1962. Origin of basalt magmas: an experimental study of natural and synthetic rock systems. *Jour. Petr.*, 3, pp. 342—532.
- Yoshino, G., 1961. Structural-petrological studies of peridotite and associated rocks of the Higashi-akaishiyama District, Shikoku, Japan. *Jour. Sci. Hiroshima Univ. (ser. C)*, 3, pp. 343—402.
- 1964. Ultrabasic mass in the Higashiakaishiyama District, Shikoku, Southwest Japan. *Jour. Sci. Hiroshima Univ. (ser. C)*, 4, pp. 333—364.
- Zirker, F., 1866. *Lehrbuch der Petrographie*. 2. Adolph Marcus, Bonn, 635 pp.
- Zwart, H. J., 1954. Sur les lherzolites et ophites des Pyrénées. *Leidse Geol. Med.*, 18, pp. 281—286.